Title	Strength Model of Concrete Using Heat and Microstructure Developments
Author(s)	HAN Virak
Citation	高知工科大学，博士論文.
Date of issue	2006-09
URL	http://hdl.handle.net/10173/238
Rights	
Text version	author

Strength Model of Concrete Using Heat and Microstructure Developments

HAN Virak

A dissertation submitted to
Kochi University of Technology
In partial fulfillment of the requirements
for the degree of

Doctor of Engineering

Graduate School of Engineering
Kochi University of Technology
Kochi, Japan

August 2006

Strength Model of Concrete Using Heat and Microstructure Developments

HAN Virak

B.Eng (Institute of Technology of Cambodia, Cambodia) 1998
M. Eng (Universite Libre de Bruxelles, Belgium) 2001

A dissertation submitted to
Kochi University of Technology
In partial fulfillment of the requirements
for the degree of

Doctor of Engineering

Special Course for International Students
Department of Engineering
Graduate School of Engineering
Infrastructure System Engineering
Kochi University of Technology
Kochi, Japan

Examination Committee:

Professor SHIMA Hiroshi (advisor)
Professor OKAMURA Hajime
Professor KUSAYANAGI Shunji
Professor FUJISAWA Nobumitsu
Assoc. Professor OUCHI Masahiro

August 2006

ACKNOWLEDGEMENTS

First of all, I would like to write down some of my gratitude owed to all persons who have offered directly or indirectly their useful helps for the completion of this thesis. The particular thanks are pronounced to my advisor, Prof. Hiroshi SHIMA for his advice in steering my studies of concerned theories as well as experimental works and for his opinions in discussion since the beginning of the research. Without his considerable contributions, this thesis can not be successfully published.

Thanks are not forgotten to Prof. Hajime OKAMURA for his important advice in establishing a strength model which is the target of the research and to Prof. Masahiro OUCHI for his useful suggestions for the research.

In my study, I have learned from the seminars which were held every week in a manner so friendly and educational that a diversity of ideas can be exchanged between researchers. Thanks are frankly expressed to all the concrete laboratory members.

It is really my great delight to have the jury board composed of Prof. Hiroshi SHIMA, Prof. Masahiro OUCHI, Prof. Hajime OKAMURA, Prof. Nobumitsu FUJISAWA and Prof. Shunji KUSAYANAGI. Their constructive suggestions and kindness made me not only write the names in this piece of paper but also engrave deeply in my heart forever.

The analysis in the research is concerned with strength, porosity and heat. I acknowledge the kindness of Prof. Toshiharu Kishi in providing the code written in Fortran with which the heat calculation was operated. Sincere thanks to Dr. Supakit Swatekititham and Dr. Ming-Hung Hsieh are kept in heart for their kind explanations in guiding me during when I was very new to the concrete laboratories of KUT. Thanks are also owed to Miss Sachie Kokubo for her helpful contributions during my study. The experimental works were conducted with help of my classmate Mr. VONG Seng, particularly when the work was hard and could not be conducted alone. His contribution was gratefully considered as an indispensable intervention.

I acknowledge the SSP scholarship of KUT with which I could live and study in Japan for 3 years. In addition, IRC (international relation center) members have undertaken very kind helps in solving living problems as well as in facilitating many administrative procedures. Without their effective interventions, life was not happy. They deserve my great gratitude.

ABSTRACT

In concrete engineering, strength of concrete is one of the important indexes that concrete engineers should know. The strength has been found basing on some basic formula called the strength model which is usually used for the purpose of mix adjustment in the mix design method. In general, a number of trial mixes are always needed before obtaining a target mix proportion. According to the properties required, it takes at least one month or more in order to achieve enough satisfaction. Many researchers have made their efforts in creating strength models able to give more precise prediction with a reduced amount of trial mixes. Many models were proposed basing on some practical parameters which may not the determinant ones and the applications were limited. The main purpose of this research is to establish a strength model capable of estimating the strength of cement, mortar and concrete at any age without conducting any trial mixes and basing only on the provided data including composing powders, mix proportions, curing conditions and ages. The mechanism of strength development is very well concerned with an increase of hydration products accompanying the pore reduction. Recently the theories of microstructure development and multi-component hydration development were successfully proposed and were widely used in estimating concrete durability. With these theories, the porosities of any kinds and heat of hydration of any component powders as well as minerals can be accurately calculated only if the chemical and physical properties of materials used are known. So the attempt to create the strength model without trial mixes becomes a good challenge. The microstructure and heat models can give good results only when the proportion of good mixes is provided, too bad mixes are not recommended. The first work is then to find the simulated mixes that are not so much segregated or bleeded that the strength is affected. One remarkable property of cement that is contrary to the ideal property of the multi-component heal model is that when mixing the flocculation of particles occur unavoidably due to the absorption without dispersion however in the model, powder particles were considered as well dispersed in uniform spaces and hydration was uniform at each particles. The problem of particle flocculation can be solved by introducing dispersing agents known as super-plasticizers (SP) which are widely used in concrete production. Daimon *et al.* clarified that SP possesses principally 3 actions in dispersing cement particles. These actions are repulsive force due to the increase of zeta-energy, liquid-solid affinity and steric hindrance. The higher the dispersion, the more hydration products are precipitated the strength is then increased so the suitable mix which has the ideal dispersion is the mix of high strength among different mixes of the same mix proportion with variation of the dispersing SP dosages. Beside the dispersion

effect, other effects on strength played by aggregate content and mixing times were also studied. The authors made 3 main series of mortar mixes after which the SP dosage, sand content and mixing time could be decided. When the mixes were defined, more mixes were produced for the purpose of modeling. The modeling is conducted by formulating strength tested on cylindrical specimens as function of hydration heat of each compounds and effective porosity of mixes which are calculated. Different types of Portland cements were used and a wide range of w/c ratios with the wet and sealed curing conditions were considered. The results have shown that strength holds linear relations with the heat of each compound coupled with porosity. The combination of heat and pore as a single parameter is hereafter called as heat-pore component. It becomes clear that the strength can be modeled with a sum of each heat-pore component multiplied by strength contribution of each compound. Basing on the authors' experimental data, the strength contribution of each compound is determined. The strength model is created for wide application of Portland cements. The models for blended cements were also studied by introducing the powder contribution coefficients. The model applicable for blended cement is then proposed. The model was established with mixes free of sand content effect so when it is used for concrete, aggregate effect should be considered as another parameter.

TABLE OF CONTENTS

Names Page numbers

LIST OF TABLES

LIST OF FIGURES

CHAPTER I: INTRODUCTIONS

I. Introductions

It is clear that concrete has offered a lot of advantages including shaping flexibility due to its fresh workability, mechanical strength due to bonding of aggregate by cement paste and durability due to the resistance against natural and chemical attacks. This section reviews the reason why this research was proposed for investigation, how much it is required and how many researchers have already invested in this kind of research.

I.1. Research requirements

Concrete has been used as a main construction material in public works for centuries and is still keeping its importance in civil engineering. This material can effectively suit needs of construction design only when its properties are well predicted and produced. Many interesting and delicate properties are being investigated in different areas of the globe. Among these properties, compressive strength of concrete is an important one that concrete engineers must know as long as they are in charge of either concrete production or concrete structure. Strength is not only the identification for itself but also for other properties of concrete. It is used for the following purposes:

- Need for structural designs: once a concrete building of any kind is projected, concrete strength has to be known because it determines the feasibility of the project and the dimension designs. Furthermore, the corresponding mix proportions are the basic parameters in handling the quantity and cost estimation.
- Index to evaluate concrete performance including permeability and durability: it is common to hear someone say higher strength higher durability even though a durable concrete of low strength can be produced with some cement replaced by powders providing hydrates of sheet structures that can reduce permeability. In general, for the same type of materials, higher strength always leads to higher durability.
- Parameter in statistical data for ensuring the quality control system: one important attention is that concrete should be well placed and the quality should be satisfactorily guaranteed. According to the security importance of a project, construction can be stopped if compressive strength is found lower than the required one. In addition, the degree of variation of strength recorded for different parts can indicate how uniform the concrete production is and how well the delivery is qualified.

The above-cited purposes are very relevant to concrete engineers however the only way to know the compressive strength is to conduct a strength test of some tried mix proportions before deciding a suitable mix. Until now, there is no prediction method that provides surely the strength without testing. The purpose of this research is to find a model able to tell strength of concrete without testing if material properties, curing conditions and ages are known. This purpose underlines the essence of strength prediction which is the main point treated in this research.

I.2. Strength model history

Many models have been proposed and used in concrete engineering for strength prediction since concrete was first used. Some models needed some experimental coefficients any time material properties changed and some other gave a prediction of high variation. Those models were normally employed by producing a series of trial mixes and then the target mix would be selected with the engineer's skillful experience.

Feret (1892) said the strength was proportional to $[c/(c+w+a)]^2$, where c, w and a were the volumes of cement, water and air. The relation did not cover all relevant parameters and its use was limited. The coefficient of proportionality had to be determined with the available materials by trial mixes.

Powers (1962) found that the paste of various degrees of hydration and w/c ratio conformed to the following relation:

$$\sigma = \sigma_o . X^A \quad \text{.....eq. 1}$$

where X was the gel/space ratio and equaled to the volume of hydration products divided by that of hydration product plus capillary porosity. The A value was 3 and typical values for $\sigma_o = 130 - 190\, MPa$. The model was used for general mixes but the parameters taken in account were not enough and the range of variation was very high.

Feret's formula has been used by some ready-made concrete plant as a basis to make some adjustments in trial mixes and made records. Some practical ready mix producers kept a large record of mixes with a gradual variation of cement, water and aggregate content. With that record, the mix proportion could be found by fitting the required strength and workability with the data listed. It is not surprising that one concrete producer can keep in a list as many as 5000 mix designs. Even this is very practical but not very systematic and the use is limited only to the producer himself.

To create mix design methods which are widely applicable, some research establishments studied on a large tested data and proposed a set of tables and charts easy to find the mix proportions from the requirements imposed. These methods included DOE, ACI, Dreux-Gorisse, ConAd and others. According to the increase of computers available, many mix designers were interested in making their method computerized.

Until now, many mix design methods have been computerized and are potentially used in concrete engineering for example Dreux-Gorisse Method (in France), ConAd Method (in Australia) and some others currently used in some other places. Even these methods are different from each other but they have the two same purposes: slump and strength. The purposes can be obtained first by an approximation basing on the experimental charts or on a set of data programmed in software and finally some adjustments have to be operated with a few trial mixes.

Dreux-Gorisse Method

1. Determine the maximum size of aggregate
   Basing on the rebar reinforcement and the concrete placement condition
2. Composition of sand and coarse aggregate
   Using the sieving curves of both materials
3. w/c
   Using $f_{c28} = G\sigma_{c28}\left(\frac{V_c}{V_c + V_e + V_v}\right)^2$,
   G is a coefficient obtained experimentally and changing with an aggregate type.
4. Water and cement content
   Using workability charts
5. Mix proportion
   Using the equation of volume balance

ConAd Method (KEN W. DAY, 1999)

1. SS (Specific surface)
   Basing on aggregate sizes and grading curves
2. MSF (Mix Suitability Factor), EWF (Equivalent Water Factor)
   MSF is obtained from the workability table then EWF can be calculated.
3. w/c
   Using $f_{c28} = \frac{25}{w/c} - 8$
4. Water and cement
   Using SS and MSF
5. Mix proportion
   Using SS, sand and aggregate proportions are determined.

Dreux-Gorisse was one of the methods that were easy and objective to use however KEN W. DAY claimed that ConAd was an easy method and needed less input data than others. The

two different points interesting to the author are the objectivity and subjectivity of the methods. According to my own opinion, ConAd was subjective and without a lot of experience a young concrete producer can not become familiar.

The methods have just been described presented that the computerizing methods were already applied but the disadvantages that were not overcome were the adjustment by trial mixes. The question here is how a mix design method can be operated with computerization and without trial mixes. Answering to this question, two recent researches were already done: one by Kato Kishi (1994) and another by Otabe and Kishi. Kato and Kishi proposed a model relating the differential increase in the strength to the increase in the average degree of hydration of major components. It was expressed as:

$$df_c^{'} = 25\,dQ_{C_3S} + 40\,dQ_{C_2S} + 27\,dQ_{SG} + 40\,dQ_{FL} \quad \text{.....eq. 2}$$

$$dQ_i = w_i\,d\alpha_i \quad \text{.....eq. 3}$$

where w_i is the weight ratio of the *i*th clinker mineral in powder to mix water and $d\alpha_i$ is the incremental increase in the degree of hydration of *i*th clinker mineral component. This model was created in an idea for general application without trial mixes to tell strength by knowing only the properties of the materials and curing conditions. The authors share this idea. Kato model showed the prediction values very different from the test values. According to Kato's model, the degree of hydration was considered as the main factor determining strength development. This may not always be true because the degree of hydration is just the ratio of heat hydrated at any time divided by the ultimate heat of hydration and two mixes of different w/c and of the same degree of hydration do not have the same strength. He should have included porosity and heat of hydration instead of using degree of hydration alone. Before Kato's works, Relis, M. (1988) made an attempt in generating strength prediction equations for mortar on the basis of parameters which include main compounds and some oxides and w/c ratio but the reliability was marginal. Odler, I. (1991) made an extensive review that a generally applicable strength prediction equation for commercial cement was not possible due to the interaction between compounds, the influence of the alkalis and of gypsum, the influence of particle size distribution and the presence of glass.

The very new research for strength prediction was just finished by Otabe and Kishi, they proposed a relation:

$$f_c = f'_\infty \left[1 - \exp\left\{ -\alpha' \left(\frac{D_{hydr.out}}{\theta} \right)^{\beta'} \right\} \right] \quad \text{.....eq. 4}$$

where $D_{hyd.out}$ is the ratio between the outside hydration volume and initial capillary pores. θ is related to initial capillary pores, $\alpha' = 1.055, \beta' = 2.9$ and f'_∞ is the contribution by ultimate strength of C2S and C3S.

According to their presentation, the model shows a good prediction. I have no experience using this model but on my own opinion, this model included both heat (hydration products) and microstructure (capillary pore). These parameters are also considered as important in this research. Differences of creative ways will be shown in the whole paper.

The above description of strength prediction in mix design can be summarized as shown in Fig.I.2-1. The mix design originated since the birth of concrete by trying many mixes and then the suitable mix was selected. According to the concrete market competition, the design strategy developed fast and nowadays' method is to use a mix design that can predict all properties without any trial mixes.

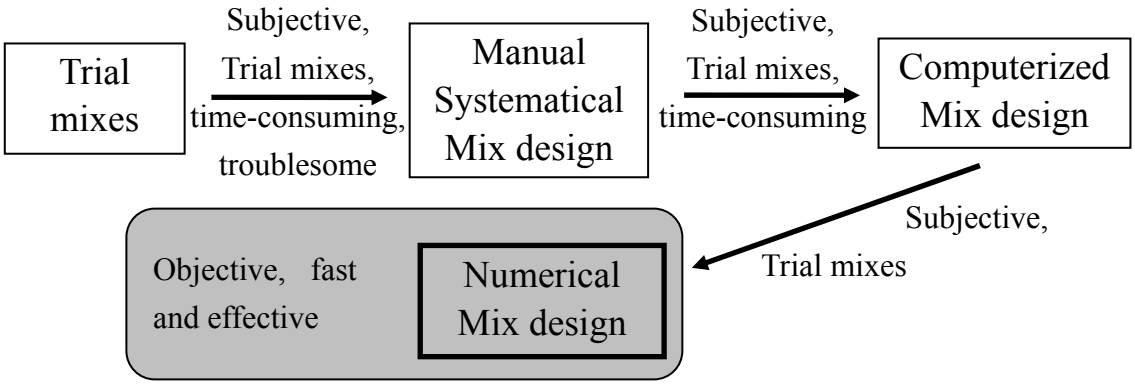

Fig I.2-1: Mix design method development history

The route to achieve this goal is to use the microstructure and the energy of hydrate formation. The lack in Kato's works may be the negligence of microstructure and his parameter that is degree of hydration was not direct and not unique for identifying strength. So in order to avoid the lack in Kato's works, the first task in this research is to find the very determinant and potential parameters and then study them with strength.

Many researchers have investigated in the effect of porosity on strength. In material science, materials of the same type have higher strength when porosity is lower. In concrete technology, it is well known that lower w/c will certainly lead to lower porosity and then

higher strength. Mindess (1970) concluded that for a given porosity, the strength increased with the proportion of fine pores and Odler and Rossler (1985) concluded that while the main factor influencing strength was porosity, pores with a radius below 10 nm (10^{-8}m) were of negligible importance. Their conclusions clarified that strength had close relation with porosity and porous structure even this relation was not unique.

In this research, strength was modeled with a new proposed formula relating two important parameters: total hydration heat and porosity of mix (see section II). Hydration heat was taken into account because heat was the energy of hydrate formation. As hydration processes, the strength increases as well due to the increase of hydrated products filling porous space and replacing un-hydrated particles and porosity was included in modeling because of its close effect on strength [1]. An appropriate type of porosity will be studied for modeling. The main idea of works was to create a model for strength prediction basing on mix proportion properties including: cement chemical compositions, curing methods and ages. This model would not be the time-consuming method which needed a long series of trial mixes.

I.3. Research programs

The research program was established to show the general flow of work and the final target (see Fig.I.3-1).

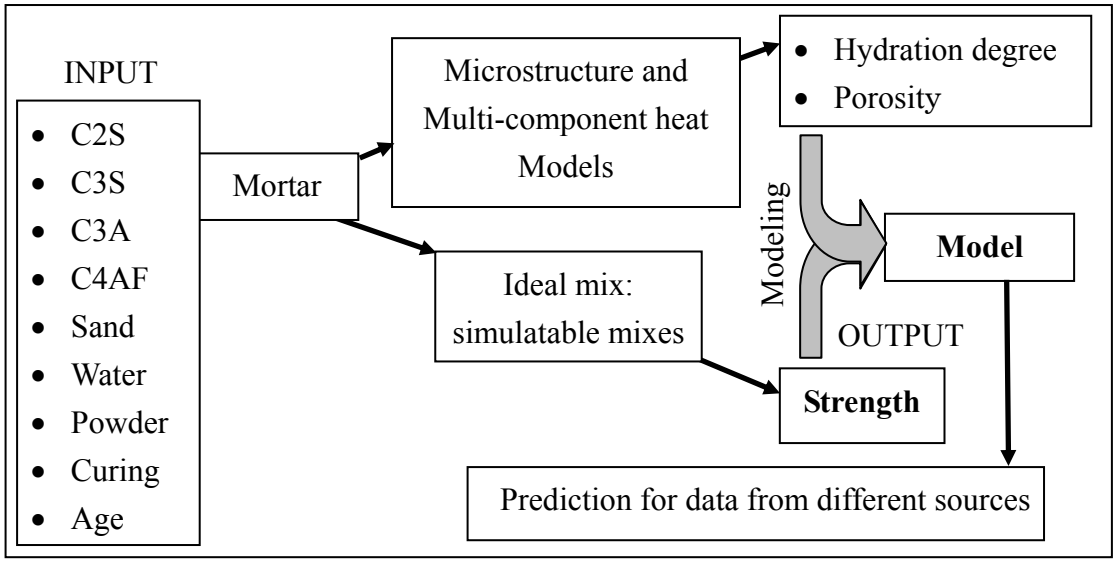

Fig I.3-1: research program

The research was started with many mixes of mortars in order to study factors playing the coherent effects on compressive strength. Among those mixes, some ideal mixes were selected because they show the same properties as those of the mixes in the microstructure

and multi-component heat models.

Once the ideal mixes were identified, their properties were calculated with the combined model of microstructure and multi-component heat theories by inputting cement compounds, mix compositions, curing method and age. Modeling was studied basing on the behavior of the tested strength of mortars investigated as function with the calculated properties. A general form of strength related to heat and effective porosity was discovered but the form still contained some unknown coefficients needing to be determined with experimental works. A model was then created after collecting experimental data. After the model was proposed, it would be refined with data from other sources and for different types of cements.

CHAPTER II: LITERATURE

II. Literature Reviews

In this research, the microstructure and heat development of hydration products were calculated using the microstructure model and the multi-component heat models which were proposed by Toshiharu Kishi *et al*. Their models were created with some suppositions which constituted the ideal conditions of cement particles and aggregate. The mix of the same ideal condition has to be defined and produced before modeling its strength with calculated heat and porosity. In this section, the models for calculating heat and porosity are reviewed as follows.

II.1. Microstructure model

When cement, powders and water are mixed continuously the particles are supposed to be dispersed uniformly and the reaction of the particles is all at the same degree of hydration (see Fig.II.1-1).

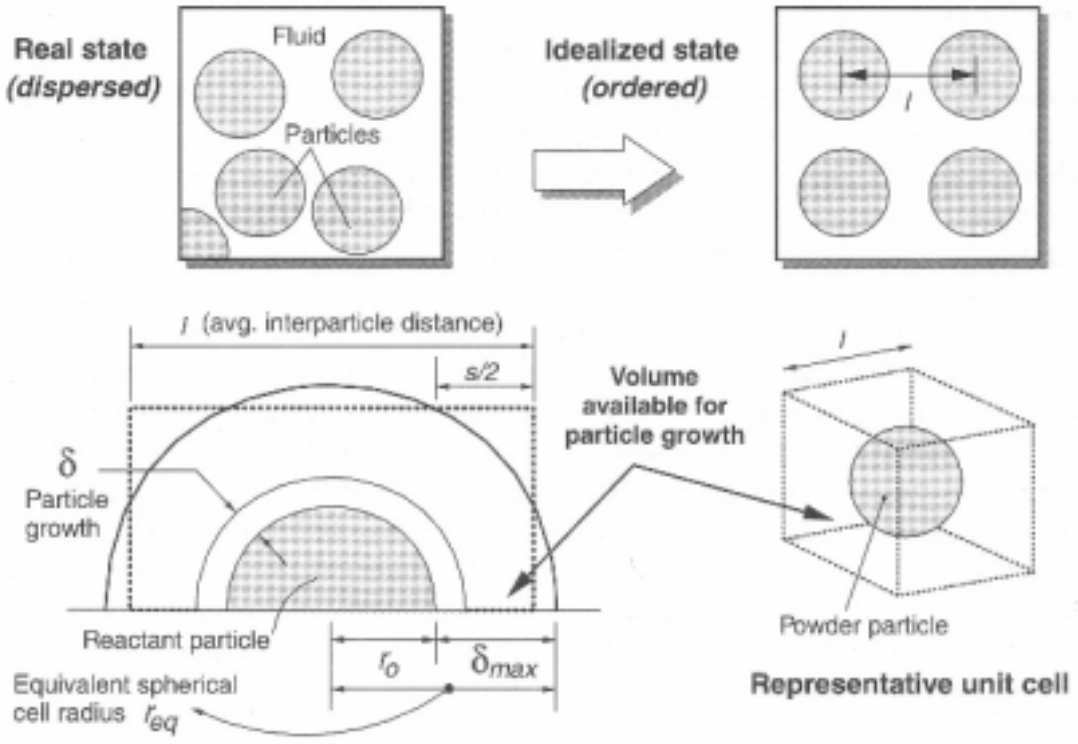

FigII.1-1: Dispersion of particles

Fig.II.1-1 shows the particles are dispersed and the spaces between particles are available for the hydration growth. Each cement particle hydrates outwards as well as inwards. The outer hydration products are more porous than those of inner hydration. For a given w/p and a given type of cement or powder whose fineness modulus and specific gravity are known, the space between particles can be calculated. As the particles are in colloidal suspension, the volumetric concentration of powder is

$$G = \frac{G_0}{(1 + s/2r_0)^3} \quad \text{.....eq. 5}$$

G : average volumetric concentration.
G_0 : maximum volumetric concentration
r_0 : radius of particles.
s : space of particles.
$G_0=0.79(BF/350)^{0.1}$ and $G_0=<0.91$.
BF : Blaine fineness index.
r_0= 10μm and BF=340m^2/kg.
The particles' space is:

$$s = 2r_0\left[\left\{G_0(1+\rho_p w_0)\right\}^{1/3} - 1\right] \quad \text{.....eq. 6}$$

ρ_p : average specific gravity.
Each particle has a free cubic volume l^3 to which corresponds a representative spherical cell of radius r_{eq}.

$$r_{eq} = \left(\frac{3}{4\pi}\right)^{1/3} l = \chi l \quad \text{.....eq. 7}$$

l : cubic side.
χ : stereological factor.
Maximum thickness of the expanding cluster is

$$\delta_{\max} = r_{eq} - r_0 = r_0\left[2\chi\left\{G_0(1+\rho_p w_0)\right\}^{1/3} - 1\right] \quad \text{.....eq. 8}$$

At any stage of hydration, the matrix contains hydrates and various compounds: gel, un-reacted powder particles, calcium hydroxide crystals, traces of other minerals and large void spaces filled with water. 3 porosities are found: interlayer pore (between layers of CSH or other hydrates), gel pore (inside gel but between groups of layers CSH) and capillary pore (between gels or groups of gels).

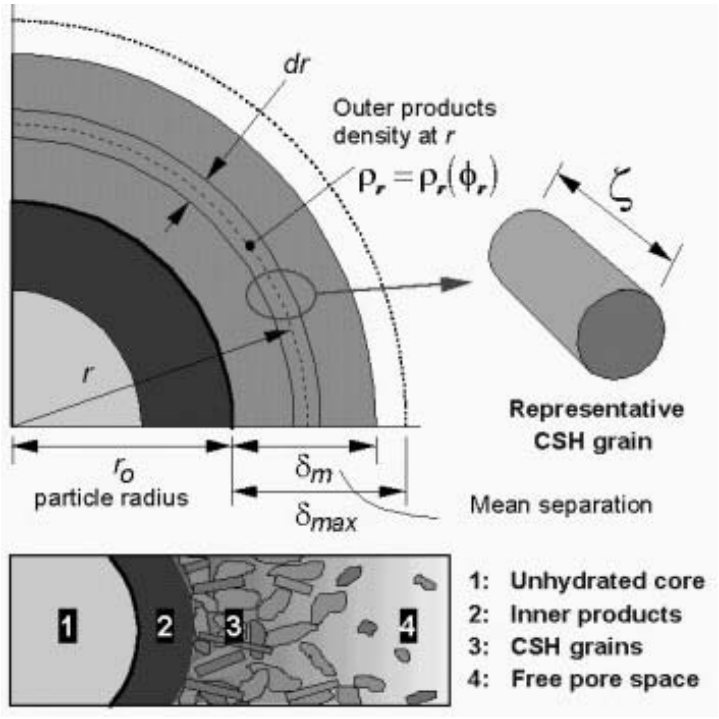

FigII.1-2: Hydration of cement and pozzolans

Fig.II.1-2 illustrates the hydration of one particle of powder. As can be seen, hydration processes outwards and inwards. Outer development gives a more porous medium than the inner part. During hydration, hydrates are produced and precipitated in such an arbitrary manner that different pore types are distinguished. The space between hydration of cement particles are normally capillary pores however in the hydration products (gel or gel products) interlayer and gel pores are formed.

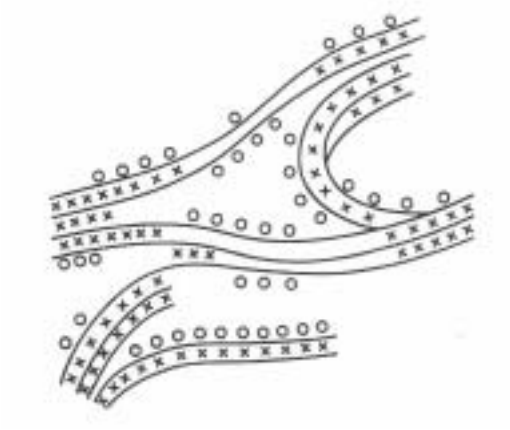

FigII.1-3: Interlayer and gel pores

Fig.II.1-3 illustrates a cement gel composed of hydrates structured with gel and interlayer pores. Interlayer pores (cross marks) are formed between hydrates and gel pores (circle marks) are formed between groups of hydrates. The group of hydrates is formed by the hydrates of same precipitation direction. The characteristic porosity in gel is ϕ_{ch}=0.28 for cement (OPC). This value is adopted and used for all types of powders.

The volume V_s of gel products (hydration products) in a unit of volume of the paste can be calculated using the following expression:

$$V_s = \frac{\alpha W_p}{1-\phi_{ch}}\left(\frac{1}{\rho_p}+\frac{\beta}{\rho_w}\right) \quad \text{.....eq. 9}$$

α : average degree of hydration.
β : mount of chemical combined water per unit weight of hydrated powder.
W_p : weight of powder per unit paste volume.
ρ_p, ρ_w : density of powder and chemical combined water.

The interlayer porosity (ϕ_l) and gel porosity (ϕ_g) are calculated by eq.10 and eq.13

$$\phi_l = (t_w s_l \rho_g)/2 \quad \text{.....eq. 10}$$

t_w : interlayer thickness (=2.8 A^o)-(Anstrom = 10^{-10}m).
ϕ_l : is interlayer porosity per volume of gel product.
s_l : specific surface area in (m^2/g) and is calculated by eq.11

$$s_l = 510 f_{pc} + 1500 f_{sg} + 3100 f_{fa} \quad \text{.....eq. 11}$$

f_{pc}, f_{sg}, f_{fa} : weight fractions of cement, slag and fly ash.

The dry density of gel products is given by eq.12.

$$\rho_g = \frac{\rho_p \rho_w (1+\beta)(1-\phi_{ch})}{(\rho_w + \beta\rho_p)} \quad \text{.....eq. 12}$$

The gel porosity is then deduced with eq.13

$$\phi_g = V_s \phi_{ch} - \phi_l \quad \text{.....eq. 13}$$

Finally, the capillary porosity is calculated by

$$\phi_c = 1 - V_s - (1-\alpha)(W_p/\rho_p) \quad \text{.....eq. 14}$$

α, which is the degree of hydration which will be reviewed in the next section.

Some parameters that derive from interlayer, gel and capillary porosity are effective porosity and total porosity. The effective porosity (EP) is the sum of gel and capillary porosity on the other hand the total porosity is the sum of interlayer, gel and capillary porosities.

$$EP = \phi_g + \phi_c \quad \text{.....eq. 15}$$

II.2. Multi-component heat model

The heat of hydration of cement and pozzolanic materials were the main topics in concrete engineering in order to model the development of cementitious materials. Many of models were proposed by different researchers, some were totally empirical and some others were very scientific. The multi-component heat model used in this research was proposed by Kishi *et al*. The model was based on the fundamental values ($H_{i,To}$) of heat rate of each cement

component obtained from experiments [9]. The reference heat rate is function of accumulated heat. The total heat rate can be calculated by eq.16.

$$\begin{aligned} H_c &= \sum p_i H_i \\ &= p_{C3A}(H_{C3AET} + H_{C3A}) + p_{C4AF}(H_{C4AFET} + H_{C4AF}) \\ &\quad + p_{C3S}H_{C3S} + p_{C2S}H_{C2S} + p_{SG}H_{SG} + p_{FA}H_{FA} \end{aligned} \quad \text{.....eq. 16}$$

H_i : heat generation rate of mineral i per unit weight

p_i : weight composition ratio.

H_{C3AET}, H_{C4AFET} : heat rates in formation of ettringite.

The heat generation rate of each mineral compound was calculated with the proposed equation eq.17 which depended on the actual temperature, delaying effect, water reduction effect, effect of $Ca(OH)_2$ lack, mineral interaction effect and fineness effect.

$$H_i = \gamma\beta_i\lambda\mu s_i H_{i,T}(Q_i)\exp\left\{-\frac{E_i}{R}\left(\frac{1}{T}-\frac{1}{T_0}\right)\right\} \quad \text{.....eq. 17}$$

$$Q_i = \int H_i dt \quad \text{.....eq. 18}$$

E_i : activation energy of component i.

R : gas constant.

$H_{i,To}$: reference heat rate of component i at constant temperature To.

γ : coefficient expressing the delaying effect of admixtures.

β_I : reduction coefficient in heat generation rate due to availability of free water.

λ : change coefficient of heat generation rate of blast furnace slag and fly ash due to the lack of calcium hydroxide.

μ : change coefficient of heat generation rate in term of the difference of mineral composition of Portland cement.

$s_i=S_i/S_{io}$: change coefficient of reference heat rate according to the fineness of powders.

$-E_i/R$: thermal activity which is determined by the experimental works.

- **Reference Heat generation rate and thermal activity**

The heat generation rate is calculated based on the reference heat generation rate measured on the clinker minerals of OPC. In this proposed scheme, the reference heat rates are represented

with multiple breaking lines divided into typical stages of hydration including: dormant period, control process and diffusion control.

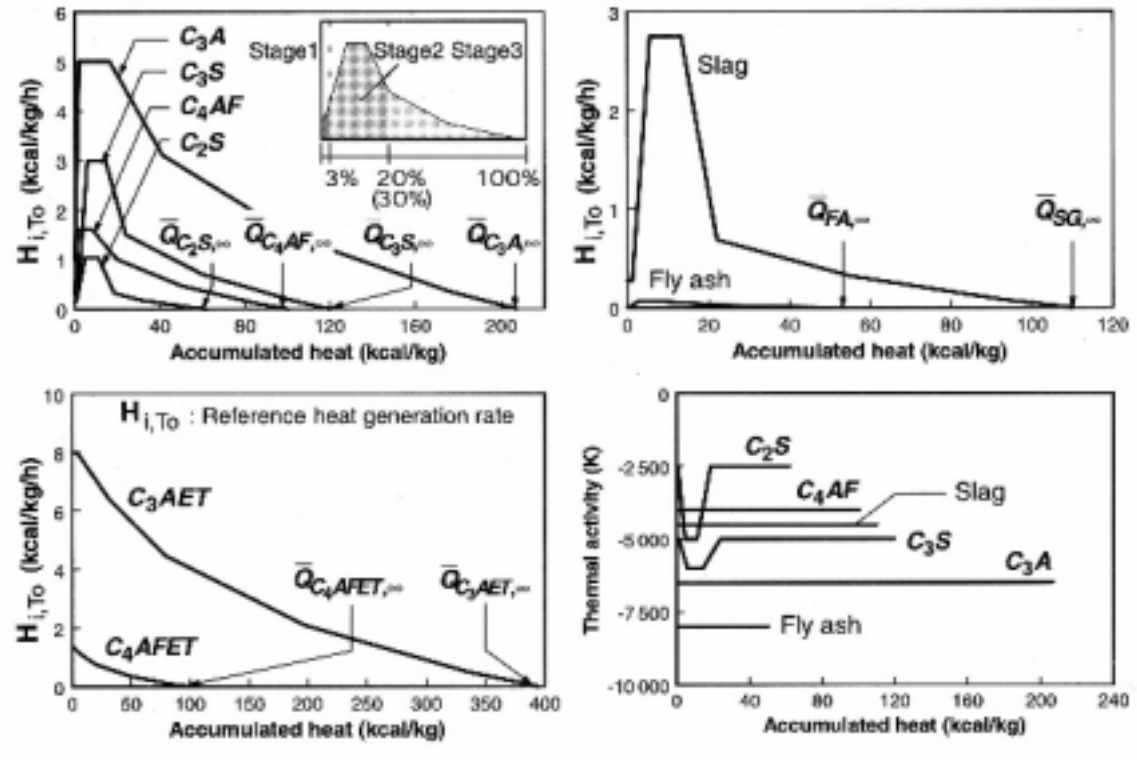

FigII.2-1: Reference heat generation rate of cement and pozzolans

Fig.II.2-1 shows the heat generation rate of cement compounds and pozzolans and the thermal energy as function of accumulated heats. In the heat model 2005, the thermal activities showed in the Fig.II.2-1 are changed to be constant. When this is used for cement of different compositions, the effect of compound interaction and micro filler effect must be taken into account. The modification factors of C2S and C3S are shown in Fig.II.2-2 and are represented by r_{CH}

$$r_{CH} = r_{\max} - a\exp\left\{-b\left(\frac{p_{C3S}}{p_{C2S}}\right)^{C}\right\} \quad \text{.....eq. 19}$$

where, b and c are respectively equal to 0.025 and 7.0. r_{max} and a are respectively 1.05 and 0.9 for alite case and 1.3 and 1.0 for belite case.

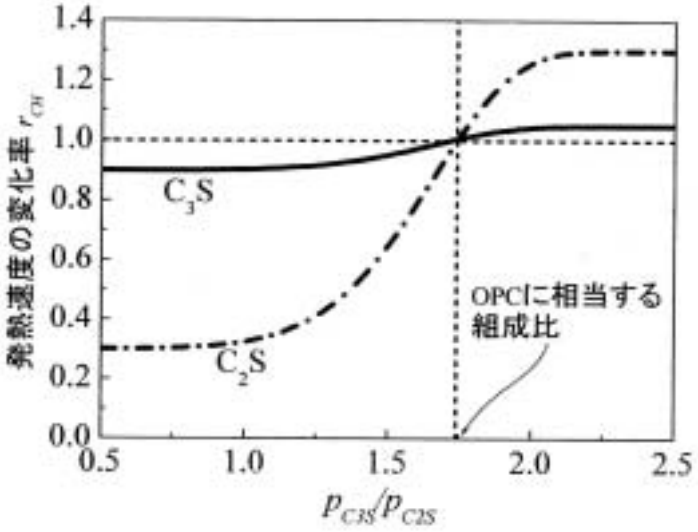

According to Fig.II.2-2, C3S is much affected by C2S however C3S is less affect by C2S. The heat rate of C2S is much different between when C3S content is low and when C3S content is high.

FigII.2-2: Modification factor for heat generation rate due to mineral composition

After the heat rate is modified with the mineral composition effect, it must be rectified with the micro-filling effect which is calculated in the following equations:

$$HS'_j = (1+rs)\,HS_j \quad (3 \le j \le 5) \qquad \text{eq. 20}$$

$$Q'_j = Q_{\max} - \frac{Q_{\max} - Q_j}{1+rs} \qquad (4 \le j \le 6) \qquad \text{eq. 21}$$

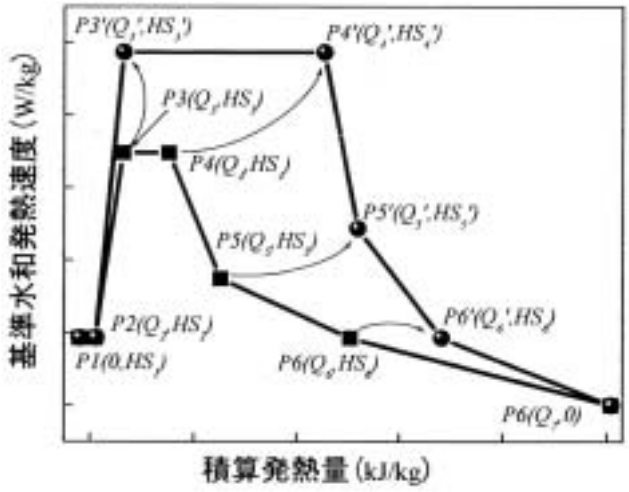

Fig.II.2-3 shows the change of heat rate due to the fact that cement particles are so fine that the filling effect occurs.

FigII.2-3: Change of heat rates due to micro-filler effect

$$rs = rs_{\max}\left[1-\exp\left\{-d\left(\frac{p_{C2S}}{p_{C3S}+p_{C2S}}\right)^{e}\right\}\right] \quad \text{.....eq. 22}$$

where, rs_{max}, d and e are respectively 1.2, 3.0 and 5.0.

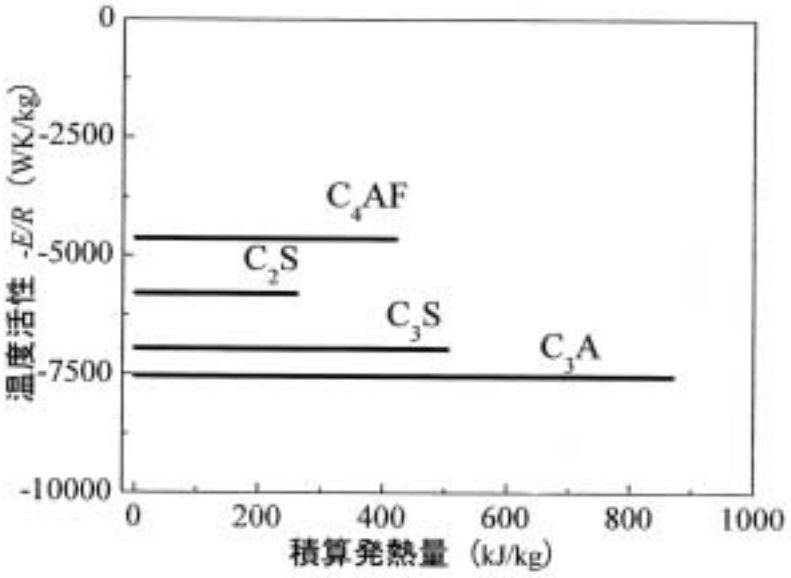

FigII.2-4: Thermal activity (modified 2005)

- **Free water-missing effect**

$$\beta_i = 1-\exp\left\{-r\left[\left(\frac{w_{free}}{100\eta_i}\right)/s_i^{1/2}\right]^{s}\right\} \quad \text{..... eq. 23}^{1}$$

r = 5 and s = 2.4 : material constants.

$$w_{free} = \frac{W_{total}-\sum W_i}{C} \quad \text{.....eq. 24}$$

$$\eta_i = 1-\left(1-\frac{Q_i}{Q_{i,\infty}}\right)^{1/3} \quad \text{.....eq. 25}$$

Where

W_{total} : unit water content.

W_i : water consumed and fixed by the reaction of constituents.

[1] reference:[17] and [18]

C : unit cement content.

Q_i : accumulated heat of component i.

$Q_{i,\infty}$: final heat generation.

In case that slag or fly ash is used separately or in combination, the free water reduction due to a shortage of $Ca(OH)_2$ was taken in account and treated by eq.26.

$$W_{free} = \frac{W_{total} - \sum W_i}{C.\left(p_{PC} + m_{SG}.p_{SG} + m_{FA}.p_{FA}\right)} \quad \text{.....eq. 26}$$

$$m_i = \lambda / \beta_i \quad \text{.....eq. 27}$$

- **Inter-dependence coefficient.**

The inter-mineral interaction effect was considered to depend on the percentage of C3S and C2S which were believed to play a role in both heat and strength developments. According to Fig.II.2-5, the hydration stages other than stage 3 are not affected.

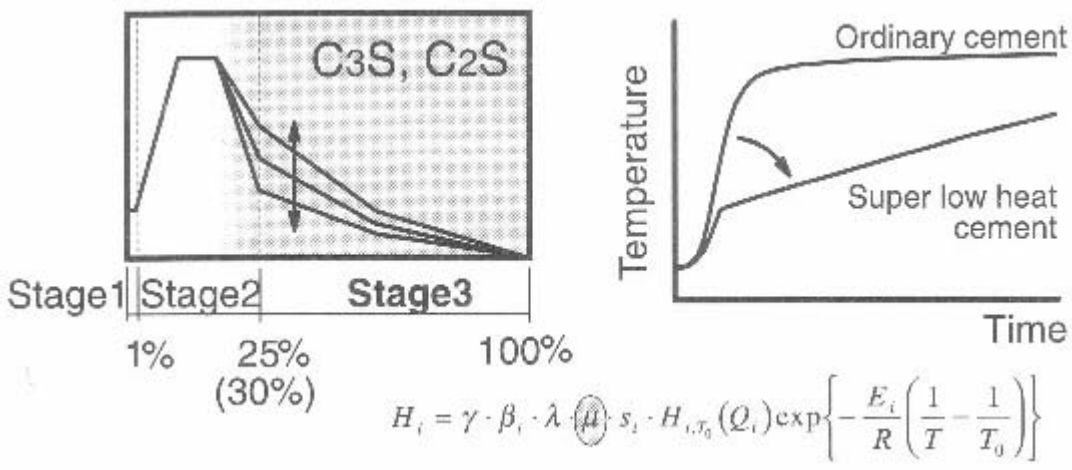

FigII.2-5: Inter-dependence effect

The following equation was proposed for the inter-dependence effect:

$$\mu = 1.4\left\{1 - \exp\left[-0.48.\left(\frac{p_{C3S}}{p_{C2S}}\right)^{1.4}\right]\right\} + 0.1 \quad \text{.....eq. 28}$$

- **Coefficient of left and need of $Ca(OH)_2$.**

The reaction of slag and fly ash was reported to take place only with sufficient supply of $Ca(OH)_2$ left by cement reaction. The reaction of cement is accompanied with release of $Ca(OH)_2$ which is consumed by slag, fly ash and some other pozzolans. This shows that the

prediction of hydration of pozzolans must be concerned with the factor controlling the supply and consumption of $Ca(OH)_2$. As can be illustrated in Fig.II.2-6, fly ash consumes $Ca(OH)_2$ from cement and retards cement hydration however, slag consumes without retarding. In ternary case, fly ash keeps playing its role as retarding agent. This retarding effect is reckoned in with the coefficient γ. When the $Ca(OH)_2$ supply is reduced in the reaction medium, water availability is also affected then the free water-missing effect is to recalculate as in the section free water-missing effect.

The lack and need of $Ca(OH)_2$ for pozzolanic reaction was accounted for by using the following equation:

$$\lambda = 1 - \exp\left[-2.0 \left(\frac{F_{CH}}{R_{SGCH} + R_{FACH}} \right)^{5.0} \right] \quad \text{.....eq. 29}$$

F_{CH} : is the amount of $Ca(OH)_2$ produced by C_3S and C_2S and not yet consumed by C_4AF.

R_{SGCH} and R_{FACH} : is the amount of $Ca(OH)_2$ necessary for reaction of slag and fly ash.

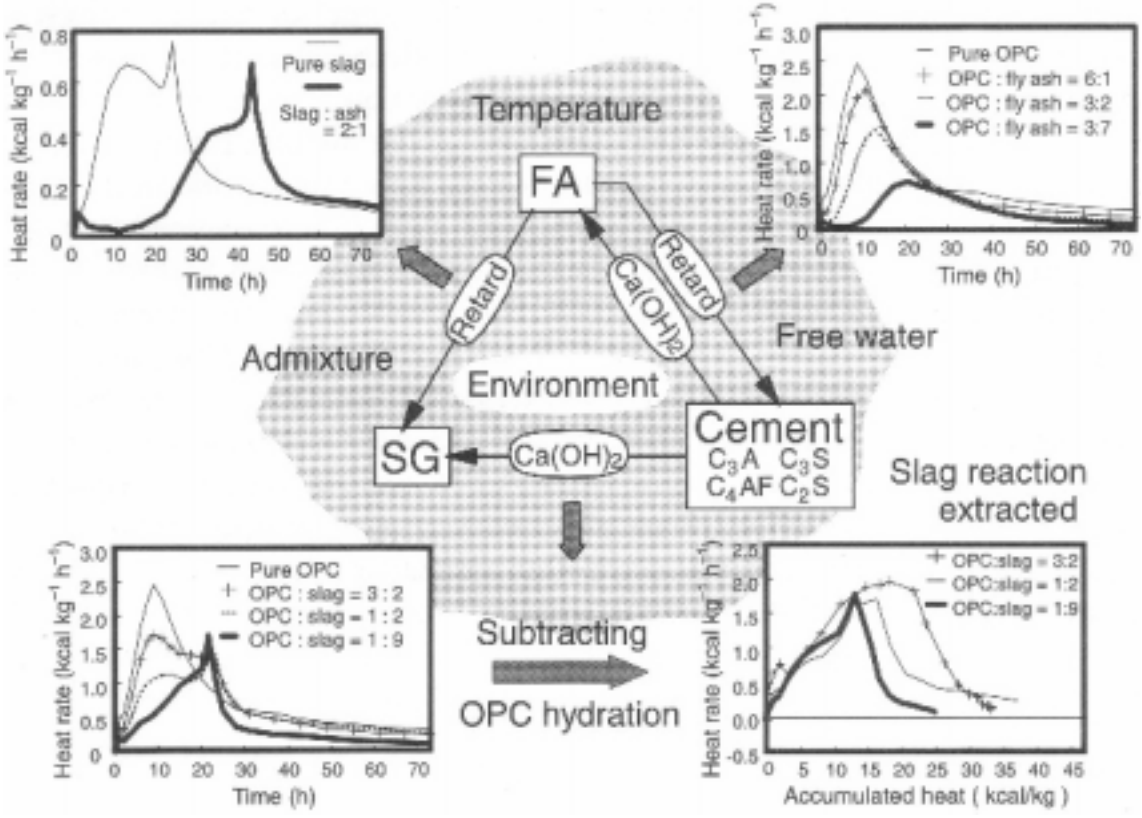

FigII.2-6: Connection between heat rates of blast furnace slag and fly ash with OPC

- **Effective Delaying coefficient.**

When a super-plasticizer (SP) was used, the delaying effect short or long was sure to occur.

The effective SP was calculated by eq.31 then the delay coefficient was proposed by eq.30.

$$\gamma = \exp\left[-\frac{1000(\vartheta_{SPef} + \vartheta_{FAef})}{10 p_{C3S} s_{C3S} + 5 p_{C2S} s_{C2S} + 2{,}5 p_{SG} s_{SG}} \right] \quad \text{.....eq. 30}$$

γ : delaying coefficient of heat generation reduction in stage 1.

$$\upsilon_{SPef} = p_{SP} \cdot \chi_{SP} - \upsilon_{Waste} \quad \text{.....eq. 31}$$

$$\vartheta_{Waste} = \frac{1}{200}(16 p_{C3A} s_{C3A} + 4 p_{C4AF} s_{C4AF} + p_{SG} s_{SG} + 5 p_{FA} s_{FA}) \quad \text{.....eq. 32}$$

ϑ_{Waste} : Effect of chemical admixtures without influencing the delay.

ϑ_{ef} : Effective delaying capability.

χ_{SP} : Coefficient representing the delaying effect per unit weight of admixture.

Table II.2-1: Delaying effect corresponding to each type of admixtures

Main component of admixtures	χ_{SP}
Naphtalene sulfonate	1.2
Polycarboxilate	1.2
Air entraining agent	5

p_{SP} : Dosage of organic admixture expressed as additive ratio to binder (Cx%)

$$\vartheta_{FAef} = 0.2 . p_{FA} s_{FA} \quad \text{.....eq. 33}$$

After heat generation rate is calculated, the average degree of hydration is given by:

$$\alpha = \sum_i p_i \cdot \frac{Q_i}{Q_{i\infty}} \quad \text{.....eq. 34}$$

The process of calculation hydration heat on one age is to make summations of hydration of all time steps. As can be shown in Fig.II.2-7, the process begins with an initialization of accumulated heat. At zero time, accumulated heat is zero, but the reference heat rate is not zero. $H_{i,To}$ and $\frac{E_i}{R}$ are calculated from Fig.II.2-1 and at the same time $\gamma, \beta_i, \lambda, \mu, s_i$ can be calculated. The heat rate is then calculated. By multiplying with the initial time step, the

increase of heat can be known and the new heat is accumulated, this new accumulation of heat is used for determining the reference heat rate of the next loop.

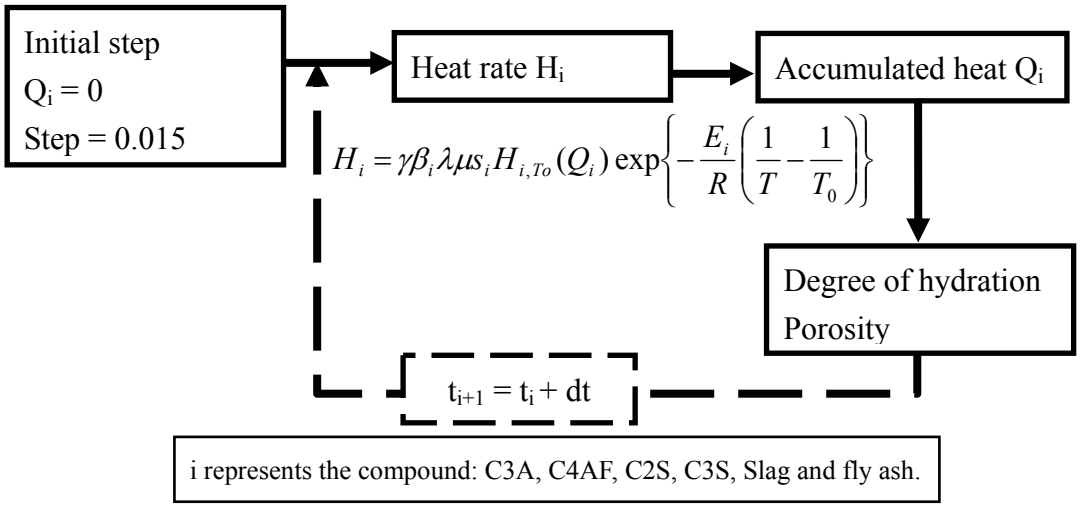

FigII.2-7: Hydration heat calculation process

II.3. Porosity measurement and the disadvantages

Paste is hardened progressively with time during reaction of cement with water. At the same time that cement particles are reacted, the paste becomes compacted and strong by interlacing cement particles with outside hydrates. The structure of hardened pastes is complex because of the complexity of forms of different types of hydration products including CSH[2], CH[3], AFm (alumino-ferrite mono), AFt (alumino-ferrite tri) and others. Jennings *et al.* reported that CSH possessed 4 main forms including CSH type I, II, III and IV. These CSH types exist in cement paste in some stages of hydration and are foil-like and fibrillar. CH, AFm and AFt have similar layer structures. Pore structures are not of fixed forms but determined by the hydrate products which are foils and fibrillar and which are interlocked. The knowledge of porosity becomes interesting since it determines many properties of concrete. Porosity and porous structures were measured with several methods among which MIP (mercury intrusion porosimetry) meets wide applications. The microstructure development model used in calculating pores in this research was established basing on MIP. So it is essential to know how fine pores can be measured with MIP. The method was based on the fact that mercury does not wet a porous solid will enter pores only under pressures. Washburn assumed that pores are cylindrical and calculated the pressure p

[2] Calcium silicate hydrate: tobermorite ($C_5S_{5.5}H_9$), CSH type I ($C_5S_5H_6$), Jennite ($C_9S_6H_{11}$) and CSH type II ($C_9S_5H_{11}$). C=CaO; S=SiO_2 and H=H_2O.

[3] Calcium hydroxide: $Ca(OH)_2$ or Portlandite.

needed to place in pores of diameter d by $p = -4\gamma\cos\theta/d$ where $\gamma;\theta$ are respectively the surface energy of liquid (Hg=0.483Nm^{-1}) and the contact angle (117^o-140^o). Even MIP is widely applied; we should pay strict attentions to the disadvantages happening in some cases. The followings are some problems not resolved yet by researchers (Taylor. H. F. W, Cement Chemistry, 2nd edition, 1997, pp. 248-249).

1. The method does not measure the distribution of pore sizes, but that of pore-entry sizes (Dullien, 1979). If large pores can be entered only through small pores, they will be registered as small pores. Previous suspicions that this effect is of major significance with cement pastes were supported by the results of computer modeling of the entry of mercury into cement pastes (Garboczi, 1991).
2. The delicate pore structure of the paste is altered by the high stress needed to intrude the mercury. This effect was shown in studies on composite cements, in which mercury was intruded, removed and re-intruded into mature pastes. Contrary to earlier conclusions, it also occurs with pure Portland cement pastes (Feldman, 1991).
3. As with other methods in which the paste has first to be intensively dried, the pore structure is also altered by the removal of the water. Isopropanal replacement followed by immediate evacuation and heating at 100^{o}C for 2h has been reported to cause the least damage (Feldman, 1991).
4. It is not clear whether the method registers the coarsest part of the porosity, intruded at low applied pressures.
5. The assumption of cylindrical pores and of a particular contact angle may be incorrect.

According to these above cited remarks, the real porosity is coarser than the one given by MIP.

When slag and fly ash are used, they can react with $Ca(OH)_2$ released from cement hydration and the reaction leads in general to a low Ca/Si ratio and $Ca(OH)_2$ are replaced with CSH. Harrison (1987), Regourd (1986) and Uchikawa (1986) concluded that the microstructures of slag cement pastes were similar to those of Portland cement paste apart from the lower CH content. Harrison continued that the similarity between slag cement pastes and Portland cement pastes were typical for fly ash-cement pastes. Basing on the TEM (Transmission Electron Microscope) these microstructures changed from fibrillar shapes to foil-like shapes which allowed slag-cement pastes to have lower permeability than cement paste (Regourd, 1992). Most researchers shared their opinion about the difficulties found in studying pore structures of composite cements using mercury intrusion due to the foil-like shapes with fine entry sizes of pore.

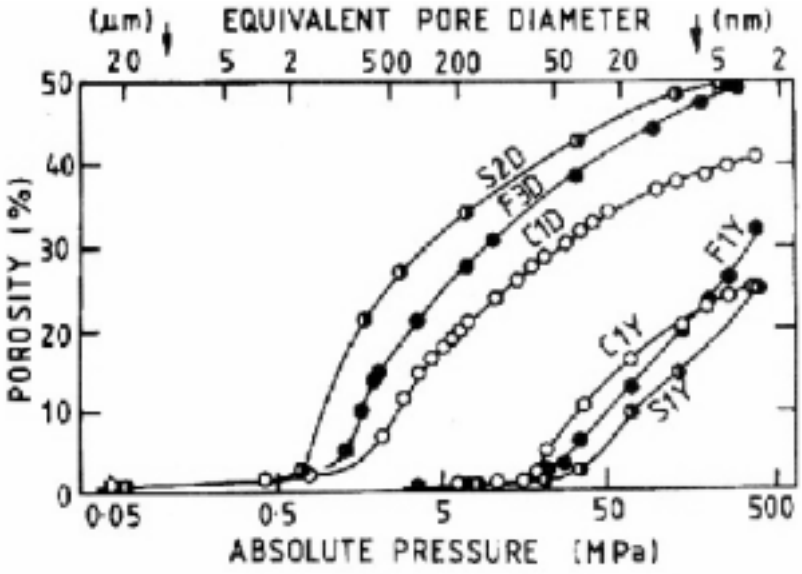

FigII.3-1: Pore entry size distribution for pastes of composite cements using mercury intrusion porosimetry

In Fig.II.3-1, (Feldman, 1981) mixes were with w/p=0.45 and curing temperature 21^{o}C. C1D, C1Y: Portland cement pastes cured for 1 day and 1 year. S2D, S1Y: Portland slag cement (70% slag) pastes cured for 2 days and 1 year. F3D, F1Y: Portland flyash cement pastes (13% CaO in flyash) cured for 3 days and 1 year.

Feldman (1981) reported using mercury porosimetry that at early ages, the distribution of pore entry sizes in fly ash or slag cement pastes was coarser than in comparable Portland cement pastes and the porosity recorded by the method at the maximum pressure was higher however at later ages, the distribution of pore entry sizes was finer than in comparable Portland cement pastes. This researcher believed that mercury could not enter all the pore space.

The above described literatures suggest that the porosity measured with mercury intrusion method for slag and fly ash replacements may not be certain due to the pore structures. The microstructure model used to calculate the porosity in this research was established based on the mercury porosimetry and on Portland cements. This uncertainty of pore measurement may be a need to take account for the pore distribution factor in modeling strength of slag and fly ash mixes.

II.4. Integration of microstructure and multi-component heat model

The above-described microstructure model and multi-component heat model were integrated in one program in order to calculate the time dependent development of hydration and microstructure and predict the strength development of concrete. The process of calculation can be seen in Fig.II.4-1. The multi-component heat model is calculated using the code developed by Prof. Toshiharu Kishi (reference [17]) and the microstructure model is calculated using the model reported in reference [1].

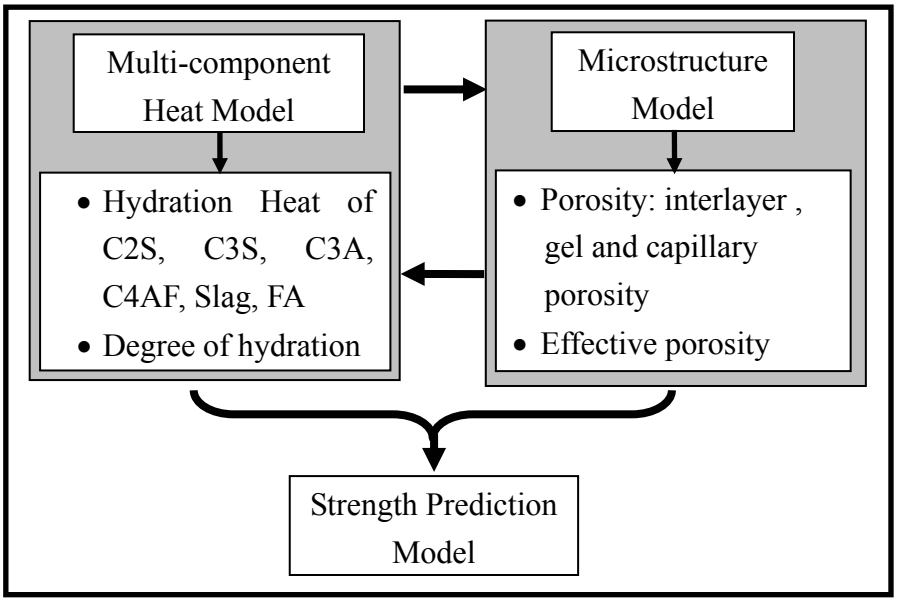

FigII.4-1: Integration of multi-component heat and microstructure models

CHAPTER III: METHODOLOGY

III. Methodology

The main concern of research was strength which had to be tested for mixes whose properties were calculated. Many researchers believed that compressive strength of concrete depends on raw material compositions and strength testing. The latter is influenced by several operational factors such as the loading rate, moisture condition, curing conditions, specimen size, machine platen size and others. Consequently, the procedures were described in the following in order to specify what has been done and to assure the quality of the authors' results.

III.1. Materials

Raw materials used in mortar or concrete production can be found in many areas where the physical and mechanical properties are quite different. Natural, industrial materials and waste can be used as components of concrete. The natural materials are sand exploited from river, sea or mountains. The industrial materials are cement, produced ash and the waste materials are blast furnace slag, fly ash, plasticizers and super-plasticizers.

III.1.A. Admixtures

Admixtures are defined as materials added to concrete before, during mixing or immediately before placing in order to improve the physical and chemical properties of paste or concrete which eventually affects the mechanical property in both short and long-term durability. According to functions offered, admixtures are categorized in ASTM C494-98 into 7 types:

- A (water-reducing admixtures),
- B (retarding admixtures),
- C (accelerating admixtures),
- D (water-reducing and retarding admixtures),
- E (water-reducing and accelerating admixtures),
- F (water-reducing, high range admixtures) and
- G (water-reducing, high range and retarding admixtures).

Among these admixtures, super-plasticizers (SP) (types F and G) become very popular because it offers a variety of flexibility to settle many concrete problems ranging

from fresh workability to long-term durability. An example of workability improvement was the production of self-compacting concrete and an example of long-term durability was the production of high performance concrete by incorporating silica fume. This very interesting capacity was due to its fundamental mechanism in dispersing cement particles by three ways such as an increase of ς-potential, an increase of solid-liquid affinity and steric hindrance (Daimon, 1978). These three effects can be high or low depending on the types of SP including sulfonated melamine formaldehyde polymers (poly(melamine sulfonate); MS), sulfonated naphthalene formaldehyde polymers (poly(naphtalene sulfonate); NS), lignosulfate materials and polycarboxylate based superplasticizers. The dispersing mechanism of the polycarboxylate types was reported based on the steric hindrance and the dispersion increased as the polymer length or the absorption thickness increased (Sakai, 2003). In this research, cement and other powders have to be well dispersed in order to simulate mixes as ideal as in the microstructure and multi-component heat models, therefore super-plasticizers were used as admixture. SP are not only good dispersing agents but are also set delayers and air-entrainers. According to Suzuki, the delaying effect varies according to the type of SP. SP used was RHEOBUILD SP8SB_Sx2 which was made of compounds of polycarboxylate ether with their cross-linked polymers. It had a density of 1.04 g/cm^3 and a pH of 9. This type of SP was the same type used by Suzuki in his experiment and according to his report, the delaying effect was 1.2.

III.1.B. Cements

Cement is defined as hydraulic powder which can react with water and harden under water to form a hardened rock. Cement, according to its manufacturing process, is an expensive powder among powders used in concrete engineering. Cement compositions are not unique however are variable due to sources of raw materials and production purposes. In concrete, cement is the first component that reacts with water; its reaction is always accompanied with hydration heat whose value may be high or low according to the cement components mainly including: C2S, C3S, C3A, C4AF and gypsum. Strength of cement is of first importance because its role is to bond all aggregate together to form a unique rock. In Japan, low heat Portland cement is pure cement; it is selected for use in the first investigation to find the ideal mixes prescribed by the microstructure and multi-heat component models.

After determining some effective parameters which have a close influence on strength, these parameters have to be studied and modeled with the strength tested on the specimens. The model has to be applied with different types of cement characterized with the composition of C2S, C3S, C3A and C4AF. The properties and compositions of these cements were listed as following:

Table III.1.B-1: Cement compositions

Mineral types	Percentage by weight		
	LH (Low heat)	HES (High Early Strength)	OPC (Ordinary Portland Cement)
C3S (tricalcium silicate or alite)	28	63	58
C2S (dicalcium silicate or belite)	53	11	15.5
C3A (tricalcium aluminate)	3	9	11.4
C4AF (tetracalcium ferro-aluminate or ferrite)	10	8	7.6
Physical properties			
Specific gravity in g/cm^3	3.24	3.13	3.13
Surface area in cm^2/g	3280	4770	3400

III.1.C. Powders

Defined as powders, all materials finer than 0.075 mm they can be hydraulic, pozzolanic, latent hydraulic. Many powders are available for concrete production. They are used to enhance the fresh (flowability, bleeding retention) and hardened properties (strength, durability) of concrete. Powders excluding cement have been broadly categorized as pozzolanic or latent hydraulic. Neither type reacts significantly with water at ordinary temperature in absence of $Ca(OH)_2$ supply. Pozzolanic powders are always low in CaO and high in Si_2O or Al_2O_3, they react with water and CaO supplied by cement reaction and finally give hydration products of low $Ca(OH)_2$ even the structure is almost the same as pure hydraulic cement products. Included in this type, are fly ash class F, natural pozzolana and silica fume. However, latent hydraulic powders have reaction property between hydraulic cements and pozzolanic materials and can react consuming a minimal amount of catalyst or activator. In general, latent hydraulic powders can be used in higher amount than pozzolanic powders to replace some cement. Considered as latent hydraulic, are slag and fly ash class C. Another powder which is neither pozzolanic nor latent hydraulic is finely ground limestone. This powder becomes now very interesting in concrete technology as cement replacement powder. In this paper, the authors also included the often-used powders in the investigation. Those powders are listed in Table III.1.C-1. The blast furnace slag is slag from factory it is not mixed with other compounds of clinker. All the powders are blended with low heat cement when batching. The replacement ratio of a powder is defined as the ratio of that powder weight to the total weight of all powders. This replacement ratio is used to identify a fraction of the powder in powder composition.

Table III.1.C-1: Powder properties

	Limestone	Fly ash (II)[4]	Blast furnace slag
Specific gravity (g/cm^3)	2.7	2.36	2.91
Fineness modulus (g/m^2)	3530	3410	3930

III.1.D. Sands

Sand is defined as an aggregate whose grain sizes ranges from 0.075 mm to 5 mm. These materials can be composed of various minerals which provide specifically a diversity of physical and mechanical properties. In concrete, despite of the reactivity of some minerals with cement, sand is considered as an inert component that may affect the resulted mix property by its texture, size, sieving distribution, strength and other secondary properties. In general, sand contains water some of which is absorbed inside and some other is attached to surface. The inside absorbed water content with dry surface is called SSD water content or water absorption content, on the other hand the water content attached to surface is called surface free water. The latter is a cause of variation of mix properties because of its downward movement which makes the water content non-uniform. In order to keep water content of sand uniform, sand need to be kept with water content the same as SSD water content. Of course, sand ordered from suppliers had water content variable and different from SSD water content, so the preparation of a large required quantity was indispensable.

Table III.1.D-1: Sand properties

	First sand	Second sand
Bulk SSD specific gravity	2.57	2.59
Apparent specific gravity	2.64	2.67
Absorption	1.86	1.87
Fineness modulus	2.75	2.97

The preparations was really troublesome but was successfully managed using the following methods. First, sand was sampled and tested for SSD water content according to ASTM C-128-97. Second, an amount equal to the container volume was taken and stirred with a concrete mixer and then the actual water content was checked with a moisture meter. Third, if the actual water content was higher than the SSD water content, sand had to be dried. Fourth, if the actual water content was lower than the SSD water content, the amount of water needed to add in order to make the whole sand become at SSD condition was calculated and added and finally sand was uniformly stirred. Fifth, sand was inserted into the storage

[4] Fly ash type II, Japanese product.

container and kept in the control room with a regular check. The storage condition was shown in Fig.III.1.D-2.

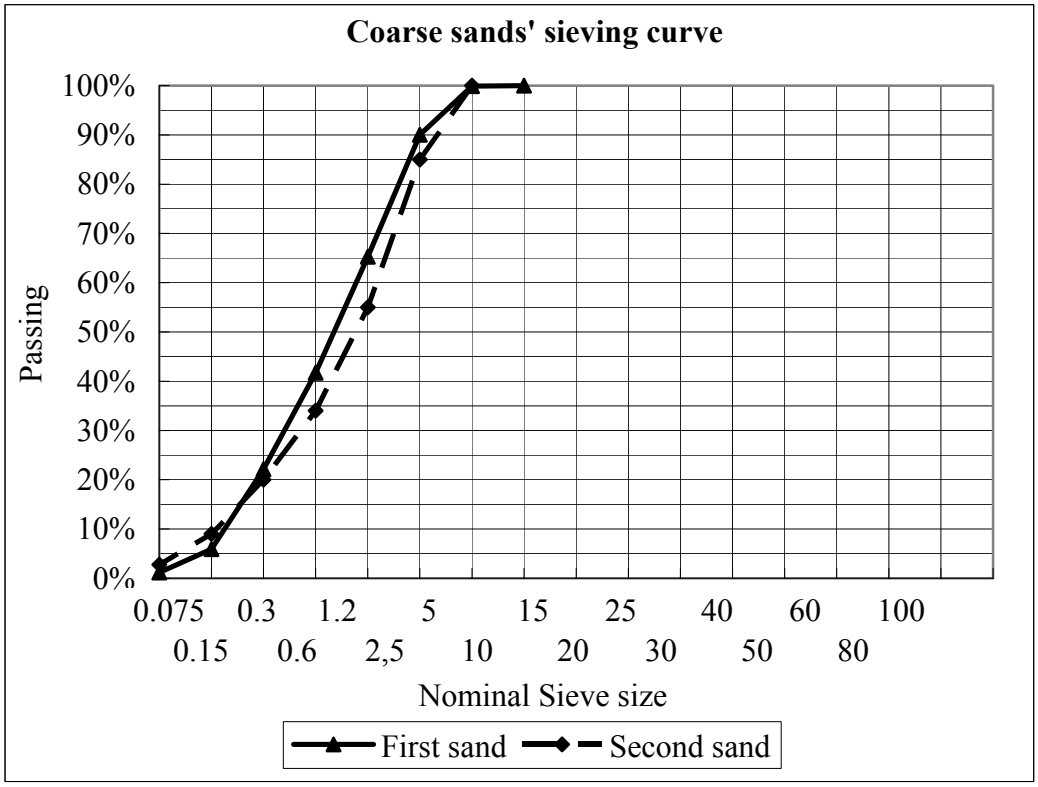

Fig III.1.D-1: Sieving curve of crushed sands

In this experimental works, sand as well as other materials were prepared and kept in a room with well-controlled conditions. The room condition was always maintained at temperature 20^{o}C and at RH=60%. In this condition, the remarkable problem was the early evaporation of water from sand at the top part of the storage containers and the non-uniform water content was observed between the top and the bottom of sand container.

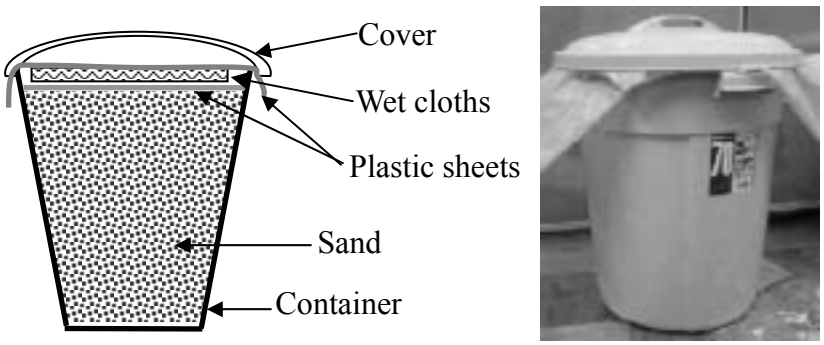

Fig III.1.D-2: Storage condition of sand

A solution was to put two separate sheets of plastic between which exist some wetted cloths at the top of sand. This solution allows keeping sand for a long time without changing its water content but cares had to be taken to prevent the wetted cloths from drying.

III.2. Mixer and mixing

Mixer is an apparatus in which materials of different types are uniformly mixed. The mixers are classified into 2 main types: batch mixers and continuous mixers. The first type produces concrete one batch at a time and the second type produces concrete at a constant rate. The mixer and mixing method are effective contributions to the concrete performance. Fig.III.2-1 shows the shape of the mixer used in this research. The mixer was a fixed cylinder inside which, there were 3 spatulas that turned around the axis of the cylinder. The maximum volume that can be mixed is 50 liters however all mixes were conducted with only 22 liters (for 12 specimens).

Fig III.2-1: Mixer

Mixing is an operation in which three stages including loading, mixing and discharging are successfully completed. In loading stage, some components are introduced in an order which is believed to affect good concrete properties. Mixing can be divided into dry mixing and wet mixing. Paillere (1990) concluded that the delayed addition of high range water reducer admixture (HRWRA) leads to a better dispersion of cement. So in order to achieve good dispersion, super-plasticizer was input one minute after water introduction. Cares should be taken during discharge in order to prevent segregation. Before mixing, all the necessary materials were correctly dosed and kept aside the mixer with covers to prevent eventual evaporation or desiccation. ASTM C192 suggests that a plastering mix of the same proportion as the main mix should be made in order to compensate the effect of material consumption by

apparatuses.

The materials were introduced in the following order:

1. Sand
2. Cement (or/and powder)
3. Water
4. SP (super-plasticizer)

The mixing was processed following the order of material introduction. Sand and powder were uniformly introduced into the mixer and blended in 30s. Then water was added and mixture was done for 60s, stopped for 15s rubbing spatulas and SP was added if SP was used before continuing mixture until unloading. The mixing duration which is considered from water introduction time to unloading time were varied from 2 minutes to 10 minutes.

III.3. Curing conditions

Curing is defined as a technique in which the essential care is to keep moisture and temperature of specimens during periods of time at an age for some specified conditions. The moisture is presented by a moisture status (water supply, water loss or no water exchange) and a speed of moisture exchange, at the same time the temperature is specified by a temperature status and a temperature rate. In addition, different moistures and temperatures can be applied in some separate periods of time.

Fig III.3-1: Curing methods: wet curing and seal curing

In this research, sealed curing and wet curing conditions were applied. All specimens which are sealed-cured are stored in the temperature control room with a relative humidity 60% and a temperature 20^{o}C until the test age. The specimens, which are wet-cured, are kept in water tank with constant temperature 20^{o}C until the test age.

III.4. Testing methods

Real compressive strength is obtained when a specimen is ruptured under uniaxial loading and fracture types are columnar, this happens to the case of free effect of end restrain between specimen surfaces and the machine platens however in practices, the often rupture type is conical. This means that conventional strength tested is not real but lower compared to the real strength. The following shows how strength testing is affected by other factors.

III.4.A. Sampling, specimen size and age

After unloading mortar, slump or slump flow were measured then poured into moulds. The moulds were cylindrical of 100 mm diameter and 200 mm height and made of plastics.

Some researchers had investigated the effect of specimen size on strength and gave some useful conclusions. Gonnerman, H.F (1925) claimed that the compressive strength of concrete decreased with the increase of specimen size. Neville, A.M. (1987) identified rupture types affected by platen size and specimen size due to the platen restrain. The cylinder is a better specimen than a cube because of less end restrain and more uniform distribution of stress. According to some technical reports, the smaller specimen size would induce the higher platen restrain which increased the difference between the conventional strength and the real strength however the specimen of high strength must have a limited size because of limit of machine capacity. Owing to the restriction of machine capacity and the ability to obtain the least end restrain, the cylinder100x200 should be decided.

3 specimens were sampled for one age of strength test. The 7^{th} day and 28^{th} day ages were used for series of mixes conducted for investigating sand content effect, dispersion effect and mixing time effect. These series were fundamental experimental works because they were used to investigate the ideal condition of mixes and then to determine the mixes which had components dispersing almost in the same manner as assumed in the microstructure and multi-heat models. The ages 7^{th}, 14^{th}, 28^{th} and 91^{st} days were used for strength modeling whose purpose was to be able to predict both early and long-term strengths.

III.4.B. Surfacing

End surfaces of a specimen have to be horizontal and perpendicular to the axe of the specimen during strength testing. The inclination of end surfaces were believed to cause the deviation of strength values among a set of 3 specimens and give a value lower than the real one. Three methods have been often reported effective in avoiding the effect of friction between end surfaces and the platens. This effect affected the rupture type and strength. The first method is

to use pure sulfur, a sulfur-sand mix or early strength mortar to cap both end surfaces of specimen. Due to the strength limit of capping materials, the method is suitable for normal strength testing. The second method is to use a bearing cap which can remove the friction by simply putting between the specimen surface and the platen. The third method in which a grinder machine is used to grind the end surfaces can be simply and reliably operated. According to some experienced engineers, the comparison among the 3 methods shows that the third one is the most reliable and suitable in this research. The grinder machine, as can be seen in Fig.III.4.B-1, can be used to grind three specimens at a time however in this experimental works, one specimen at a time was ground because some workers reported that grinding 3 specimens at a time would not offer a horizontal plane surface. Both top and bottom surfaces of specimens were ground.

Fig III.4.B-1: Grinder machine

III.4.C. Compressive strength test

Shimadzu Testing Machine was used to test compressive strength. The machine has a capacity of 1000 kN which corresponds to the possible maximum stress of 127 MPa as 100x200 cylinders were used. The test operation was ordered with an automatic mode and a constant stress speed of 0.21MPa/sec that was in the range recommended by ASTM-C39-96 standards. This stress speed was kept constant for all tests. Specimens were placed centrally onto the bottom plate carved with central guidelines. The top plate was then slowly moved downward to contact the specimen top surface. The specimen was covered with a security cylindrical cover to protect exploded debris. When preparation was ready, loading was started. One

strength point was the average of three specimens which showed a small deviation.

Fig III.4.C-1: Universal testing machine

CHAPTER IV: MIX PROPORTIONING

IV. Mix proportioning

The mix proportion is the first operation taken in a mix design which is aimed to find a proportion correspondent to an imposed requirement including fresh properties (workability) and hardened properties (strength and durability). It is aimed only to calculate quantities of all components. Basing on one cubic volume balance, a mix proportion must respect to eq.35.

$$V_V + V_W + V_C + V_P + V_S + V_g = 1 \quad \text{.....eq. 35}$$

Where the indexes V, W, C, P, S and g represent respectively void, water, cement, powder, sand and coarse aggregate.

IV.1. Fundamental proportioning

The mix proportion is defined in the manner that all components form one cubic meter, so the amount of a component depends on the others. If one component increases (decreases), another or others decrease (increase).

The following symbols are used for fundamental mix proportioning:

a) *w/c*: this is believed to play an important role in strength development and porosity. The higher w/c, the more porous and then the weaker strength.

b) w/p: the water-powder ratio is used instead of w/c when powder other than cement is used. Even powder is not reactive (latent-hydraulic or pozzolanic), the presence of powder increases degree of hydration by giving more surface area.

c) W: water content is an important index for workability, strength and durability.

d) s/a: this is a ratio of sand in volume compared to total aggregate volume (sand and coarse aggregate), it is defined basing either on strength or workability. This is equal to 0.45 for the best workability with Japanese materials. It can also be defined basing on many other methods including: Bolomey, Fuller, Faury…These methods aim to determine a ratio s/a with a proposed optimum line considering that sand-aggregate will give a mix with

less porosity. s/a can be calculated numerically using packing density theory proposed by Francois De Larrard (1999) [3].

Symbols for Physical properties and compositions

- ρ_c: specific gravity of cement in g/cm^3.
- ρ_s: specific gravity of sand in g/cm^3.
- ρ_g: specific gravity of coarse aggregate in g/cm^3.
- ρ_{pi}: specific gravity of powder i in g/cm^3.
- R_{pi}: replacement ratio of powder i in weight.
- *w/p*: water-powder ratio in weight.
- *w/c*: water-cement ratio in weight.
- W: water content in kg.
- C: cement weight in kg
- P: total powder weight in kg including cement.
- P_i: weight of powder i in kg excluding cement.
- V_{Pi}: volume of powder i in m^3.
- S, G: sand and coarse aggregate weight respectively in kg
- p_a: assumed entrapped air in %.
- *s/a* sand-aggregate ratio in volume.

Using the equation (35), the proportion is calculated either by weight or by volume; the following is given in weight:

✧ In case that only cement is used as powder,

The known parameters are: W, w/c, s/a, p_a, and physical properties of concerned materials. The unit of weight is in kg and that of volume is in m^3.

$$C = \frac{W}{(w/c)};\quad W = (w/c).C \qquad \text{.....eq. 36}$$

$$S = (s/a).1000.\rho_s.\left[1 - \frac{p_a}{100} - \frac{W}{1000} - \frac{C}{1000.\rho_c}\right] \qquad \text{.....eq. 37}$$

$$G = (1-(s/a)).1000.\rho_g.\left[1 - \frac{p_a}{100} - \frac{W}{1000} - \frac{C}{1000.\rho_c}\right] \qquad \text{.....eq. 38}$$

✧ In case that other powders are used with cement,

$$P = \frac{W}{(w/p)}; \quad W = (w/p).P \quad \text{.....eq. 39}$$

$$S = (s/a).1000.\rho_s.\left\{1 - \frac{p_a}{100} - P.\left[\frac{1-\sum R_{pi}}{1000.\rho_C} + \sum\frac{R_{pi}}{1000.\rho_{pi}} + w/p\right]\right\} \quad \text{.....eq. 40}$$

$$G = (1-(s/a)).1000.\rho_g.\left\{1 - \frac{p_a}{100} - P.\left[\frac{1-\sum R_{pi}}{1000.\rho_C} + \sum\frac{R_{pi}}{1000.\rho_{pi}} + w/p\right]\right\} \quad \text{.....eq. 41}$$

$$P_i = P.R_{pi}; \quad V_{pi} = \frac{P_i}{1000.\rho_{pi}} \quad \text{.....eq. 42}$$

$$C = P - \sum P_i \; ; \quad V_C = P.\frac{1-\sum R_{pi}}{1000.\rho_C} \quad \text{.....eq. 43}$$

IV.2. Mortar in concrete

As coarse aggregate affects strength of concrete by its size, texture and strength so in order to avoid the coarse aggregate effect, it should be extracted, the mix becomes then a mortar. In this paper, mortar mixes which were used are all calculated by taking from concrete of normal ranges. A pair of concrete and mortar was defined basing on the same void percentage between concrete and mortar. To define a pair concrete-mortar, the composition diagram on Fig.IV.2-1 was drawn.

Symbols

V_C: unit volume of cement in concrete
V_S: unit volume of sand in concrete
V_G: unit volume of coarse aggregate in concrete
C: unit weight of cement in concrete
C_M: unit weight of cement in mortar
S: unit weight of sand in concrete
S_M: unit weight of sand in mortar
P_i: unit weight of powder i in concrete
P_{iM}: unit weight of powder i in mortar
V_{Pi}: unit volume of powder i in concrete
V_{PiM}: unit volume of powder i in mortar
W: unit water in concrete
W_M: unit water in mortar

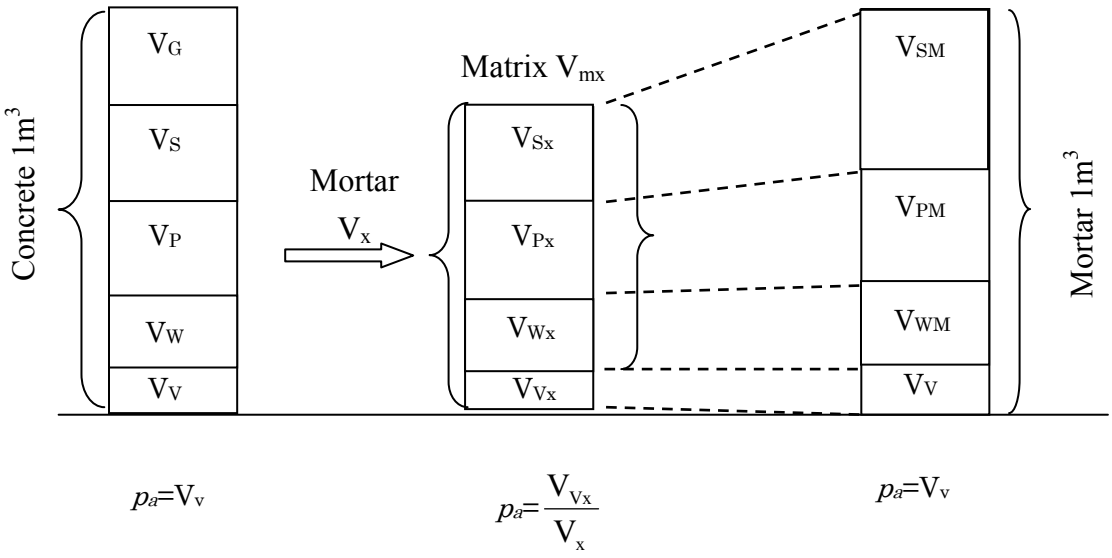

Fig IV.2-1: Representation of components of a pair concrete-mortar (C-M)

✧ In case that only cement is used

From concrete to mortar, the following formulae are used:

$$V_{SM} = V_S \frac{1 - p_a/100}{1 - V_{CA} - p_a/100} \quad \text{.....eq. 44}$$

$$V_{CM} = V_C \frac{1 - p_a/100}{1 - V_{CA} - p_a/100} \quad \text{.....eq. 45}$$

From mortar to concrete, the following formulae are used:

$$V_C = V_{CM} \frac{1 - p_a/100}{\frac{S_M}{(s/a)\rho_S.1000} + \frac{C_M}{1000.\rho_C} + \frac{W_M}{1000}} \quad \text{.....eq. 46}$$

$$V_S = V_{SM} \frac{1 - p_a/100}{\frac{S_M}{(s/a)\rho_S.1000} + \frac{C_M}{1000.\rho_C} + \frac{W_M}{1000}} \quad \text{.....eq. 47}$$

$$V_G = (1 - s/a).\left[1 - p_a/100 - \frac{C}{1000.\rho_C} - \frac{W}{1000}\right] \quad \text{.....eq. 48}$$

✧ In case that powders other than cement are used

From concrete to mortar, the following formulae are used:

$$V_{SM} = V_S \frac{1 - p_a/100}{1 - V_{CA} - p_a/100} \quad \text{.....eq. 49}$$

$$V_{CM} = V_C \frac{1 - p_a/100}{1 - V_{CA} - p_a/100} \quad \text{.....eq. 50}$$

$$V_{PiM} = V_{Pi} \frac{1 - p_a/100}{1 - V_{CA} - p_a/100} \quad \text{.....eq. 51}$$

From mortar to concrete, the following formulae are used:

$$V_C = V_{CM} \frac{1 - p_a/100}{\frac{S_M}{(s/a)\rho_S.1000} + \frac{C_M}{1000.\rho_C} + \sum \frac{P_{iM}}{1000.\rho_{Pi}} + \frac{W_M}{1000}} \quad \text{.....eq. 52}$$

$$V_{Pi} = V_{PiM} \frac{1 - p_a/100}{\frac{S_M}{(s/a)\rho_S.1000} + \frac{C_M}{1000.\rho_C} + \sum \frac{P_{iM}}{1000.\rho_{Pi}} + \frac{W_M}{1000}} \quad \text{.....eq. 53}$$

$$V_S = V_{SM} \frac{1 - p_a/100}{\frac{S_M}{(s/a)\rho_S.1000} + \frac{C_M}{1000.\rho_C} + \sum \frac{P_{iM}}{1000.\rho_{Pi}} + \frac{W_M}{1000}} \quad \text{.....eq. 54}$$

$$V_G = (1 - s/a).\left[1 - p_a/100 - \frac{C}{1000.\rho_C} - \sum \frac{P_i}{1000.\rho_{Pi}} - \frac{W}{1000}\right] \quad \text{.....eq. 55}$$

In the data discussion, the authors use the notation type xM-CWy-SPz which means the mortar taken (by calculation) from concrete of w/p=x, water content=y and SP dosage=z. For example, 0.3M-CW210-SP06 means the mortar in concrete of w/p=0.3, water content = 210 liters and SP dosage=0.6%.

CHAPTER V: DATA DISCUSSION

V. Data discussion

This section describes the experimental works and its interpretation in order to find the suitable mixes for modeling which will be presented in the next section. Sand content effect, SP effect and mixing time effect were interrogated. In addition to the findings of ideal mixes of cement without powders, the effect of limestone powder was therefore studied and ideal mixes for powders were concluded.

V.1. Strength and sand content

Sand as well as coarse aggregate can affect strength if its content is increased. In this experimentation, mixes of different sand contents are made for different SP. The interaction between sand particles in mortars is also contributed by the thickness of paste that can retain its form around particle. The higher thickness of paste can surround sand particles, the lower sand volume can allow interaction between sand particles (see Fig.V.1.1). This can explain the reason why for high w/c, the critical volume of sand is higher than for w/c low.

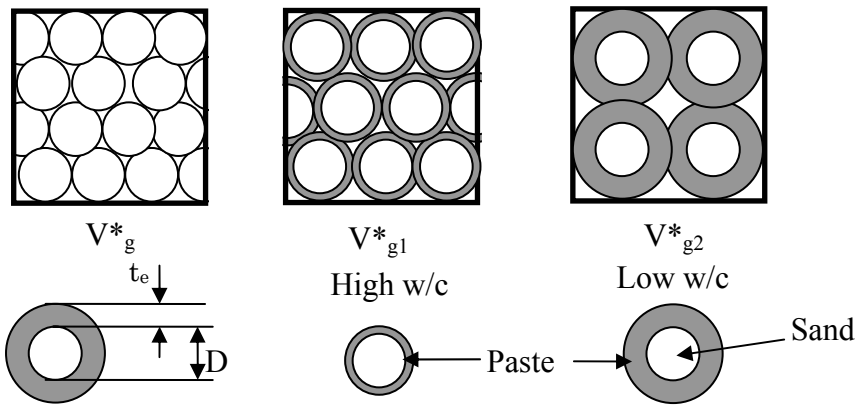

Fig V.1-1 Sand volume with different effective thicknesses of paste

According to Scrivener (1988) *et al*, aggregate is normally surrounded with a layer thick of 15mm-50mm called Interfacial transition zone (ITZ). The thickness of the zone is weak due to high porosity even it is filled with increasing hydrates as can be shown in Fig.V.1-2 and due to the presence of Ca(OH)2 crystallized with good cleavages in the ITZ. The high porosity was reported due to the localized bleeding happening after mixing. This weak layer even thin but constitutes the source of crack and fracture. Some researchers have

been interested in producing high strength and durable concrete by improving the ITZ with incorporation of silica fume. Bentur (1988) concluded that partial replacement of cement by silica fume increases strength in concrete but not in pastes. This shows that the ITZ has certainly an effect on strength.

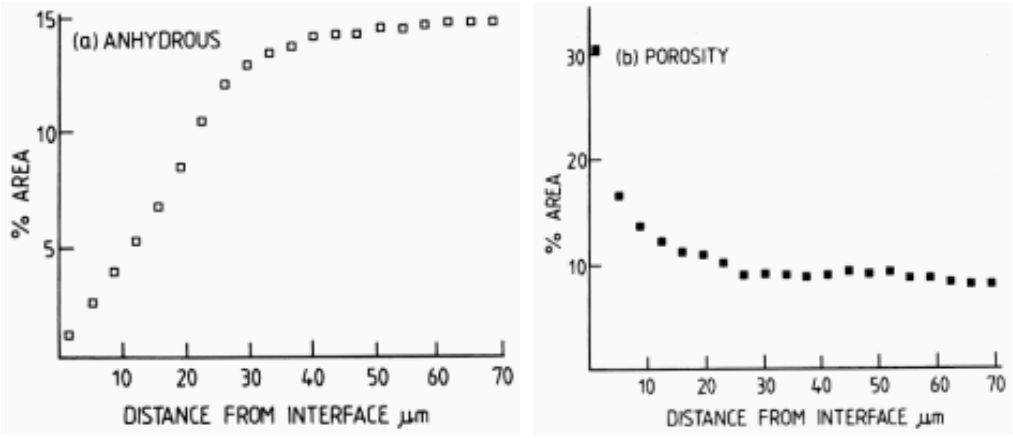

Fig V.1-2 Interfacial transition zone properties

As can be shown on Fig.V.1-3, two parts are distinguished, one is for sand volume less than 0.37 and another is for sand volume more than 0.37. Each line represents a series of mixes with one SP dosage corresponding to one level of dispersion. Sand effect plays different roles when the mix is at good dispersion, sand effect decreases strength however when the mix is at low dispersion, sand effect increases strength. This behavior is conserved by both 7 and 28 day strength.

With good dispersion (SP dosage=0.8%, see Fig.V.1-3), strength decreases as sand volume increases. This is explained by the presence of the interfacial zone around sand particles. The interfacial zone of 15-50 µm constitutes weak layers however cement matrix (in good dispersion) and sand are strong parts, so the increase of sand content will increases the amount of weak zones then implies the decrease of strength.

Contrarily, when the paste is not yet dispersed (SP dosage=0.3% and 0.6%, see Fig.V.1-3), the paste is a weak matrix and sand interfacial zones are weak as well, on the other hand, only sand is a strong part. So the increase of sand content will increase the strong parts in mix then strength increases.

As can be shown on Fig.V.1-4, the behavior of mixes with w/c=0.6 is the same as that of mixes with w/c=0.3. In order to find mixes free of sand content effect, for w/c=0.3, a mix of sand content equal to 0.38 should be used and for w/c=0.6, a mix of sand content equal to 0.52 should be used.

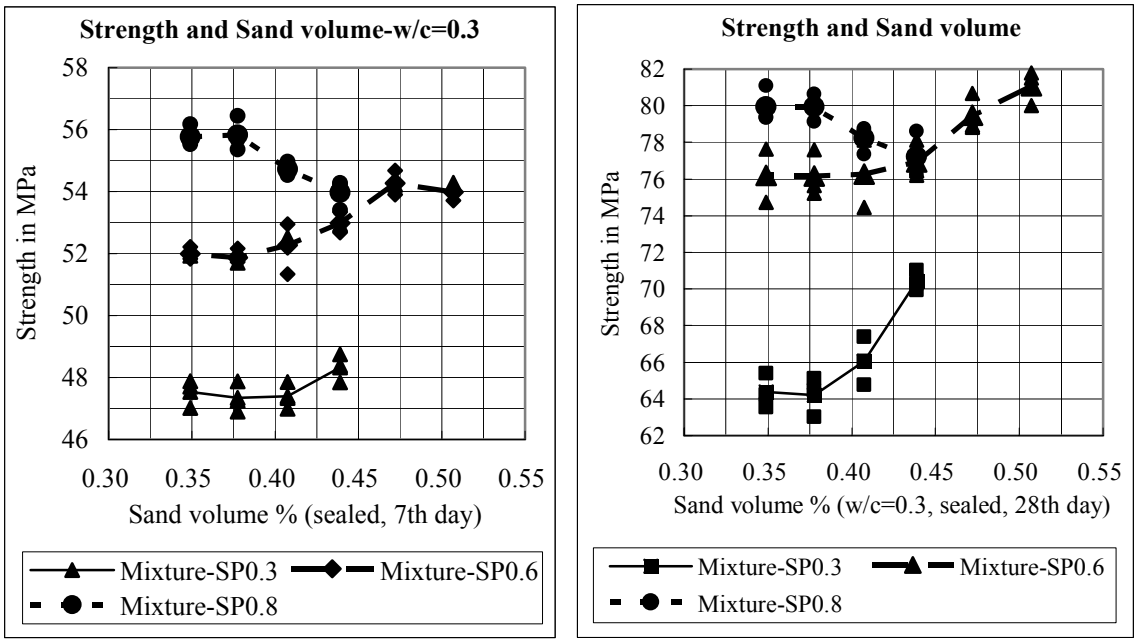

Fig V.1-3: Strength behavior versus sand content at different dosage of SP

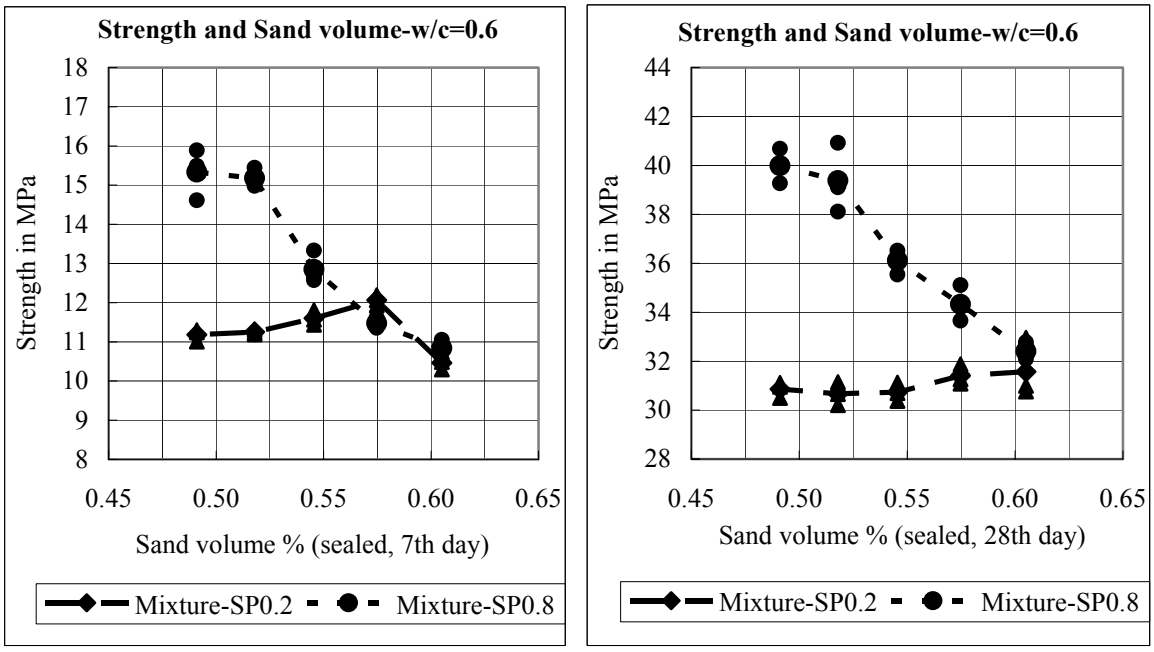

Fig V.1-4: Strength behavior versus sand content at different dosage of SP

The critical volume of sand that can affect strength is different for different w/c, this is due to the effective thickness of paste around sand particles are different (see Fig.V.1-1). For low w/c, the paste is stronger and then the effective thickness is thicker than for high w/c. As illustrated on Fig.V.1.1, critical volume of sand for low w/c is lower than for high w/c and the experimental results are confirmed.

In conclusion, there existed a critical volume for a given w/c, and the increase of sand volume higher than V_{cr}, strength variation would be affected according to the dispersion levels. The critical volume were found 0.38 for w/c=0.3 and 0.52 for w/c=0.6.

V.2. Strength and dosage of SP

As dispersion is a status of well spaced particles of cement, this implies that higher dispersion (see Fig.V.2-1) will give higher hydration and then higher strength, so dispersion and strength are two parallel terms. In this study, for w/c=0.3 all mixes have the same sand content (0.38) and the degree of compaction are all the same range (0.99). For w/c=0.6, all mixes have the same sand content (0.52) and the degree of compaction are all the same range (0.99-1.00).

As can be seen on Fig.V.2-2 and V.2-3, strength shows a particular relation with dosage of SP. There exists an amount of SP which is absorbed by cement and it can not disperse cement. For the range of absorbed SP, strength does not increase. When SP is higher than the absorption amount, SP plays a role in dispersing cement particles and then increases strength of the mix, this increase continues until a maximum point where mix's particles are well dispersed and after which there is a tendency to segregation. The segregation is well shown by a fall in Fig.V.2-3 (data of mixes w/c=0.6).

From data shown on Fig.V.2-2 and V.2-3, the maximum dispersion should be obtained by mixing with SP 1.0% for both w/c=0.3 and w/c=0.6.

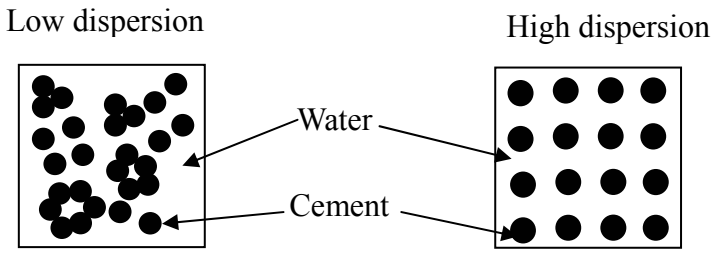

Fig V.2-1: Status of cement particles in case of low and high dispersion

The dosage of SP absorbed on cement particles is called non-effective SP (NESP) and it is equal to 0.3% (see Fig.V.2-2). This SP is not active in dispersing cement particles apart. This means that this dosage does not depend on cement compounds but powder content.

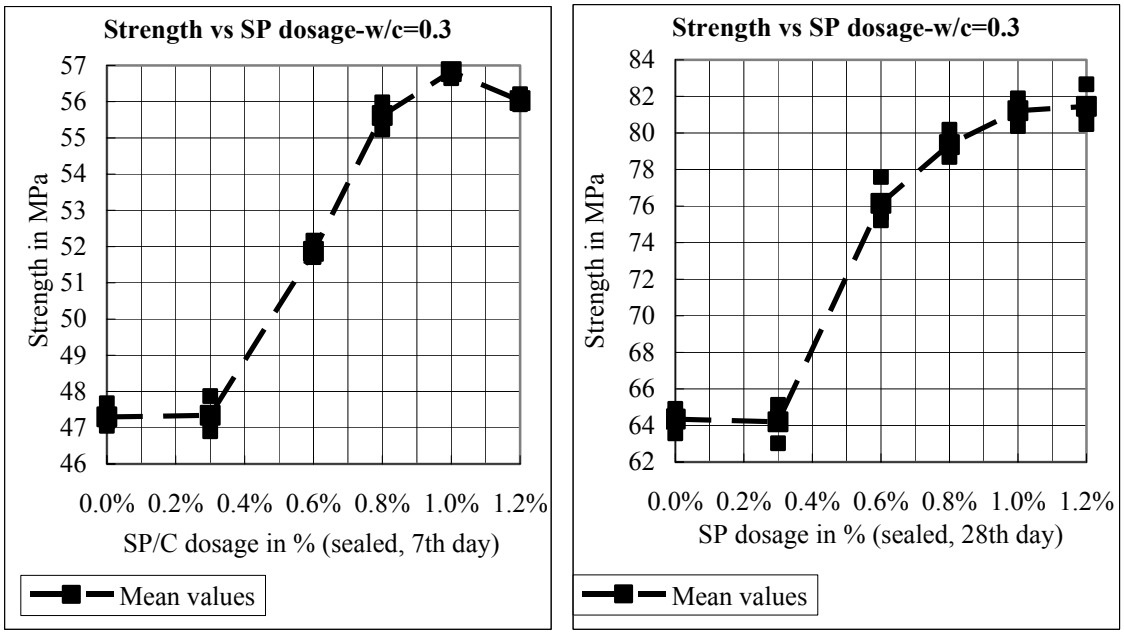

Fig V.2-2: Strength behavior versus dosages of SP (w/c=0.3)

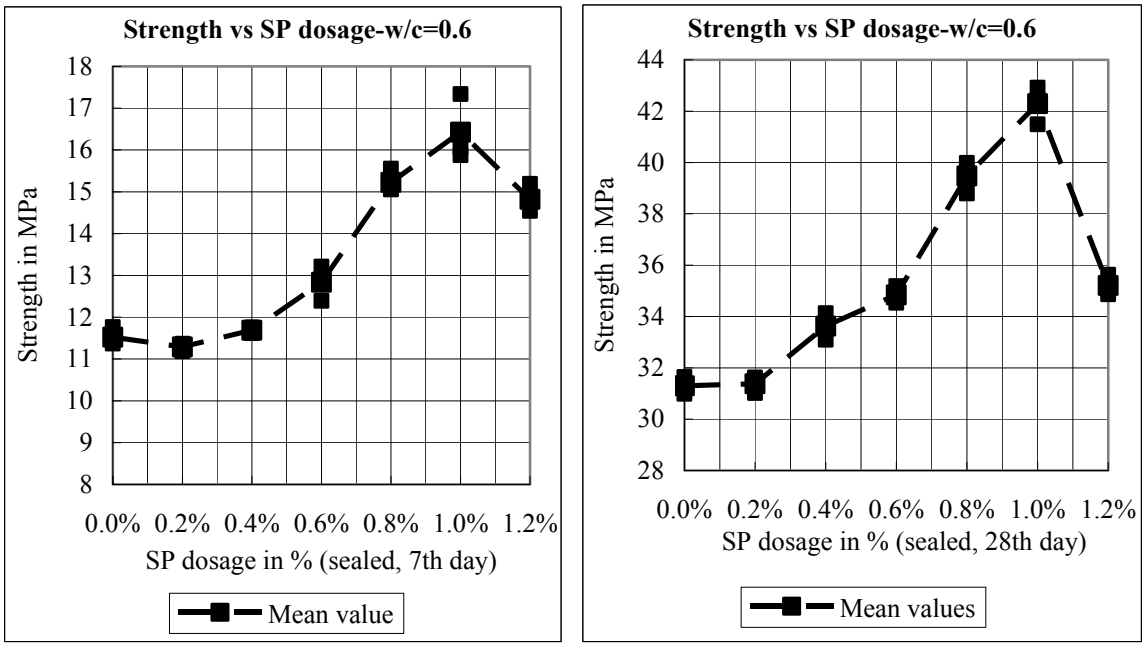

Fig V.2-3: Strength behavior versus dosages of SP (w/c=0.6)

The difference of SP dosage between the absorbed SP and the SP of any mix is called effective SP (ESP) for that mix. This SP plays an active role in dispersing particles. The activity of SP is formed by the increase of electro-chemical surface charge on cement particles, ESP dosage depends only on chemical compounds. For example, the effective SP for maximum dispersion is equal to 0.7% (total SP=1.0% for maximum dispersion, see Fig.V.2-2).

The non-effective was found the same for different w/c ratios and either is the effective SP for the maximum dispersion.

Table V.2-1: SP maximum effect for different w/c

w/c	Strength in MPa on 7th day			Strength in MPa on 28th day		
	Min	Max	SP effect	Min	Max	SP effect
0.3	47.3	56.83	9.53	64.3	81.2	16.9
0.6	11.52	16.43	4.91	31.3	42.29	10.99

It is remarkable that for w/c=0.3, the increase of strength played by SP is 9.53 MPa (7^{th} day), 16.9 MPa (28^{th} day) and for w/c=0.6, 4.91 MPa (7^{th} day), 10.99 MPa (28^{th} day) (see table V.2-1). This means that the effect of SP depends on w/c, the lower w/c the higher dispersion effect. This may be explained that at high w/c, excessive water dispatches already some cement particles and at the same time reduces the effect of SP however at low w/c, water can not dispatches cement particles and much flocculation exists. If a lot of the flocculation is all dispersed, strength increase is high.

One often posed question is why the strength decreased after the maximum. The answer is based on the segregation caused by SP. SP can disperse cement particles but it will cause segregation if its dosage is higher than the optimum dosage. The manner how the segregation decreases strength can be illustrated in fig.V.2-4.

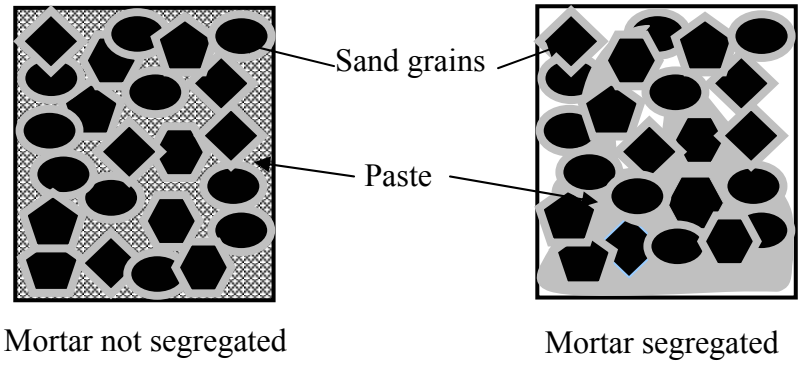

Fig V.2-4: Status of cement paste and sand particles in mixes with and without segregation

When the segregation does not occur, sand particles are uniformly surrounded and the inter-particle spaces are filled with cement paste however when the segregation occur, some inter-particle spaces are not filled and sand particles are not well surrounded with paste because sand particles are separated upwards from the cement paste settling downwards. The

separation of sand and paste makes the strength decreased. The strength decrease can be observed with experimental data in Fig.V.2-2 and Fig.V.2-3.

In conclusion, the maximum strength can be obtained with SP dosage=1.0% and the SP dispersion effect is higher when w/c is lower. This means the dispersion depends on w/c.

V.3. Strength and mixing times

The mixing time is an index of mixing power as a longer mixing time provides a higher mixing power. This is a mechanical power able to separate particles apart so that one kind of dispersion is obtained. This dispersion can be called a mechanical dispersion however SP can disperse cement particles by its chemical activity and its thickness absorbed on cement surfaces. It was found that the dispersion is dependent of w/c when w/c is high the cement particles can not keep the distance equally due to bleeding. The bleeding is a phenomenon by which the particles settle downwards at the same time that water moves upwards reducing the w/c of the mix.

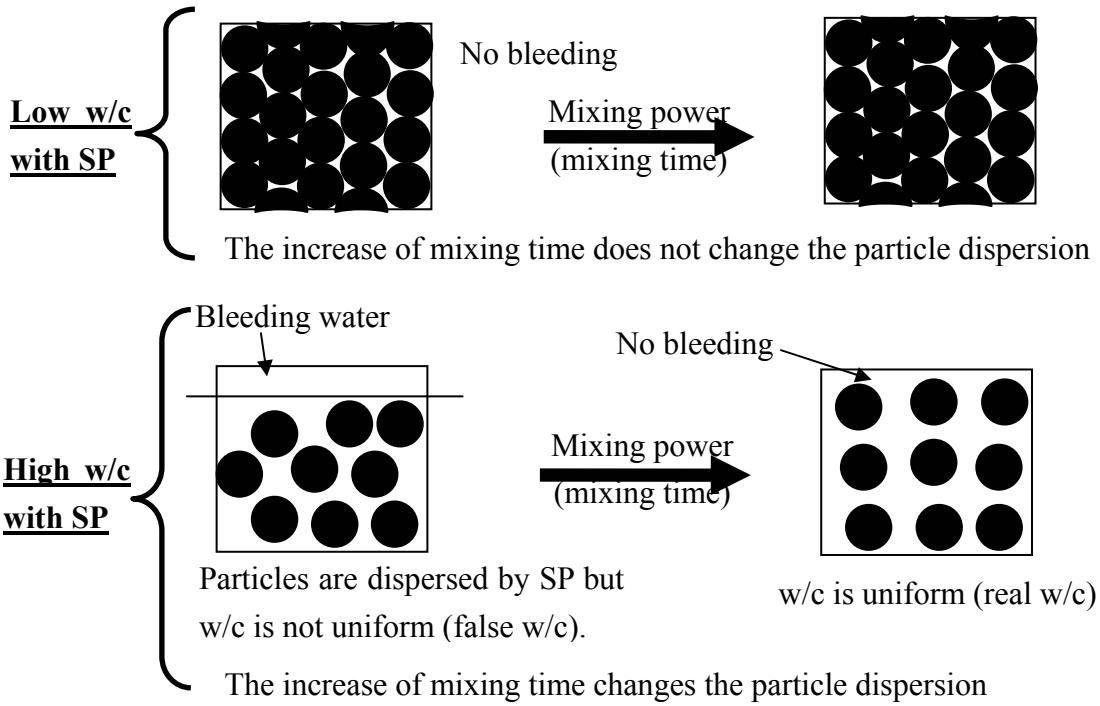

Fig V.3-1: Status of cement particles when the mixing time is increase

Fig.V.3-1 shows the situation of dispersed particles when the mixing time (MT) increases for low and high w/c. In case of low w/c, the particles that are already dispersed by SP do not show the change in its particle arrangement when MT increases. So the strength should not

change before and after increasing MT. However in case of high w/c, the particles are already dispersed with the existence of bleeding water. The bleeding water does not take part in the reaction and does not constitute the real w/c. When more mechanical powder is applied by increasing MT, the distance of particles are more dispatched and then bleeding is reduced at the same time the real w/c increases. The increase of w/c (up to the mixing w/c) leads to the decrease of strength. This explanation is justified by the following data.

As can be shown in Fig.V.3-2 for w/c=0.3 and in Fig.V.3-3 for w/c=0.6, the behavior is contradictory. For w/c=0.3, strength increases until the optimum mixing time = 3 minutes after which strength is found constant however for w/c=0.6 the increase of mixing time longer than 3 minutes shows the decrease of strength.

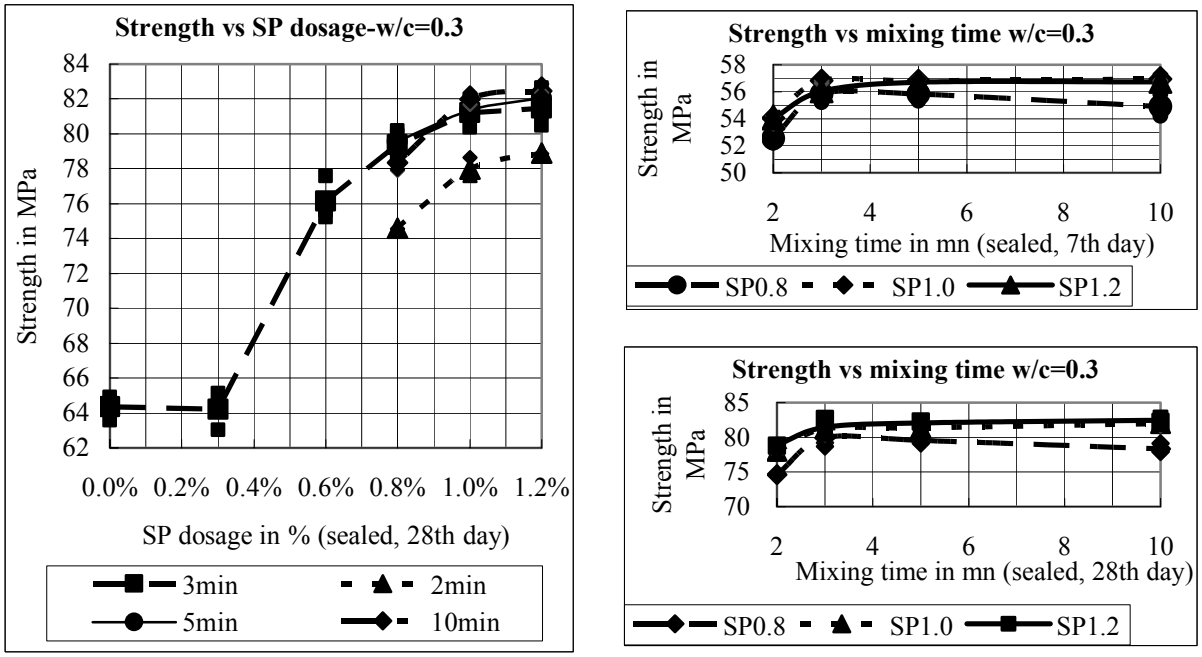

Fig V.3-2: Strength behavior versus mixing time and dosage of SP (w/c=0.3)

The hydration reaction can be represented with the following chemical equations:

$C_3A+6H \rightarrow C_3AH_6$ .....eq. 56

$C_4AF+2CH+10H \rightarrow C_3AH_6\text{-}C_3FH_6$ .....eq. 57

$2C_3S+6H \rightarrow C_3S_2H_3+3CH$ .....eq. 58

$2C_2S+4H \rightarrow C_3S_2H_3+CH$ .....eq. 59

Using the above chemical reaction equations, the water required for cement reaction is 23% and the water un-reacted and integrated in the structures of hydrates is 15% so the total water enough to supply reaction with cement is 38%. Compared with the w/c of these two

experimental works, w/c=0.3 is below the adequate amount of water, this means that there is no excess of water which may be a source of bleeding however w/c=0.6 is higher than the amount of water strictly needed by cement, this means some water is free from reaction and constitutes bleeding which may decrease the real w/c.

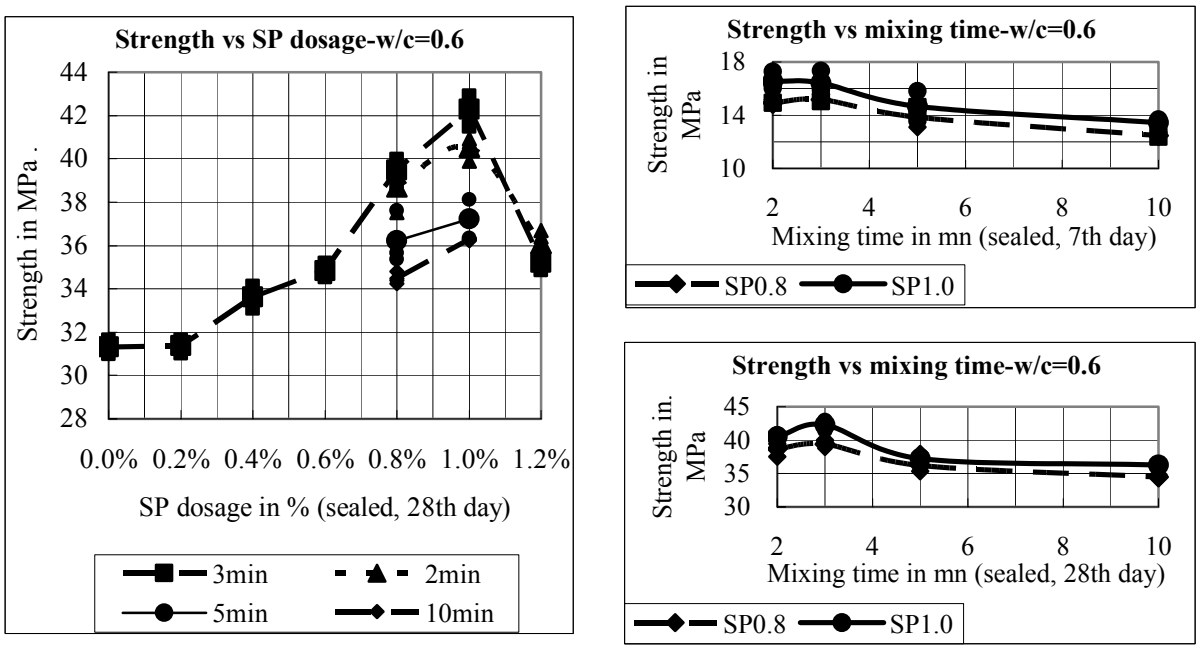

Fig V.3-3: Strength behavior versus mixing time and dosage of SP (w/c=0.6)

For w/c=0.3 at high SP dosage, the first increase of time below 3mn increases the strength, this may be explained that the presence of flocculation of cement at low mixing time is broken when the mixing time increases and that the water distributed to each cement particles becomes uniform at 3mn mixing time. After 3mn, the increase of mixing time does not increase strength this may be due to the uniformity of w/c that is kept even the mixing time is increased so strength is found constant as well, this can be seen on Fig.V.3-2.

For w/c=0.6 at high SP dosage, the range of mixing time 2-3mn gives strength nearly constant however, when mixing time increases strength is found decreased. The explanation is that the excessive water which bleeds at low mixing time and which does not bleed at high mixing time (see Fig.V.3-1) makes the real w/c different from the mixing w/c. As we know w/c=0.6 is higher than the required amount (0.38) for reaction, so $\Delta w/c=0.22$ is the excessive amount which causes bleeding then the real w/c becomes lower than the mixing one. When the mixing time is prolonged, the water continues to uniformly surround particles and then the real w/c increases by reducing bleeding; this decreases strength, as can be seen on Fig.V.3-3. The values of real w/c increase with the mixing times as can be seen in Fig.V.3-4.

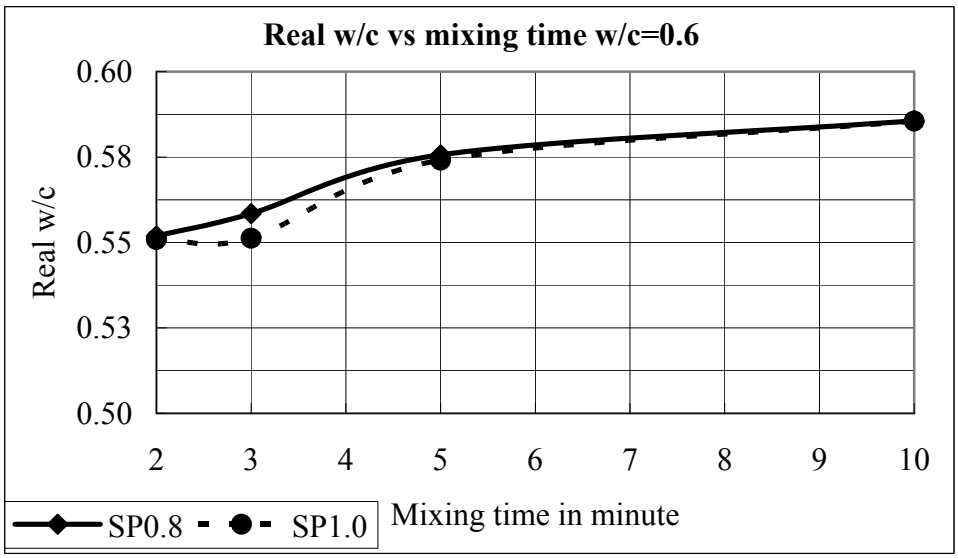

Fig V.3-4: Real w/c as function of mixing time (w/c=0.6)

In conclusion, the 10 min mixing time is the suitable for mixing due to its ability to reduce bleeding and to reach the real w/c. One more observation is that SP dosage=1.0% provides the maximum strength for different w/c and for different mixing times.

V.4. Strength behavior when limestone powder is used

A question was posed if dispersion of cement particles keeps the same when LS is used. LS is a powder of which very small amount can react with cement hydration products to give mono-carboaluminate $(CaO)_3(Al_2O_3).CaCO_3.11H2O$ and mono-sulfoaluminate $(CaO)_3.(Al_2O_3).CaSO_4.12H_2O$. LS can absorb some of SP even LS is believed not chemically reactive however according to recent research, LS was reported reacted with SP. The reaction mechanism was the absorption of SP on the surface of LS. Many engineers use LS as a filler that can replace un-hydrated particles.

The following experiments were mixes with limestone powder replacement ratio 20%. To study the strength behavior with different dispersing effect of SP, SP was calculated supposing that limestone powder reacted with SP by absorbing SP around itself. SP/P were 0.70%, 0.86%, 1.02%, 1.18% and 1.34%, these values were calculated from mixes without LS for SP/C=0.8% (ESP=0.5%), SP/C=1.0% (ESP=0.7%), SP/C=1.2% (ESP=0.9), SP/C=1.4% (ESP=1.1%) and SP/C=1.6% (ESP=1.3%) making assumption that LS absorb SP the same amount as cement (eq.60).

$$\frac{SP}{P} = NESP + ESP.\frac{C}{P} \quad \text{.....eq. 60}$$

In the formula, P is powder including cement and non-hydraulic powder and ESP and NESP (0.3%) are defined in Section V.2. The corresponding values of SP dosage with and without LS were listed in Tab.V.4-1.

Table V.4-1: SP dosage with and without LS

Mix type	Dosage of SP/P in %				
SP/C (no LS)	0.8	1.0	1.2	1.4	1.6
ESP	0.5	0.7	0.9	1.1	1.3
SP/P (with LS)	0.7	0.86	1.02	1.18	1.34

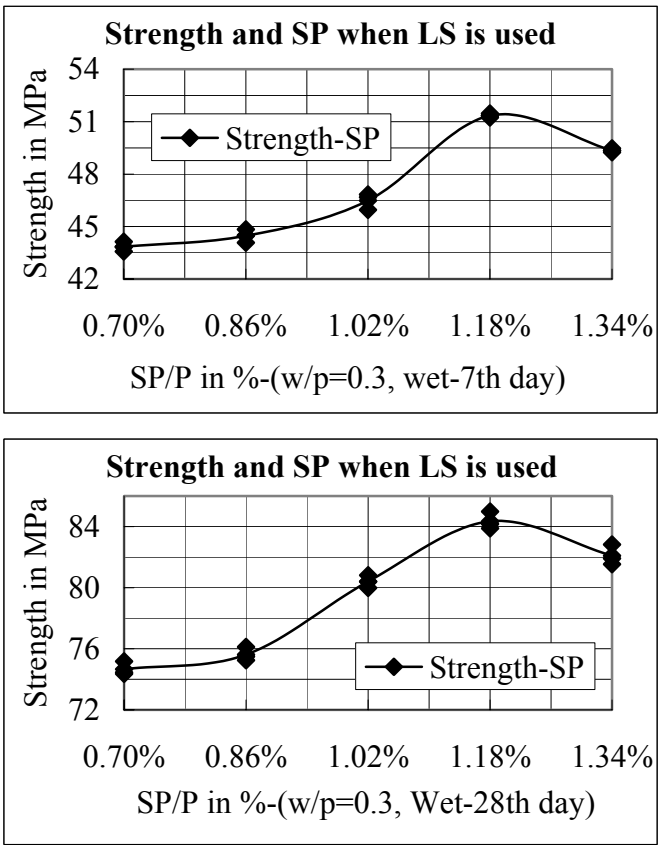

Fig V.4-1: Strength behavior versus SP/P for 20% LS replacement

As can be seen on Fig.V.4-1, the maximum strength was reached with 1.18% of SP/P when limestone powder was used. This optimum dosage was higher than 1.0% in the case without limestone. This may be due to the reason that limestone powder absorbed some SP and made SP lacked for cement dispersion and when all LS particles absorb SP on their surface at SP/P=0.86% (inflexion point), more SP will disperse LS particles. This is the reason why when LS was used, SP dosage needed to increase to attain the maximum strength.

The dispersion of cement and LS can be more explained in the following detail. The dosage SP/P=0.86% corresponded to SP/C=1.0% without LS, the case of maximum dispersion of cement. The increase of SP implied a decrease of strength in mixes without LS however in mixes with LS the increased SP dosages until 1.18% implied the increase of strength (see Fig. V.4-2). This may be explained with the filling of LS between cement particles after cement was well dispersed at SP/P=0.86%. At SP/P=0.86%, cement particles were dispersed with a limited space into which LS particles could not fill however when SP increased more than SP/P=0.86% (in case of LS replacement), cement particles (without LS) dispersed and tended to segregate and gave spaces for LS fillers. The filling of LS was confirmed until SP/P=1.18% where strength was found maximum after which the cement paste (without LS) was severely segregated and then LS powder (in case of LS replacement) was expulsed upwards and cement particles settled downwards, the strength were then reduced.

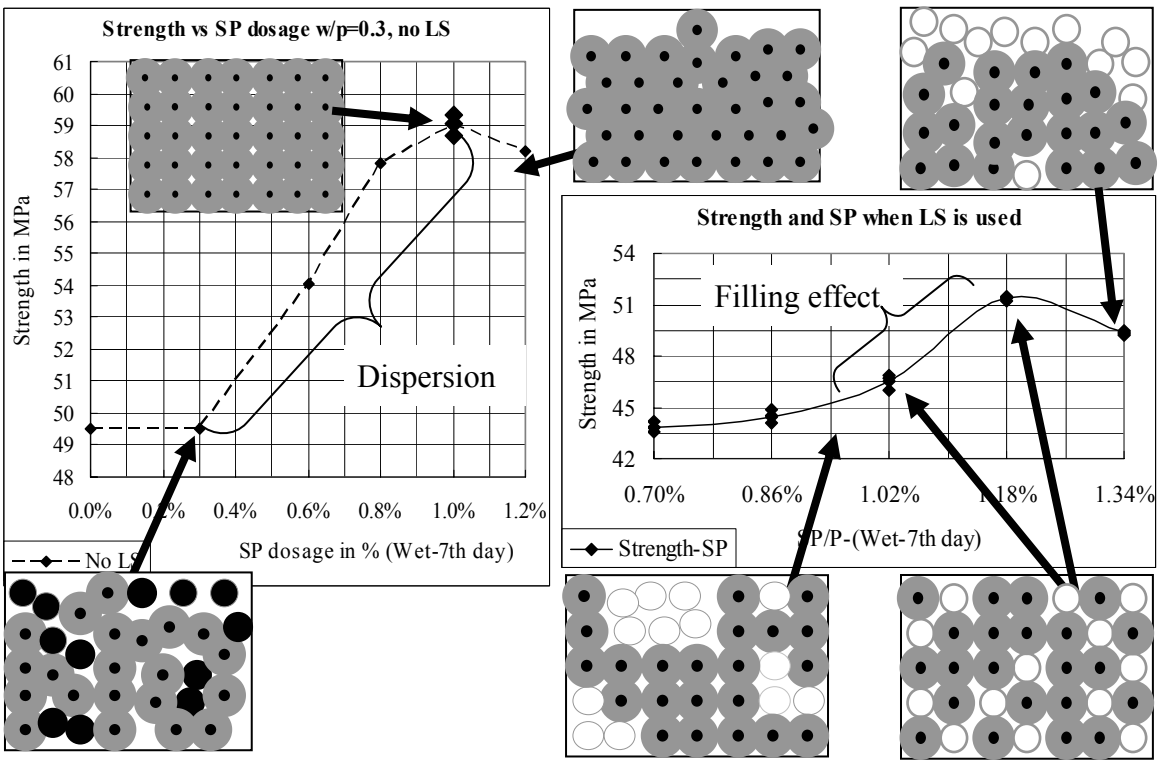

Fig V.4-2: Strength behavior versus SP/P for mixes with and without limestone powder replacement

It was also shown on Fig.V.4-2 that the maximum strength for LS replacement case was comparable to the strength of mixes without LS and at SP/C less than 0.3% where the dispersion was not confirmed and the un-hydrated existed. This means that LS in well dispersed mixes could be used instead of some un-hydrated cement to save money spent for the same strength achievement. Bentz (2005) [15] concluded that LS powder could replace

the coarse grains of cement in low w/p.

From this series of experiments, the mix 03M-CW210LS20SPP1.18 had the particles that were dispersed and was the ideal mix, so it would be used as a model mix in the microstructure and multi-component heat models.

More mixes were done for the same powder replacement ratio and different w/p (0.6 and 0.45). The results were illustrated on Fig.V.4-3 and V.4-4 (see table.VIII.1-6 and VIII.1-7). According to the data for w/p=0.3, the attempt in finding the mix of high dispersion was to add SP at dosages around the strength peak. For w/p=0.45, the dosages of SP/P were 0.86%%, 1.02% and 1.18%. The higher dosage of SP lead to a severe segregation and the mix was not practically handled. As can be seen in Fig.V.4-3, two mixes were found of similar strength, they were: the mix with SP/P=1.02 and the mix with SP/P1.18.

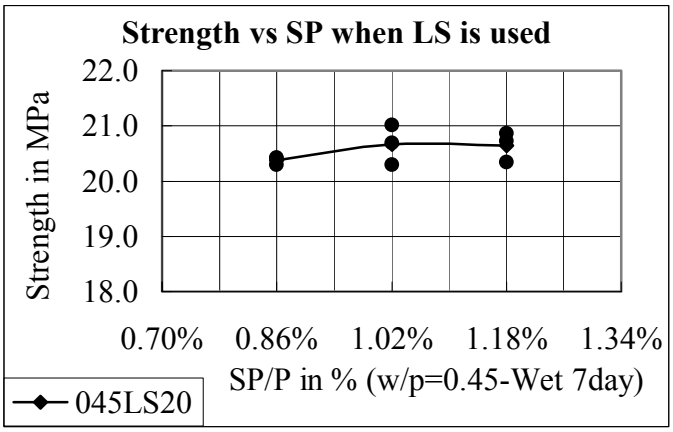

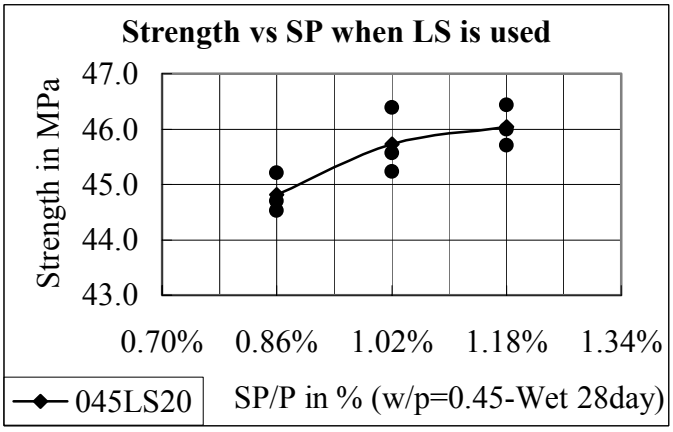

Fig V.4-3: Strength behavior versus SP/P for w/p=0.45 and 20% LS replacement

The maximum strength was attained with SP dosage lower than the one required in case of

w/p=0.3. So the model mix should be conducted with SP/P=1.02.

In case of a series of mixes w/p=0.6, SP/P were 1.02%, 1.18% and 1.34%, the strength was found maximum at the dosages SP of 1.18% and 1.34%. The same manner as for w/p=0.45 and w/p=0.3, the mix with SP/P=1.18% should be the model mix.

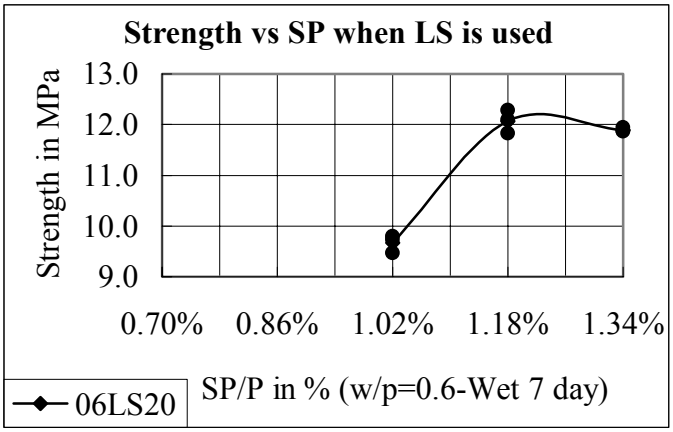

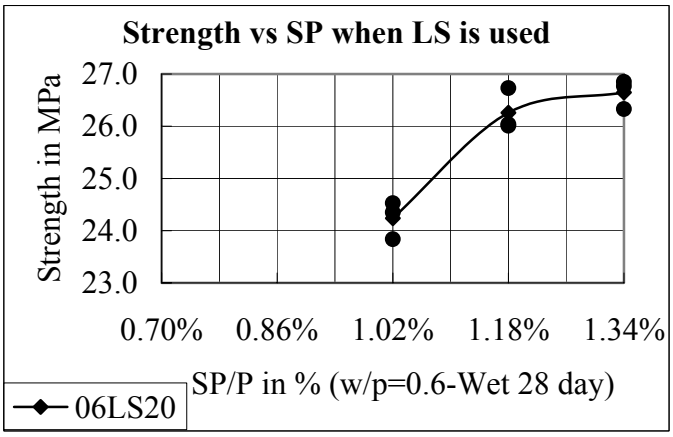

Fig V.4-4: Strength behavior versus SP/P for w/p=0.6 and 20% LS replacement

In conclusion, LS affected the requirement dosage of SP providing the maximum strength and that SP dosage is SP/P=1.18% for different w/p. LS was found able to absorb SP as have been reported by Sakai 2003.

CHAPTER VI: MODELING

VI. Modeling

In the previous section, mixes were conducted in order to find the mixes ideal to the microstructure and heat multi-component models. The porosity, heat developments of all ideal mixes were calculated with the formulae given in the microstructure and heat multi-component models which were combined and programmed in Fortran. In this section, the first task is to find reliable parameters determining strength development before taking the next step in proper modeling.

VI.1. Ideal mixes and their properties

After the investigation of sand content effect, SP dosage effect and mixing time effect, the ideal mixes were found for LH cements. More ideal mixes were made using HES cements and OPC cements for wet and seal curing conditions, the strength test results were shown in table VI.1-1, VI.1-2 and VI.1-3.

Table VI.1-1: Strength of ideal mixes with LH

		Strength in MPa			
Mix name	SP/C	7^{th} day	14^{th} day	28^{th} day	91^{st} day
045M-CW210-wet	1.0%	27.75	42.50	61.32	83.13
045M-CW210-seal	1.0%	33.89	45.33	56.53	78.14
06M-CW195-seal	1.0%	13.4	-	36.28	-
06M-CW195-wet	1.0%	13.90	23.40	38.73	50.30
03M-CW210-seal	1.0%	56.95	-	81.97	-
03M-CW210-wet	1.0%	59.02	77.33	100.19	116.35

Table VI.1-2: Strength of ideal mixes with OPC

		Strength in MPa			
Mix name	SP/C	7^{th} day	14^{th} day	28^{th} day	91^{st} day
06M-CW195-wet	1.0%	33.70	39.85	46.53	51.56
045M-CW210-wet	1.0%	54.90	62.48	71.98	77.05
03M-CW210-seal	1.0%	75.48	83.82	91.68	96.18
03M-CW210-wet	1.0%	84.25	91.74	100.42	108.32

Table VI.1-3: Strength of ideal mixes with HES

		Strength in MPa			
Mix name	SP/C	7th day	14th day	28th day	91st day
06M-CW195HES-seal	1.0%	36.78	40.62	44.42	47.20
045M-CW202HES-seal	1.0%	57.01	62.24	67.61	69.67
03M-CW210HES-seal	1.0%	85.60	92.95	96.90	97.67
03M-CW210HES-wet	1.0%	90.65	96.39	104.74	111.87

Some parameters including porosity (interlayer, gel, capillary and total porosity) and heat of hydration (C3S, C2S, C3A and C4AF) were calculated for all ideal mixes. The relations between strength and the couple of heat and porosity (Heat divided by porosity (Hi/P) or Heat multiplied by (PI-P)/PI are presented in figures shown in section VIII.2 and VIII.3.

Fig.VI.1-1 shows the strength tested for mortar w/c=0.3 and wet curing condition. Fig.VI.1-2 and Fig.VI.1-3 show respectively the porosities and hydration heats of each component for the case of LH cement. Heat of hydration is one source of microstructure development that can not be neglected for strength prediction. In addition, porosity is one characteristic of microstructure that should be coupled with heat. The questions are how the porosity affects strength and what type of porosity that gives close influence on strength. Some calculations are made to show the effect of each pore type and the manner in which pore and heat are coupled.

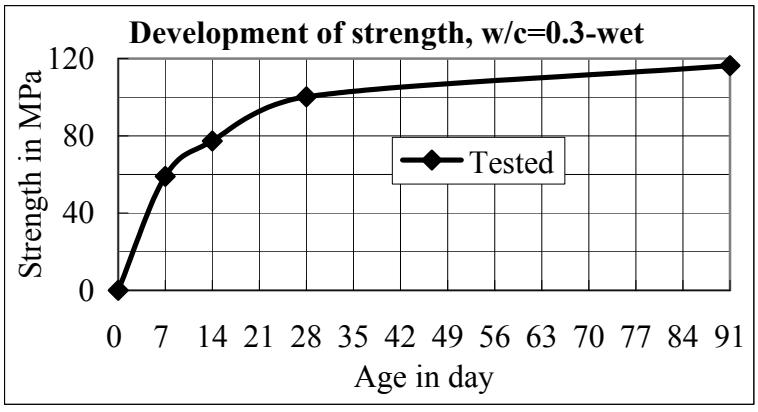

Fig VI.1-1: Development of tested strength

As can be seen in Fig.VI.1-1, strength increases even after 28th day. This is typical for strength development of other w/c (Low heat Portland cement). The strength developments for HES and for OPC are a little different and much different from LH particularly at early ages.

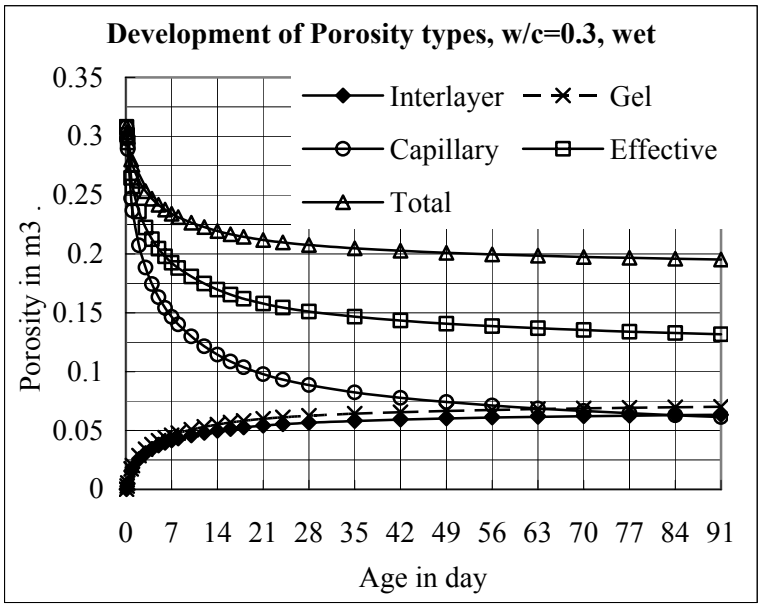

Fig VI.1-2: Development of porosities

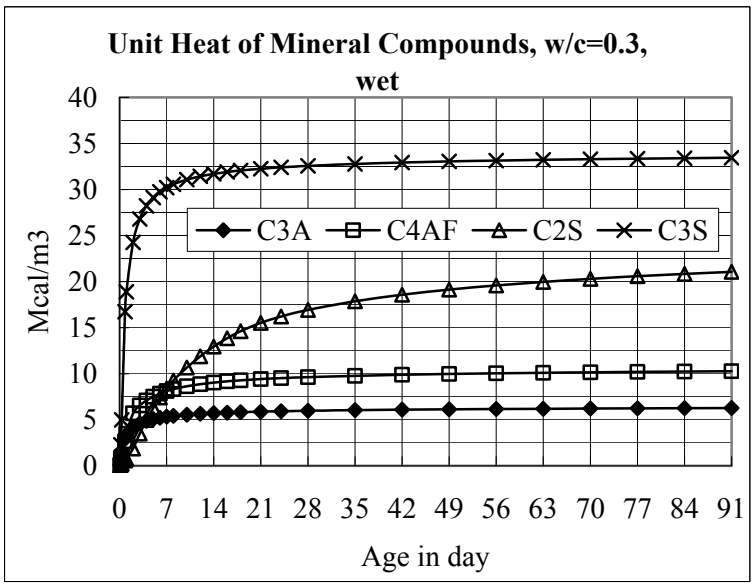

Fig VI.1-3: Development of hydrations

According to the behavior of porosity illustrated in Fig.VI.1-2, the interlayer and gel porosities increase and keep constant after 21st day however capillary, effective or total porosities show their continual decrease until 91st day. In general, Strength is inversely proportional to porosity. Capillary, gel and interlayer pores should be combined in some manner in order that the determinant parameter is found.

As can be seen in Fig.VI.1-3, all components give heats of hydration that are not negligible. C3S and C2S show their heat increase until 91 however C3A and C4AF show their heat increase only before 7th day. This may explain their less important contribution to long-term strength.

VI.2. Strength with its determinant factors

VI.2.A. Strength mechanism

Concrete is composed of hydration structure, un-hydrated products, pores with more or less water and aggregate. Once concrete is compressed, hydrated and un-hydrated structure deforms by resisting at the same time, pores shrink and a disjoining pressure is then originated

to some extent in saturated pores. In some pores, water moves to bigger pores through porous connectivity and then reduces the disjoining pressure but most of pores have narrow entrances which do not allow water to flow and this will increases the disjoining pressure. The latter depends much on permeability and a displacement rate of testing machine. Owing to permeability and testing displacement rate this pressure is not significantly reduced and initializes cracks. The cracks may be originated in some places where the pores are sharp even no water exists. Once cracks are formed, they spread to form a cracking network with other pores whose forms and positions are essential to the spreading. The spread of cracks depend on the pore connectivity and the cohesion of hydrate layers CHS that hold the particles together. The amount of hydrates can be expressed as proportioned to the heat of hydration. According to the strength mechanism, both porosities and heat of hydration are important for strength prediction.

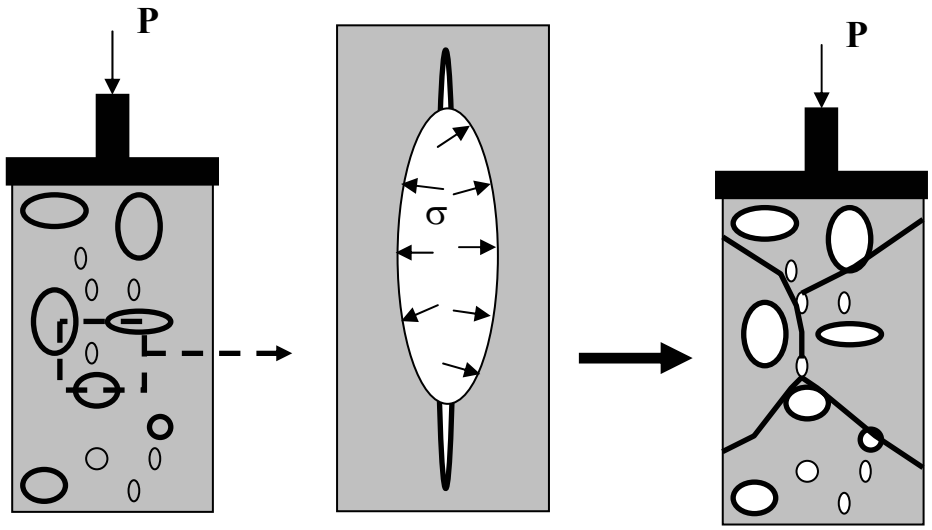

Fig VI.2.A-1 Initialization and spread of cracks

VI.2.B. Strength with heat and porosity

Heat is the only source producing hydrates which constitute the solid parts of paste, mortar and concrete. A study was done to investigate the relation of strength with hydration heat of C2S and C3S; it was found that the scatters of data were not acceptable as can be shown in Fig.VI.2.B-1. This means that heat is not a unique parameter for strength prediction. On the other hand, another study was also conducted to find the relation between strength and porosity alone. As can be seen in Fig.VI.2.B-2, strength was found linear with effective porosity for the case of Portland cements but this linearity was not respected for the case of powder replacement mixes. This study shows that strength is not determined only by porosity but other further parameters may intervene in combination. According to the strength

mechanism, the couple of heat and porosity in a suitable way should be used for strength prediction.

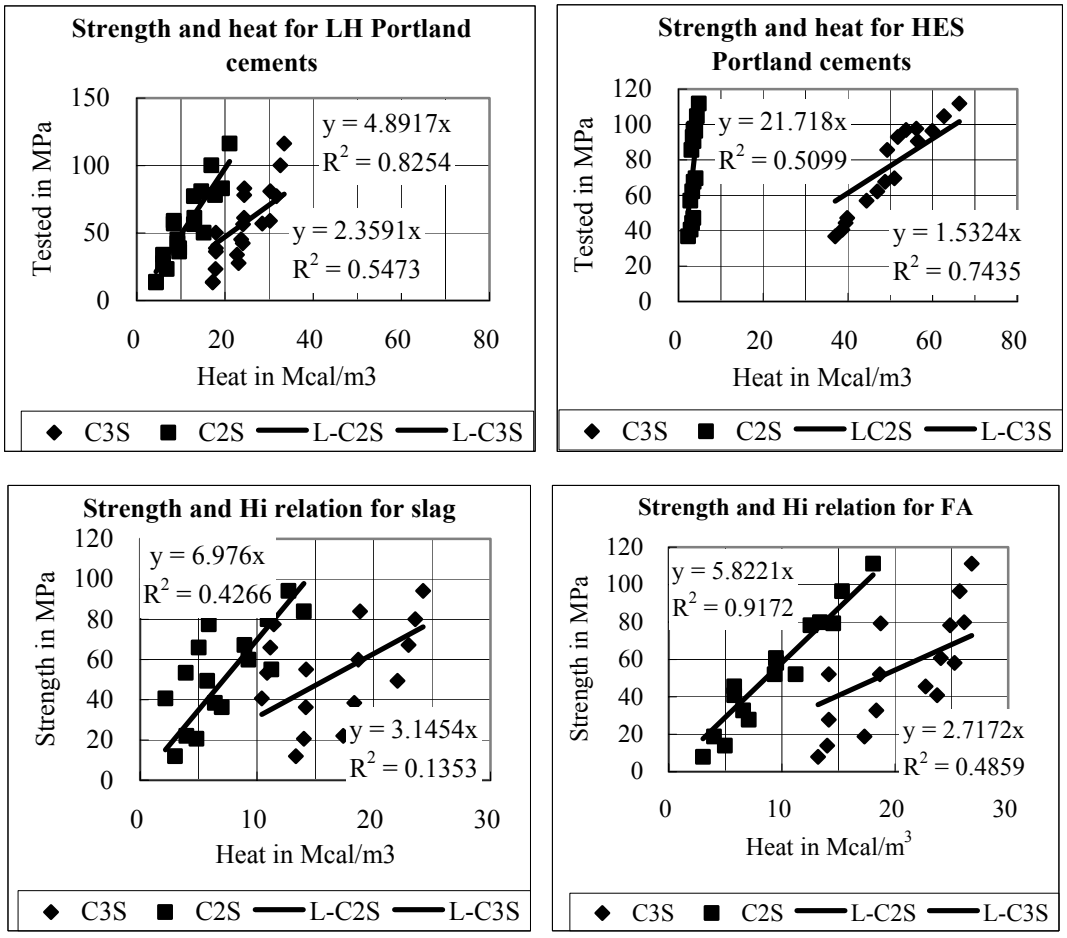

Fig VI.2.B-1 Strength with heat of hydration of C2S and C3S

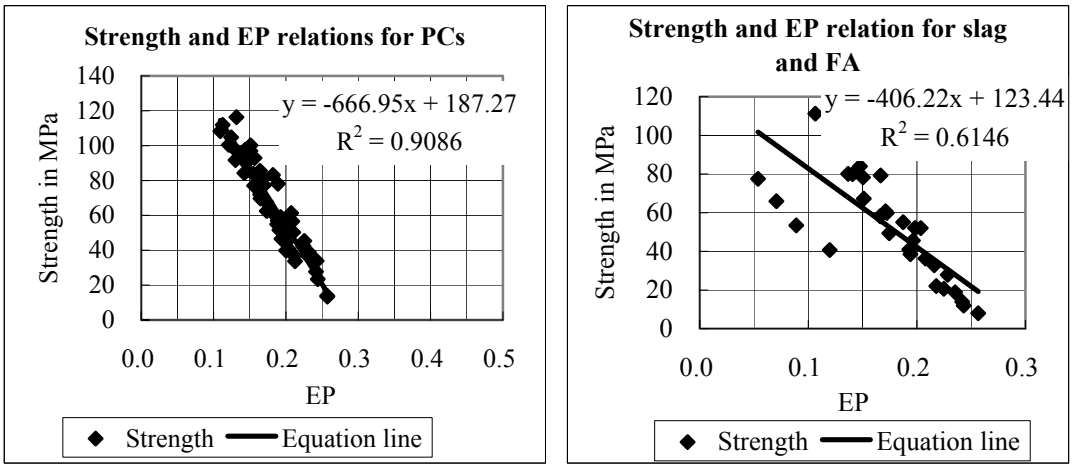

Fig VI.2.B-2 Strength with effective porosity

The strength prediction should generally bear the form given as follows:

$$f_c = g(P, H_i) \quad \text{.....eq. 61}$$

where

f_c is the strength of concrete, mortar or paste.

P, H_i are respectively porosity of mix and unit total heat of each compound.

$g(P, H_i)$ is a function in which porosity and heat are coupled together.

The function $g(P, H_i)$ can be proposed in the following forms:

$$g(P, H_i) = \sum_{i=eachcompound}^{All\ compounds} a_i \frac{H_i}{P} \quad \text{.....eq. 62}$$

or

$$g(P, H_i) = \sum_{i=eachcompound}^{All\ compounds} a_i \frac{PI - P}{PI} . H_i \quad \text{.....eq. 63}$$

In these forms, P represents one pore type or a combination of pore type. It can be gel pore, capillary pore, effective pore, total pore or other combination. The following study will show which type of pore should be used for strength prediction.

VI.3. Proposed model

VI.3.A. Strength function with $\frac{H_i}{P}$

The study will be based on the relation between strength with H_i and P which can be in three cases (effective pore, capillary pore and total pore). Fig.VIII.2.-1 shows, for the case of low heat Portland cement, the linearity between strength f_c with heat of each component divided by the following pore types:

- Effective porosity (EP): $\frac{H_i}{EP}$
- Total porosity (TP): $\frac{H_i}{TP}$ and
- Capillary porosity (CP): $\frac{H_i}{CP}$.

As can be shown, f_c has a better linearity with H_i/EP than with H_i/TP and much better than with H_i/CP.

In addition, Fig.VIII.2-2 shows, for the case of high early strength Portland cement mortar, the linearity of strength f_c with H_i/EP, H_i/TP and H_i/CP. As can be seen, f_c with H_i/CP can not be related with linear function however strength gives a linear relation a little better for H_i/TP than for H_i/EP. LH and HES cements are two cements which contain the extreme amount of C2S and C3S for Portland cements. So from this viewpoint, the conclusion is that linearity of strength with Hi/EP and Hi/TP is better than with Hi/CP for the case of all Portland cements.

The same study is conducted for the case of slag and fly ash replacement. Fig.VIII.2-3 and VIII.2-4 show the relation between strength and H_i/EP and H_i/TP. All points (strength and H_i/P) are scattered but the relation of strength with H_i/EP gives smaller scatter than with H_i/TP. So the parameter that should be used in strength prediction model is probably H_i/EP.

In general, it is found that the regression coefficient is higher than 0.75 for all Portland cements when strength is related to H_i/EP by a linear function. The scatter seems high however this scatter is not the strength prediction problem as the strength model is going to be a sum of contribution of all compounds multiplied with H_i/EP so that the scatter would be changed and that the smaller scatter of the relation between f_c and H_i/P the smaller the strength prediction scatter. So we are going now to establish the model and check if the scatter for strength prediction is acceptable. Finally the following expressions can be approximately written:

$$f_c = a_i \frac{H_i}{EP} \quad \text{.....eq. 64}$$

In order to predict as function of compound composition, f_c needs to be related to all compounds, the relation becomes:

$$f_c = \sum_i a_i \frac{H_i}{EP} = \frac{1}{EP}\left(a_{C2S} H_{C2S} + a_{C3S} H_{C3S} + a_{C3A} H_{C3A} + a_{C4AF} H_{C4AF}\right) \quad \text{.....eq. 65}$$

$a_{C2S}, a_{C3S}, a_{C3A}$ *and* a_{C4AF} are to be determined from the experimental data. Using the strength tested on Portland cement mortars, these coefficients are 0.33, 0.17, -0.032 and 0.43. So the equation eq.65 becomes:

$$f_c = \frac{1}{EP}\left(0.33 H_{C2S} + 0.17 H_{C3S} - 0.032 H_{C3A} + 0.43 H_{C4AF}\right) \quad \text{.....eq. 66}$$

Eq.66 expresses that the contributions of all compounds are positive except that of C3A which is negative. According to Bogue, all contributions are individually positive however the contribution of C3A in the model is negative. This is because when all compounds are mixed

their contributions are interacted to each other so that their contributions are different from the individual contribution. The compound C3A, which produces ettringite and monosulfate accompanying an expansion, may be a source of strength reduction as can be indicated by the equation its contribution is -0.032. Blaine R. L. (1968) and Von Euw M. (1970) *et al*. reported that C3A has a positive influence effect up to 7 or 28 days but negative influence later on.

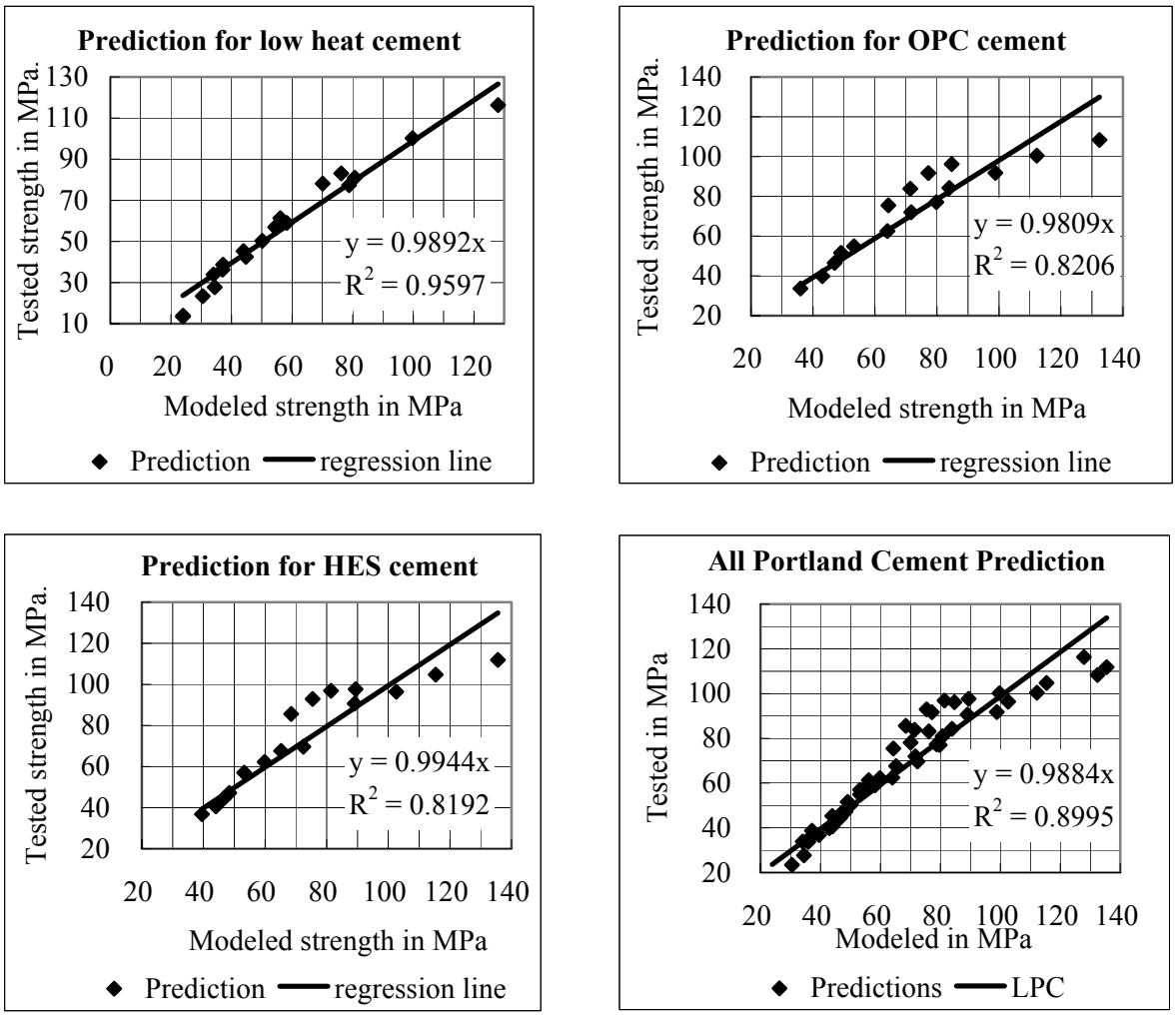

Fig VI.3.A-1: Strength Prediction by eq.66

Fig.VI.3.A-1 shows the prediction precision of each type of cement by eq.66. For LH cement, the prediction is very good with a regression coefficient of 0.96 however this regression decreases for OPC and HES cements. The reason may be the rapid hydration of OPC and HES cement which can modify the pore microstructure. Verbeck and Helmuth suggested that rapid hydration led to encapsulation of the cement grains by a product of low porosity which retarded or prevented further hydration. Another reason may be the change of fracture mechanism when strength is high.

The relation between strength and $(H_i)^a / P^b$ was also studied for the case of C2S and C3S but the variations of a and b will just make the regression coefficients of a compound increase and another decrease. The same linearity for C2S and C3S is obtained with a=1 and b=1.

VI.3.B. Strength function with $\frac{PI-P}{PI}.H_i$

In the previous section, the term 1/EP is the factor of sum of heat of compounds in powder. The problem that poses in the previous case is that when EP becomes very small or zero the strength predicted will be infinite. In an attempt that strength would be zero when P equals an initial value or one constant when P becomes zero, the strength expression should be the following:

$$f_c = \frac{PI-P}{PI}\sum_i^{all} a_i H_i \quad \text{.....eq. 67}$$

where

- PI is the initial porosity
- P is a current porosity and
- Other symbols are the same as in the previous section.

We are going to study which porosity should be determinant for strength prediction when eq.67 is used. PI is the porosity just before the hydration is started, so PI is equal to volume of water. Then eq.67 becomes:

$$f_c = \frac{V_W-P}{V_W}.\sum_{i=each\,compound}^{all\,compounds} a_i H_i \quad \text{.....eq. 68}$$

In this study, all portland cements including LH, OPC and HES are used. The w/c ranges from 0.3 to 0.6 with curing conditions alternatively wet and sealed. Fig.VIII.3-1 shows the relationship between strength and Hi*(Vw-P)/Vw for LH cement. It is found that strength is linear to Hi*(Vw-EP)/Vw, Hi*(Vw-TP)/Vw and Hi*(Vw-CP)/Vw with the same regression coefficient only the slopes of regression line are different. This may explains that either of these three parameters can be used in strength prediction modeling for LH cements. The same conclusion is found for HES cements as can be shown in Fig.VIII.3-2. However in case of slag replacement, only Hi*(Vw-EP)/Vw is a good linear relation with strength as can be seen

in Fig.VIII.3-3. Contrary to the case of slag replacement, for fly ash replacement, strength is found having a good linear relation with all of three parameters described above. In conclusion, the parameter H*(Vw-EP)/Vw should be used in strength modeling because it can provide better linearity with strength than other parameters. The equation becomes:

$$f_c = \frac{V_W - EP}{V_W} . \sum_{i=\text{each compound}}^{\text{all compounds}} a_i H_i \quad \text{.....eq. 69}$$

Using the experimental data, eq.69 becomes:

$$f_c = \frac{V_W - EP}{V_W} . \left(2 H_{C2S} + 1.8 H_{C3S} - 0.16 H_{C3A} + 11 H_{C4AF}\right) \quad \text{.....eq. 70}$$

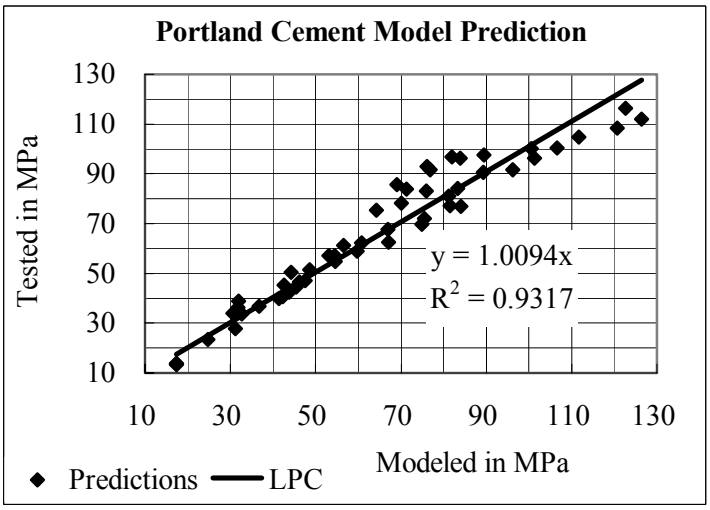

Fig VI.3.B-1: Strength prediction for all mortar made with Portland cements (eq.70)

The fig.VI.3.B-1 shows the strength tested and strength modeled with eq.70. As can be seen, the scatter of strength predicted starts when the strength of mortar is higher than 70-80 MPa and When strength is higher than 100MPa, the modeled strength has tendency to be lower than the tested strength. The reason may be the fracture mechanism which changes when strength is high.

When strength is low, it has been known that the fracture started from aggregate-paste interfaces and spread into the paste and adjacent interfaces until final rupture however when strength is high, fracture originated in the interfaces and spread by breaking the aggregate. As the fracture mechanism changes, the strength is not only affected by the cement paste but also by the surface texture and the mechanical strength of aggregate used which are not considered as the parameters in this research. These parameters should be studied more in future.

Comparing the model given by eq.66 and the one given by eq.70, it is found that eq.70 provides better prediction than eq.66 and that eq.70 gives the finite prediction in all cases however eq.66 gives the infinite value when porosity become too small or zero. So the model by eq.70 should be proposed for strength prediction. In next sections, we are going to treat the

cases of powder replacement with eq.70.

VI.3.C. Contribution of compounds with age

It was reported that pure compounds of C2S, C3S, C3A and C4AF have strength positive as can be shown in fig VI.6-1 by Bogue (1955), however the compounds have interaction effect between themselves so that the contribution of each compound under interaction can be negative as can be shown by the model equation. One question have been posed was whether the contributive coefficient of compounds change with age. The calculation is made to find contributive coefficients for each compound with age. When a cement grain is reacted with water, reaction starts at the surface and then grows inwards at the same time that the particle expands outwards as can be illustrated in fig VI.3.C-1. This means that at an age of curing, old hydrates and young hydrates exist together.

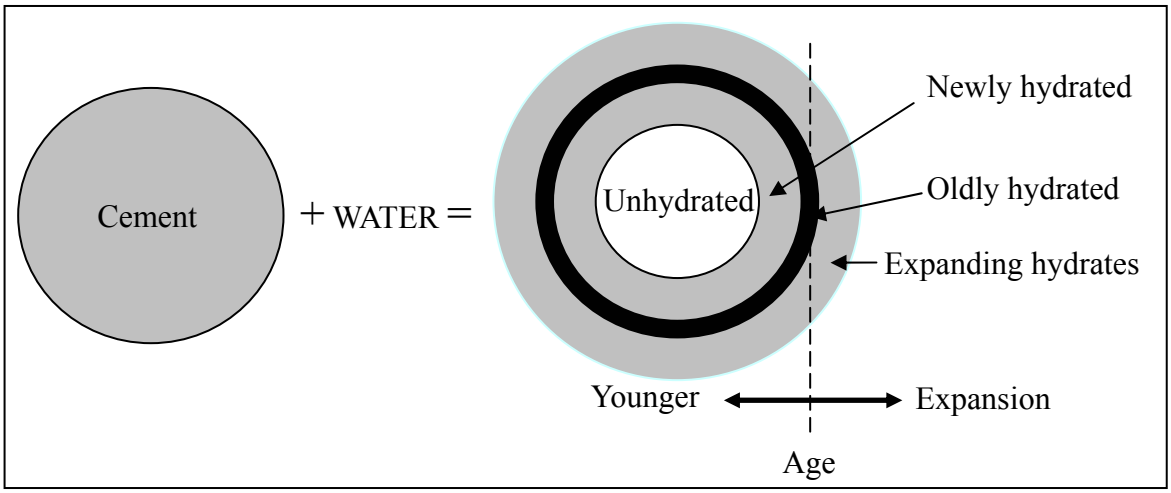

Fig VI.3.C-1 Reacting grain of cement

The contributive coefficients are calculated and shown in Table VI.3.C-1. The change behaviors of contributions are illustrated in Fig VI.3.C-2. As can be seen, for C3A the contribution is positive for early ages and negative for longer ages however C2S and C3S have negative contributions for early ages and positive ones for longer ages.

Table VI.3.C-1 Contributive coefficients of compounds as a function of age

Age	C3A	C4Af	C2S	C3S
7	6.5	55.8	-32.0	-1.9
14	1.2	22.7	-6.1	1.0
28	-0.08	13.5	0.6	1.73
91	-0.16	11.2	2.1	1.8

The reason why C3A has contribution which changes from positive to negative may be due to the hydrate fracture mechanism determining strength participation of compounds. As hydration progresses, hydrated structures are composed of Portlandite (CH) and calcium silicate hydrate of different types (CSH) with the presence of small amount of AFt and AFm.

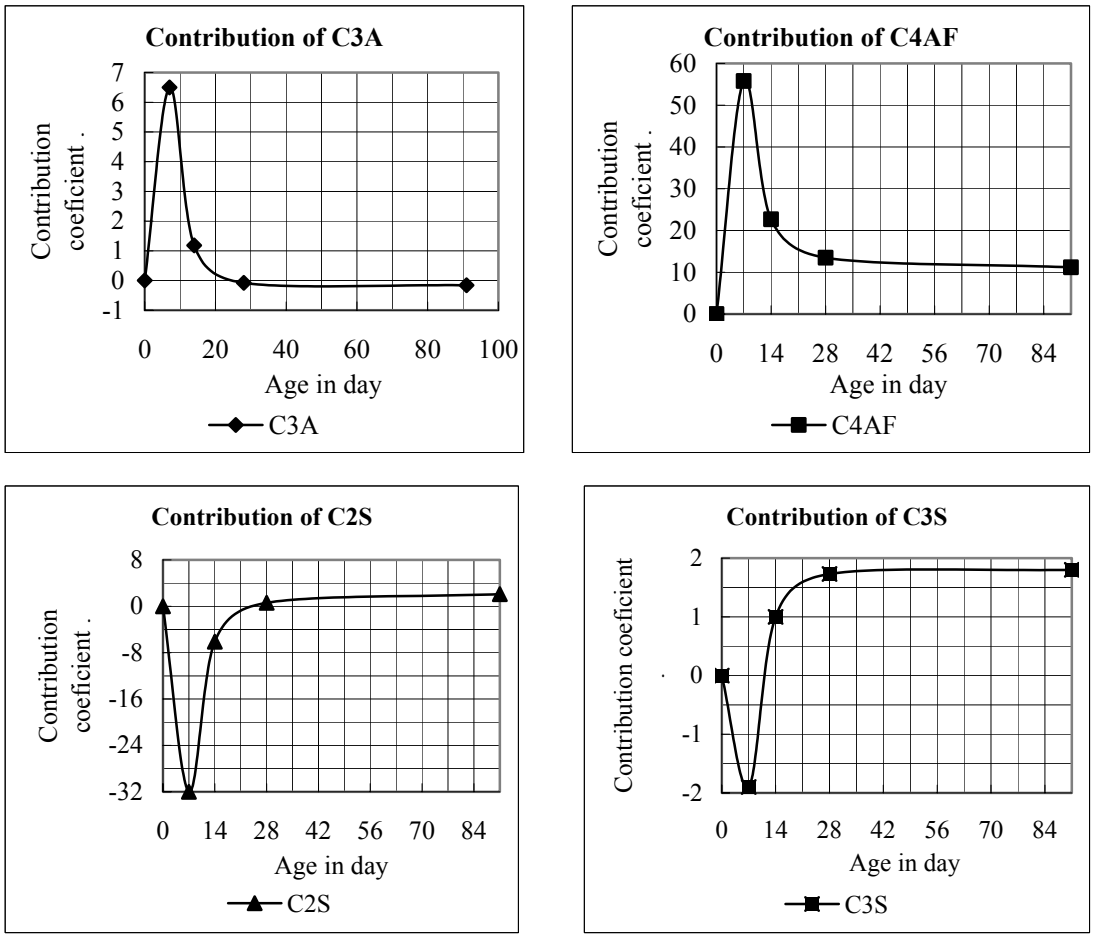

Fig VI.3.C-2 Change of strength contributions

According to fractographic studies of Dalgleish, B. J. about hydrated Portland cement, it was reported that in young pastes interparticle fracture occurs through the developing gel and around the rigid inclusions of CH with some AFt and AFm. As cement paste matures, CH crystals form a massive structure so that an interparticle crack path becomes too tortuous and the energy requirement exceeds that for CH cleavage. Alternatively, CSH becomes denser and develops strength so much that the fracturing energy becomes similar to that of CH cleavage. The failure in mature pastes occurs via a relatively straight path through extensive region of CH and dense massive CSH at the same time that AFt and AFm grows in isolated porosities. This suggests that for young paste, strength is strongly played by CH and AFt and AFm however the strength change to be played by CH and CSH when the paste ages. The growth of AFt and AFm in isolated porosities expresses the negative contribution of C3A. In addition

to Dalgleish's report, Blaine R. L. (1968) and Von Euw M. (1970) *et al*. reported that C3A has a positive influence effect up to 7 or 28 days but negative influence later on. So the change of strength contribution as function of time agrees with other researchers' findings.

VI.4. Model with slag and fly ash replacement

When slag or fly ash is used, these materials can react with catalysts produced by cement and produce the similar hydration products (CSH) as pure cement paste and take part in strength the only difference between slag or fly ash paste from the pure cement paste is the content of $Ca(OH)_2$ which high in cement paste. So slag and fly ash are also sources contributing to strength. In order to include slag and fly ash in the model, the contributions of slag and fly ash have to be determined. In case of slag, it was reported that the replacement ratio can reach 80% but in general, the maximum replacement ratio is reported 60% for low w/p. Two slag replacement ratios are used: 20% and 60% for w/p=0.3 however for w/p=0.45 and 0.6, only the slag replacement ratio equal to 20% is used. On the other hand, in case of Fly ash, the replacement ratio is 20% for w/p=0.3, 0.45 and 0.6. Using experimental data (see table.VIII.1-6, VIII.1-9 and VIII.1-11), their contributions are found and the model becomes:

$$f_c = \frac{V_W - EP}{V_W}.(2H_{C2S} + 1.8H_{C3S} - 0.16H_{C3A} + 11H_{C4AF} + 0.49H_{SG} + 1.4H_{FA}) \quad \text{.....eq. 71}$$

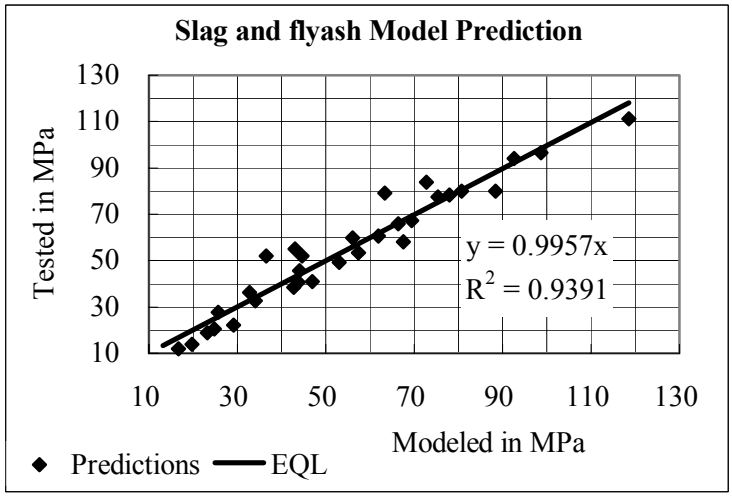

Fig VI.4-1: Strength prediction for slag and fly ash replacement case

Fig.VI.4-1 shows how much the tested strengths are different from the modeled ones in case of mixes with slag and fly ash replacements. The strength can be well predicted by the model eq.71. Comparing with the fig.VI.3.B-1, one observation is that for slag and FA mixes, even strength is high but the strength still can be predicted without fracture type effects.

VI.5. Model for mixes with LS

Limestone is not totally reactive but its physical and chemical properties allow this powder to

affect the compressive strength. Physically, limestone plays a function as filler between the clinker grains. At the same time, the additional surface area provided by the limestone particles may provide sites for the nucleation and growth of hydration products, generally enhancing the achieved hydration. Both the increase of hydrates and the presence of LS as filler are contributive to strength. Chemically, when LS is used the presence of monosulfate is not observed because LS reacts with monosulfate to give mono-carboaluminate $(CaO)_3(Al_2O_3).CaCO_3.11H2O$ and mono-sulfoaluminate $(CaO)_3.(Al_2O_3).CaSO_4.12H_2O$. The reaction takes place to an extent depending on the dosage of LS itself. The phenomena in which the hydration products are modified when LS is used can affect strength to some extent. The question is how the two properties of LS can affect the strength model. Answering to this question, the prediction of strength of LS mixes with the proposed model should be studied. Using eq.70, the prediction for limestone replacement is shown in the following figure.

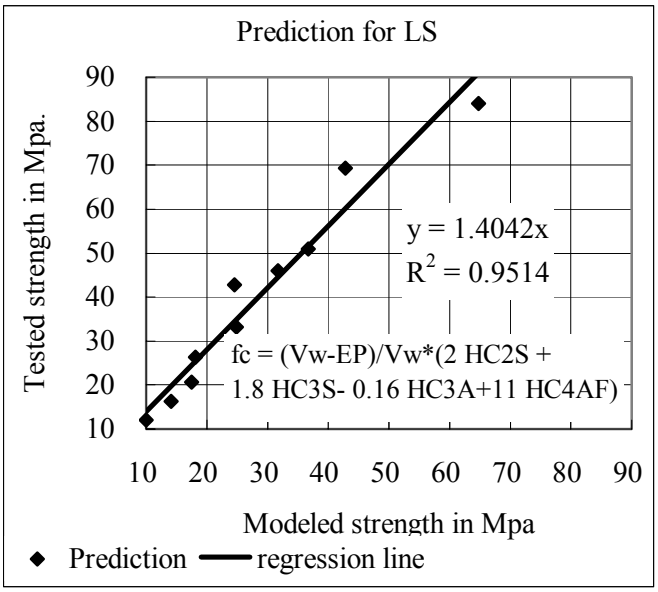

In fig.VI.5-1, the strength predicted by the model is lower than the ones tested. Even the heat model takes already in account the effect, the LS effect on strength has to be regarded. The strength of the LS mixes depends of course on the strength of four compounds of cement and also on the LS effect in filling the porosity of paste and increasing the strength. This LS effect is found 1.4 as shown with the slope of prediction line.

Fig VI.5-1: Strength Prediction for LS without effect of LS

As can be seen in Fig.VI.5-1, the strength is 1.4 times higher than the predicted strength. This is to say that the LS effect is 1.4. The LS replacement is PLS = 20% so the LS effect (LSE) can be written as

LSE = 1 + 0.02 PLS.....eq. 72

The equation becomes then

$$f_c = \frac{V_W - EP}{V_W}.\left(2H_{C2S} + 1.8H_{C3S} - 0.16H_{C3A} + 11H_{C4AF}\right)*(1+0.02PLS) \quad \text{.....eq. 73}$$

LSE is a coefficient which increases the contributions of compounds (C3S, C2S, C3A and C4AF) in cement. One question is whether LSE can be introduced as a heat rate accelerator

into the multi-component heat model. Of course, LS can affect the heat of hydration but LSE coefficient expresses only the increase of strength contributions when LS is used. This can not express that heat can be increased by multiplying with LSE. The heat was not measured in the experiment however was just calculated with the model. There may be a need to make an investigation by measuring heat to see whether LSE can be integrated into the multi-component heat model.

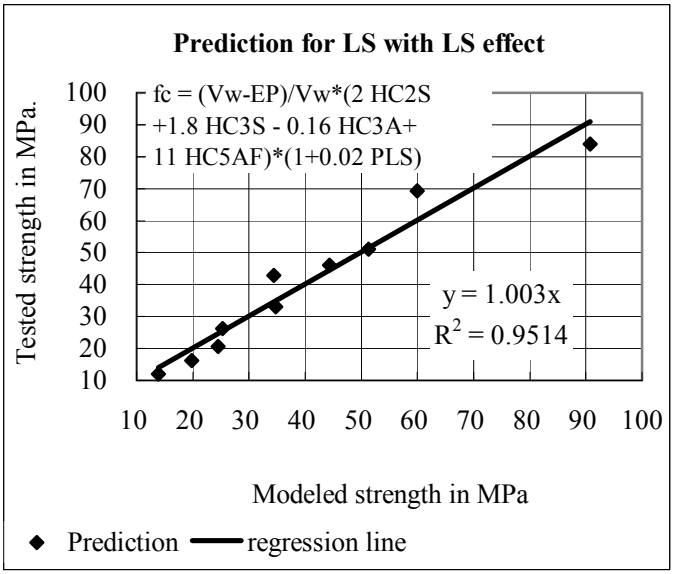

Fig VI.5-2: Strength Prediction for LS with effect of LS

As can be seen in Fig.VI.5-2, the introduction of LS effect (LSE) in the model allows a good prediction. When the LS replacement is zero, the LSE becomes 1. The LS effect is determined by supposing that the effect is linear with the LS percentage. The proposed model can predict strength with LS for different w/c.

According to the above illustrations concerning strength in function of heat and porosity for all cases including Portland cements, slag, flyash and limestone powder replacement, it was found that strength has a linear function with heat coupled with effective porosity.

VI.6. Two-compound modeling

According to Bogue (1955), each compound has its own strength as can be presented in Fig VI.6-1. The strengths of C3S and C2S are approximately the same for long time and are higher than strength of C3A and C4AF. The fact that strength of C3A and C4AF are very small can give an idea to neglect the contribution of these two compounds. In this section, an attempt is made to find a model of strength basing on two compounds including C2S and C3S.

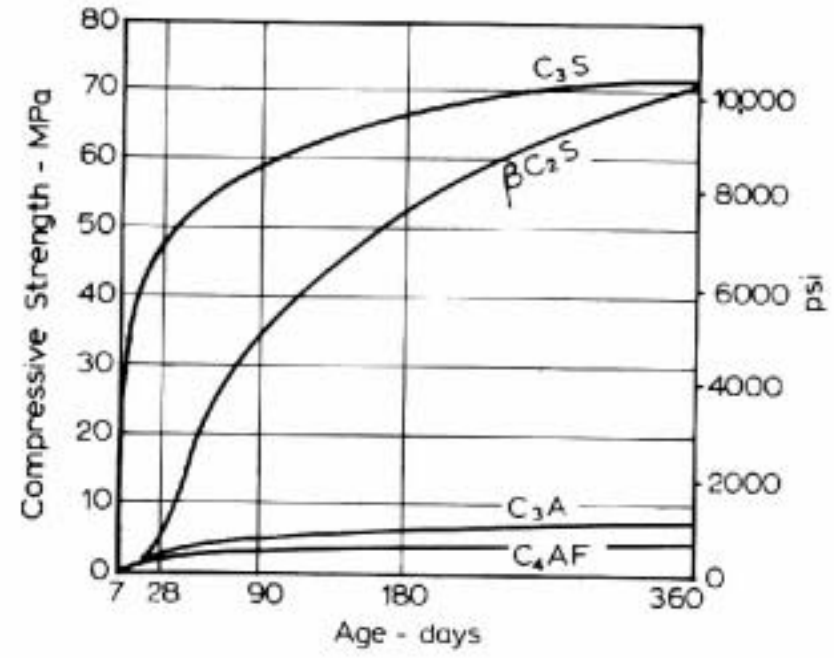

Fig VI.6-1 Strength of pure compounds (Bogue, 1955)

VI.6.A. Two-compound model for Portland cements

When only two compounds C2S and C3S are taken into account, the equation becomes:

$$f_c = \frac{V_W - EP}{V_W}.\left(6.6\,H_{C2S} + 2.6\,H_{C3S}\right) \quad \text{.....eq. 74}$$

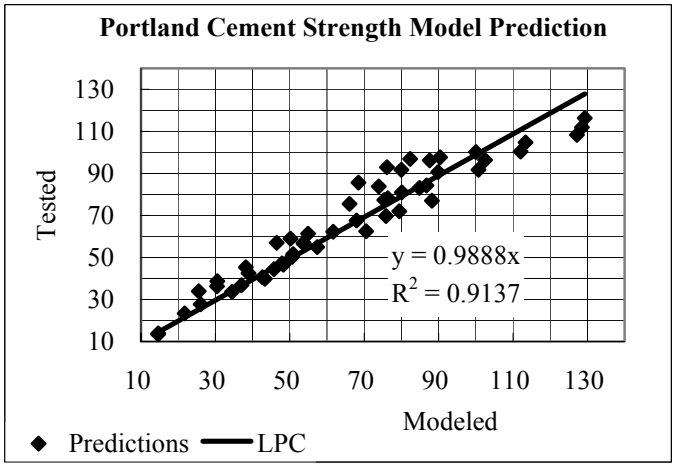

As can be shown in Fig VI.6.A-1, the strength can be predicted with two compounds for all Portland cements.

Fig VI.6.A-1 Prediction for Portland cements by two-compound model

VI.6.B. Two-compound model for Powder replacement

The model proposed with eq.74 is extended for cases of slag, fly ash and limestone replacement. The following equation:

$$f_c = \frac{V_W - EP}{V_W}.\left[6.6\,H_{C2S} + 2.6\,H_{C3S}) * (1 + 0.02PLS) + 0.49H_{SG} + 1.4\,H_{FA}\right] \text{.....eq. 75}$$

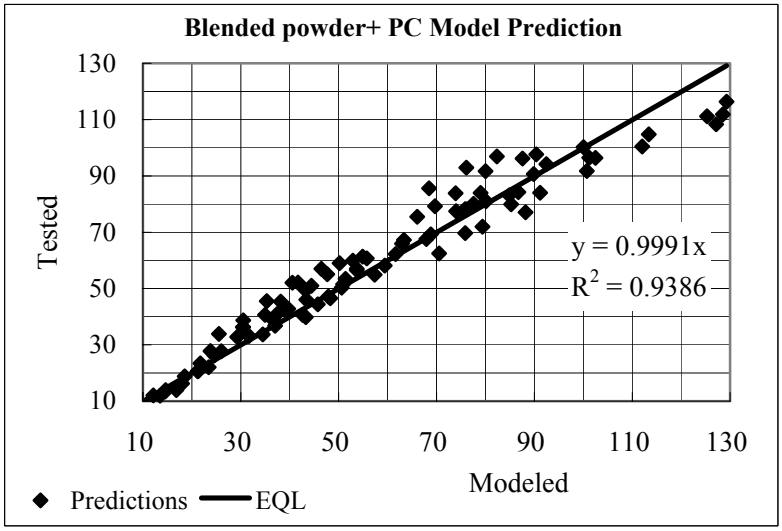

Fig VI.6.B-1 Prediction for powder replacement mixes by two compounds

VI.7. Prediction for other sources of data

The preceding section has shown that the model can predict well the strength of mortar that have the ideal conditions as in microstructure and multi-component heat models. Now the prediction for other sources of data is going to be presented in this section. The data from UBE-Mitsubishi cement corporation contains standard mortars, normal strength concrete and high strength concrete using Portland cements including LH (low heat cement), OPC (ordinary Portland cement) MH (Medium heat cement) and HES (high early strength). In addition, the data from Sumitomo Osaka cement (Meca cements) contains standard mortars using 5 different LH cements and HES.

With the sources of data from Sumitomo Osaka and UBE-Mitsubishi, some main differences are:

- Dispersion which is probably much different.
- Volume of aggregate
- Aggregate type

Table VI.7-1 shows quantitatively and qualitatively some differences between the data obtained by the authors' experimental works and the data from the external sources (Sumitomo Osaka and UBE-Mitsubishi cement Corporation).

Table VI.7-1: Main differences of other sources of data

	Own data	External sources
Dispersion	Maximum dispersion	Unknown dispersion
Aggregate volume (m^3)	• 0.37 (w/c=0.3) • 0.47 (w/c=0.45) • 0.52 (w/c=0.6)	• 0.567 (Standard mortar) • 0.7-0.71 (Normal concrete) • 0.63-0.67 (High strength concrete)
Aggregate type	Mountainous	Unknown
Sand Specific gravity	2.59	2.63

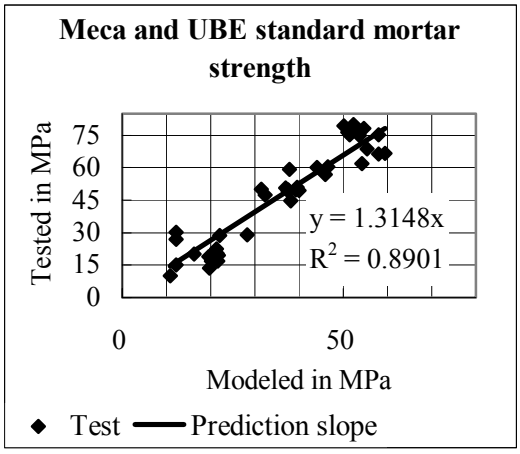

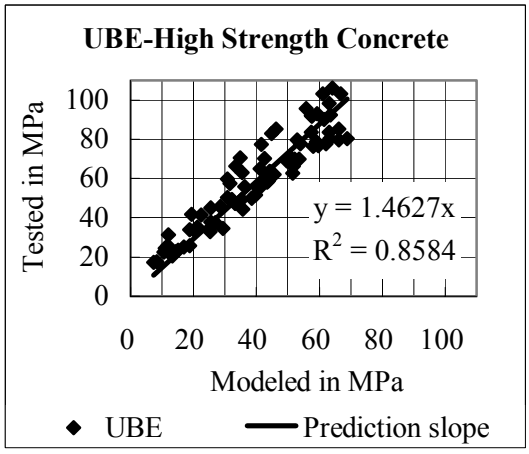

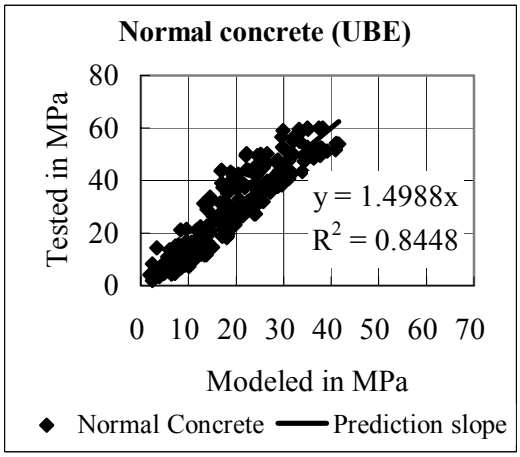

It is found that strength predicted for standard mortars and for normal and high strength concrete are linear with modeled strength. The slope of prediction is 1.3 for mortars and 1.46 for high strength concrete and 1.50 for normal concrete. This means that the predictions are lower than test results.

Fig VI.7-1: Strength Prediction for different data sources

Fig.VI.7-1 shows the strength of mortars and concrete predicted using the proposed model.

The prediction indicates different slopes for different cases but the particularity is that all tested strength points are related to modeled ones by a line. This means that strength is linear to the couple of heat and effective porosity.

The reason why the prediction gives low values is that data from UBE and Sumitomo might be produced using different sand (see table VI.7-1). In addition, sand type and aggregate effects become the new factor that more research should be conducted.

VI.8. Applicability of model

The model was established to predict strength of Portland cements and some powder replacement such as slag, fly ash and limestone. The calculation tool is microstructure and multi-component heat development models which are applicable particularly only to Portland cements and blended powders.

The Portland cements are very often used due to their properties compatible with many purposes of civil engineering however CACs (Calcium Aluminate Cements) are also used in construction for some special treatment due to their properties including rapid strength development, good resistance to sulfate and many other forms of chemical attack and are good for making refractory concrete.

CACs have the composition quite different from those of Portland cements. CACs contain high amount of Al_2O_3 and very low amount of SiO_2 however Portland cements contain low amount of Al_2O_3 and high amount of SiO_2. Due to the difference of compositions, the hydration products are quite different:

Table VI.8-1: Portland cements and CACs

	Portland cements	CACs
Hydration Products	CSH, CH	CAH10, C2AH8, C3AH6, AH3
Multi-component heat model	Applicable	Not applicable

TableVI.8-1 shows some data that can explain that strength of Portland cements and CACs are affected with contributions made by other different compounds. In addition, the multi-component heat model can calculate only the heats of hydration of Portland cements. So this proposed model is applicable only to Portland cements.

CHAPTER VII: CONCLUSIONS

VII. Conclusions

VII.1. General conclusions

After a long and careful discussion based on the experimental data from different sources and with other researchers' findings, a model was successfully proposed. On the strategic way, the authors' experimental data showed some interesting findings among which some were confirmed by other researchers and some others were originally new. The whole research could be concluded in the following summary.

1. In common sense, strength of cementitious materials was essentially dependent of w/p. In this research, some more subsidiary parameters that could make the strength vary remarkably were presented and their effects on strength were clarified. The sand content showed its effect on strength by the existence of aggregate critical volume higher than which strength varied increasingly or decreasingly depending on the dispersion level. The critical volume was found 0.37 for w/c=0.3 and 0.52 for w/c=0.6. The lower w/c, the lower critical volume.

2. The super-plasticizer was found affecting strength with a non-negligible increase when it was increased higher than the amount of SP absorbed by the surface of powder. The absorbed SP was found 0.3% that was not effective in dispersing and the dispersion increased until SP dosage=1.0% where the strength was maximum for different w/c. The effect of SP was higher when the w/c was lower.

3. The mixing time was found playing a smaller influence on strength than the sand content and the SP dosage. The mixing time 3 min was found optimum for obtaining the maximum strength and with higher mixing times, strength was kept constant for low w/p however strength was decreased for high w/p. This was explained with the fact that the false and real w/p were different at high w/p. With different mixing times, the strength was optimum using SP=1.0%.

4. LS powder has become a material currently used to replace cement for effective cost savings without long-term deterioration. To obtain the maximum strength, the SP dosage (without LS) was found different when LS was used. By using the strength data, the

discussion concluded that LS could absorb some SP and the dosage had to be increased in order to acquire the maximum strength or high dispersion. The strength of mix without LS at SP=0 was found comparable to the strength with 20% LS replacement at SP/P=1.18%.

5. Using the mixes of ideal conditions as described in the microstructure and multi-component heat models, it was clearly found that strength had a linear relation with the couple of heat of hydration with effective porosity of each compound. Strength can then be a summation of all heat-pore components.

6. The proposed model:

   After the contribution coefficients of all compounds were determined, the model was proposed with:

$$f_c = \frac{V_W - EP}{V_W}.((2H_{C2S} + 1.8H_{C3S} - 0.16H_{C3A} + 11H_{C4AF}) * (1 + 0.02.PLS) + 0.49H_{SG} + 1.4H_{FA})$$

   This was applicable to mixes made with Portland cements and powders including limestone powder, fly ash and slag for different w/c and different curing conditions.

7. If the model is simplified with the two compounds C2S and C3S, the model becomes:

$$f_c = \frac{V_W - EP}{V_W}.((6.6H_{C2S} + 2.6H_{C3S}) * (1 + 0.02.PLS) + 0.49H_{SG} + 1.4H_{FA})$$

8. Using the data from different sources, the prediction still shows that the strength had a linear relation with hydration heat and effective porosity in all cases. Owing to some intervention of further parameters listed in table VI.7-1, the current model needed to be refined considering more parameters.

VII.2. Model improvement

Even with data provided by other sources, charts of tested strength-modeled strength explain that tested strength has relation linear with the modeled strength which is linear to the couple of heat and porosity. The tested-modeled line shows some slope expressing the intervention of some further effects. The model was created with the experimental data in which the dispersion was maximum (dispersion), mixes were free of sand content effect (aggregate volume), sand was the mountainous one (type of aggregate). So when the aggregate of different types, different contents are used, the effect of aggregate content and the effect of

aggregate type play their roles in strength. In addition, when the SP of different types and different dosages are used, the dispersion effect becomes another factor affecting the strength. In order to improve the proposed model for wide application, the following should be included in the model:

1. Dispersion effect

   - SP type: there are mainly 4 types of super-plasticizers which have different delaying effects due to its structure and its manner of adhering to cement particles.

   - SP dosage: this parameter exercises a direct effect on strength. It was shown that there exist non-effective SP and effective SP which may vary with the type of SP.

2. Aggregate effect

   - Aggregate type: different types of aggregate have different surface texture which affects the aggregate-paste bonding effect.

   - Aggregate content: aggregate can interact and play an effect on strength when its content is higher than the critical volume.

   - Aggregate size: aggregate is one source of local bleeding which is the weak part of concrete. The larger the size is, the more localized the weakness is. This is a source affecting strength.

CHAPTER VIII: APPENDIXES

VIII. Appendixes

VIII.1. Preliminary mix data

Table VIII.1-1: Mix properties w/c=0.3-(3 minute mixing times), sealed condition

Mix	Slump in mm	Slump flow in mm	Water in ltr	Cement in kg	Sand volume fraction	Degree of compaction	Strength in MPa	
							7	28
03M-CW210	88		307	1023	0.38	0.99	47.30	64.3
03M-CW180-SP0.3	79		277	922	0.44	0.98	48.32	70.4
03M-CW195-SP0.3	124		292	974	0.41	0.98	47.39	66.1
03M-CW210-SP0.3	185		307	1023	0.38	0.99	47.34	64.2
03M-CW225-SP0.3	215		321	1070	0.35	0.98	47.53	64.4
03M-CW150-SP0.6	56		243	810	0.51	0.98	53.99	81.1
03M-CW165-SP0.6	133		260	867	0.47	0.98	54.27	79.5
03M-CW180-SP0.6	238		277	922	0.44	0.98	52.99	76.9
03M-CW195-SP0.6		482	292	974	0.41	0.98	52.27	76.3
03M-CW210-SP0.6		620	307	1023	0.38	0.99	51.87	76.1
03M-CW225-SP0.6		654	321	1070	0.35	0.99	51.99	76.2
03M-CW180-SP0.8		629	277	922	0.44	0.98	53.97	77.2
03M-CW195-SP0.8		744	292	974	0.41	0.98	54.72	78.2
03M-CW210-SP0.8		764	307	1023	0.38	0.99	55.83	79.9
03M-CW225-SP0.8		807	321	1070	0.35	0.99	55.77	79.9

03M-CW210-SP1.0		889	307	1023	0.38	0.99	56.83	81.2
03M-CW210-SP1.2		-	307	1023	0.38	1.00	56.03	81.5

Table VIII.1-2: Mix properties w/c=0.6-(3 minute mixing times), sealed condition

Mix	Slump in mm	Slump flow in mm	Water in ltr	Cement in kg	Sand volume fraction	Degree of compaction	Strength in MPa	
							7	28
06M-CW195		564	318	531	0.52	1.00	11.52	31.30
06M-CW150-SP0.2	110		261	435	0.61	0.99	10.46	31.57
06M-CW165-SP0.2	230		281	468	0.57	0.99	12.06	31.41
06M-CW180-SP0.2		541	300	500	0.55	1.00	11.60	30.73
06M-CW195-SP0.2		630	318	531	0.52	1.00	11.25	30.67
06M-CW210-SP0.2		784	336	560	0.49	1.01	11.18	30.86
06M-CW195-SP0.4		670	318	531	0.52	1.00	11.69	33.62
06M-CW195-SP0.6		768	318	531	0.52	0.99	12.83	34.84
06M-CW150-SP0.8	240		261	435	0.61	0.99	10.84	32.41
06M-CW165-SP0.8		577	281	468	0.57	0.99	11.47	34.33
06M-CW180-SP0.8		788	300	500	0.55	1.00	12.85	36.11
06M-CW195-SP0.8		871	318	531	0.52	1.00	15.18	39.38
06M-CW210-SP0.8		-	336	560	0.49	1.00	15.33	39.99
06M-CW195-SP1.0		-	318	531	0.52	1.01	16.43	42.29
06M-CW195-SP1.2		-	318	531	0.52	1.01	14.82	35.21

Table VIII.1-3: Mix properties w/c=0.3, seal condition

Mix	Slump flow in mm	Degree of compaction	Strength in MPa	
			7^{th} day	28^{th} day
03M-CW210SP0.8-2mn	798	0.99	52.55	74.61
03M-CW210SP1.0-2mn	-	0.99	54.06	77.99
03M-CW210SP1.2-2mn	-	0.99	54.02	78.89
03M-CW210SP0.8-5mn	810	0.99	55.83	79.55
03M-CW210SP1.0-5mn	-	0.99	56.82	81.36
03M-CW210SP1.2-5mn	-	0.99	56.71	82.07
03M-CW210SP0.8-10mn	765	0.97	54.91	78.34
03M-CW210SP1.0-10mn	-	0.98	56.95	81.97
03M-CW210SP1.2-10mn	-	0.99	56.74	82.47

Table VIII.1-4: Mix properties w/c=0.6, seal condition

Mix	Slump flow in mm	Real w/c	Degree of compaction	Strength in MPa	
				7^{th} day	28^{th} day
06M-CW195SP0.8-2mn	893	0.55	1.00	14.93	38.71
06M-CW195SP1.0-2mn	-	0.55	1.00	16.55	40.53
06M-CW195SP1.2-2mn	-	0.55	1.01	15.33	36.12
06M-CW195SP0.8-5mn	-	0.58	1.00	13.85	36.21
06M-CW195SP1.0-5mn	-	0.57	1.00	14.67	37.23
06M-CW195SP0.8-10mn	-	0.59	1.00	12.47	34.48
06M-CW195SP1.0-10mn	-	0.59	1.00	13.44	36.28

Table VIII.1-5: Mix proportion of mortars using low heat, OPC and high early strength cements

Mix name	w/p	water	Flow (small cone) in mm	Powder	Sand SSD	Sand volume
LH						
03M-CW210SP1.0	0.3	307	300	1023	970	0.38
045M-CW202SP1.0	0.45	326	303	724	1159	0.45
06M-CW195SP1.0	0.6	318	290	531	1331	0.51
OPC						
03MCW210SP1.0	0.3	306	250	1018	964	0.37
045M-CW202SP1.0	0.45	325	300	722	1158	0.45
06M-CW195SP1.0	0.6	318	243	529	1333	0.52
HES						
03M-CW210SP1.0	0.3	305	180	1017	956	0.37
045M-CW202SP1.0	0.45	316	242	701	1192	0.46
06M-CW195SP1.0	0.6	317	240	529	1330	0.51

Table VIII.1-6: Mix proportions with powders

Mix name	w/p	Water	Flow (small cone) in mm	Powder kg	Sand SSD in kg	Cement LH %	Powder replacement ratio %	Sand volume
Limestone replacement								
045M-CW202LS20	0.45	315	328	701	1190	80	20	0.46
06M-CW195LS20	0.6	317	305	529	1329	80	20	0.51
03M-CW210LS20	0.3	305	350	1016	949	80	20	0.37
Fly ash replacement								
03M-CW210FA20	0.3	303	290	1010	938	80	20	0.36
045M-CW202FA20	0.45	314	300	699	1177	80	20	0.45
06M-CW195FA20	0.6	316	280	527	1318	80	20	0.51
Slag replacement								
03M-CW210SL20	0.3	306	380	1019	965	80	20	0.37
03M-CW210SL60	0.3	303	350	1011	941	40	60	0.36
045M-CW202SL20	0.45	316	330	702	1197	80	20	0.46
06M-CW195SL20	0.6	318	360	530	1334	80	20	0.52

Table VIII.1-7: Test results of mixes with limestone replacement

	SP ratio in weight		Flow (small cone) in mm	D-ratio	Strength (MPa)				SP ratio in volume	
	SP/P	SP/C			7	14	28	91	SP/C	SP/P
03M-CW210LS20	0.70%	0.88%	220	0.97	43.85	-	74.66	-	5.2%	4.0%
	0.86%	1.08%	250	0.97	44.47	-	75.62	-	2.7%	2.1%
	1.02%	1.28%	300	0.98	46.49	-	80.40	-	3.3%	2.6%
	1.18%	1.48%	350	0.99	51.35	-	84.35	-	4.6%	3.5%
	1.34%	1.68%	405	1.00	49.35	-	82.09	-	5.2%	4.0%
045M-CW202LS20	0.86%	1.08%	301	1.00	20.37	-	44.81	-	3.3%	2.6%
	1.02%	1.28%	328	1.00	20.67	33.15	45.73	69.24	40%	3.1%
	1.18%	1.48%	380	1.00	20.64	-	46.05	-	4.6%	3.5%
06M-CW195LS20	1.02%	1.28%	267	1.00	9.67	-	24.24	-	4.0%	3.1%
	1.18%	1.48%	305	1.00	12.06	16.24	26.26	42.78	4.6%	3.5%
	1.34%	1.68%	333	1.00	11.89	-	26.65	-	5.2%	4.0%

Table VIII.1-8: Dosage of SP for mixes with fly ash replacement

	Dosage in weight		Dosage in volume	
	SP/P	SP/C	SP/P	SP/C
045M-CW202FA20-wet	1.02%	1.28%	3.06%	3.97%
06M-CW195FA20-wet	1.18%	1.48%	3.53%	4.60%
03M-CW210FA20-seal	1.18%	1.48%	3.53%	4.60%
03M-CW210FA20-wet	1.18%	1.48%	3.53%	4.60%

Table VIII.1-9 Strength of mortars with fly ash replacement

	7 day	14 day	28 day	91 day
045M-CW202FA20-wet	18.80	32.78	52.10	79.26
06M-CW195FA20-wet	7.94	13.94	27.79	52.05
03M-CW210FA20-seal	45.55	60.68	78.22	96.44
03M-CW210FA20-wet	40.90	58.14	79.92	111.19

Table VIII.1-10: SP dosage for slag replacement mixes

Mix type	SP/P in weight		SP ration in volume	
	SP/P	SP/C	SP/P	SP/C
045M-CW202SL20-wet	1.02%	1.28%	3.06%	3.97%
06M-CW195SL20-seal	1.18%	1.48%	3.53%	4.60%
03M-CW210SL60-seal	0.74%	1.85%	2.06%	5.76%
03M-CW210SL20-seal	1.18%	1.48%	3.53%	4.60%

Table VIII.1-11: Strength for mixes with slag replacement

	7 day	14 day	28 day	91 day
045M-CW202SL20-wet	22.0	38.5	59.9	83.94
06M-CW195SL20-seal	11.9	20.6	36.3	55.10
03M-CW210SL60-seal	40.7	53.4	66.0	77.48
03M-CW210SL20-seal	49.40	67.27	80.08	94.17

VIII.2. Strength and porosity: Hi/P

Table VIII.2-1: Hi/EP for LH cement mortar

Age	C2S/EP	C3S/EP	C3A/EP	C4AF/EP	Tested (MPa)
7	43.61	156.84	27.65	42.09	59
14	76.35	186.88	33.72	53.29	77.33
28	112.05	215.49	39.55	63.70	100.2
91	159.94	253.92	47.60	78.04	116.35
7	42.54	144.16	25.55	38.87	57
28	87.49	180.86	32.59	51.41	81
7	24.64	95.52	16.69	24.76	27.75
14	41.12	107.12	19.89	31.66	42.5
28	63.09	117.35	22.53	37.30	61.32
91	106.28	134.12	26.28	44.56	83.13
7	24.55	93.68	16.41	24.57	33.89
14	40.90	105.07	19.30	30.71	45.33
28	62.02	115.42	21.80	35.76	56.53
91	93.88	128.87	24.94	41.82	78.14
7	17.01	67.15	11.62	17.11	13.9
14	27.74	73.12	13.75	21.75	23.4
28	41.44	77.35	15.09	25.23	38.73
91	72.19	85.36	16.80	28.69	50.31
7	17.00	66.84	11.60	17.10	13.44
28	41.43	77.27	15.00	25.00	36.28

Table VIII.2-2: Hi/EP for HES cement mortar

Age	C2S/EP	C3S/EP	C3A/EP	C4AF/EP	Tested (MPa)
7	24.59	392.66	86.67	39.45	90.65
14	29.87	449.91	98.89	45.15	96.39
28	34.79	503.95	110.83	50.71	104.74
91	42.49	587.87	129.98	59.66	111.87
7	18.64	300.31	67.76	31.23	85.60
14	21.35	330.30	73.62	33.91	92.95
28	23.52	356.03	78.81	36.29	96.90
91	26.41	390.76	86.03	39.59	97.67
7	14.76	235.22	51.83	23.32	57.01
14	18.12	261.04	57.93	26.35	62.24
28	20.82	281.91	63.14	28.95	67.61
91	24.52	308.92	70.35	32.60	69.67
7	10.78	174.84	38.90	17.37	36.78
14	14.08	189.63	43.14	19.78	40.62
28	16.14	197.33	45.65	21.29	44.42
91	17.85	201.88	47.39	22.46	47.20

Table VIII.2-3: Hi/EP for OPC mortar

Age	C2S/EP	C3S/EP	C3A/EP	C4AF/EP	Tested (MPa)
7	33.60	355.94	120.37	37.56	84.25
14	41.66	415.21	138.96	44.04	91.74
28	48.87	468.18	156.15	49.98	100.42
91	59.77	547.87	182.78	59.12	108.32
7	25.74	271.17	95.71	29.77	75.48
14	29.59	299.69	103.89	32.61	83.82
28	32.56	323.06	110.80	35.00	91.68
91	36.35	353.58	120.08	38.18	96.18
7	20.25	229.40	75.32	23.13	54.90
14	28.03	266.79	89.05	28.51	62.48
28	34.01	292.16	99.15	32.51	71.98
91	40.74	317.40	110.20	36.99	77.05
7	13.18	156.86	50.89	15.30	33.70
14	18.85	178.71	60.46	19.37	39.85
28	23.38	188.12	65.37	21.80	46.53
91	26.23	192.04	67.70	23.10	51.56

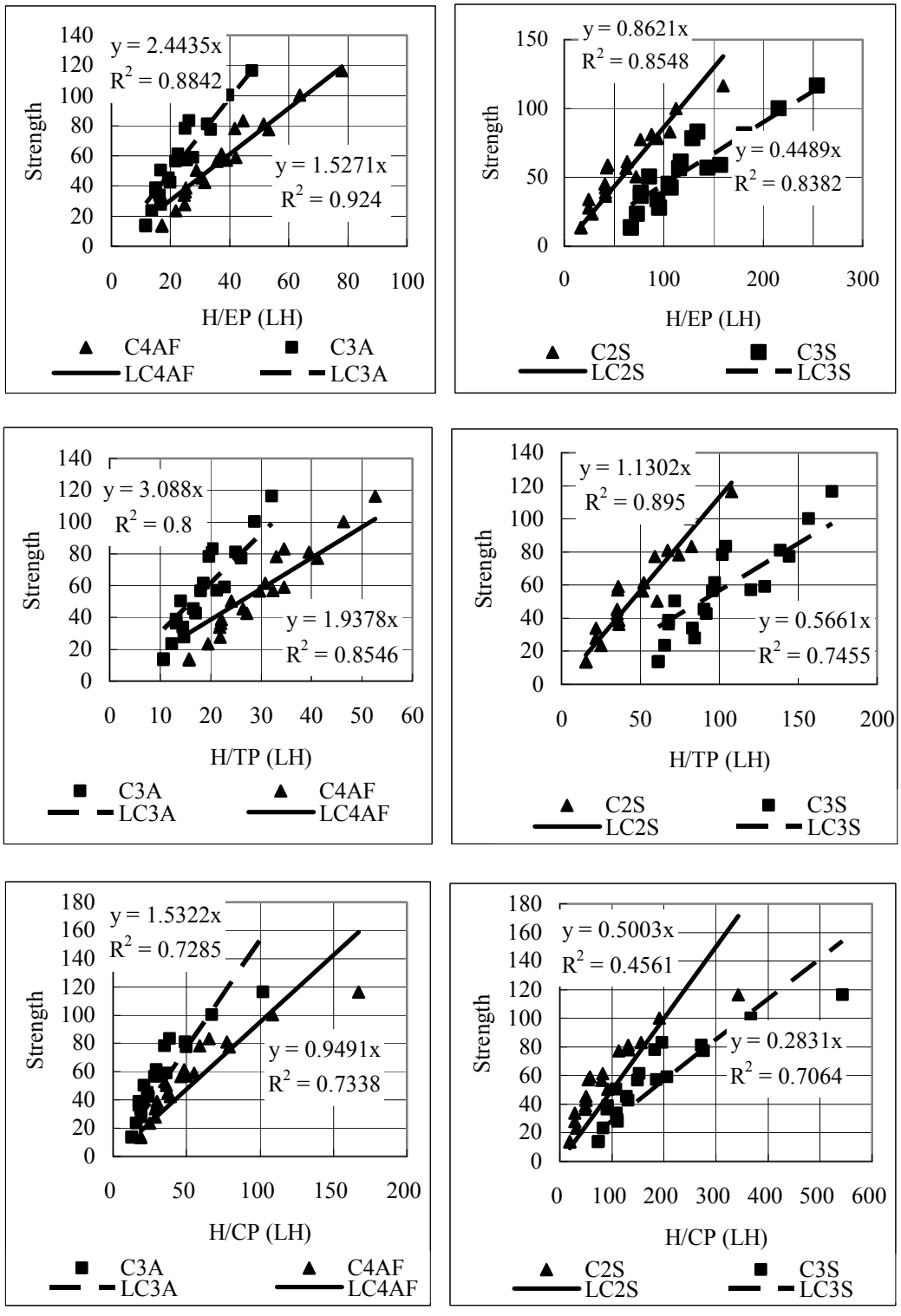

FigVIII.2-1: Strength behavior versus heat of each component divided by pore type (Low heat Portland cement)

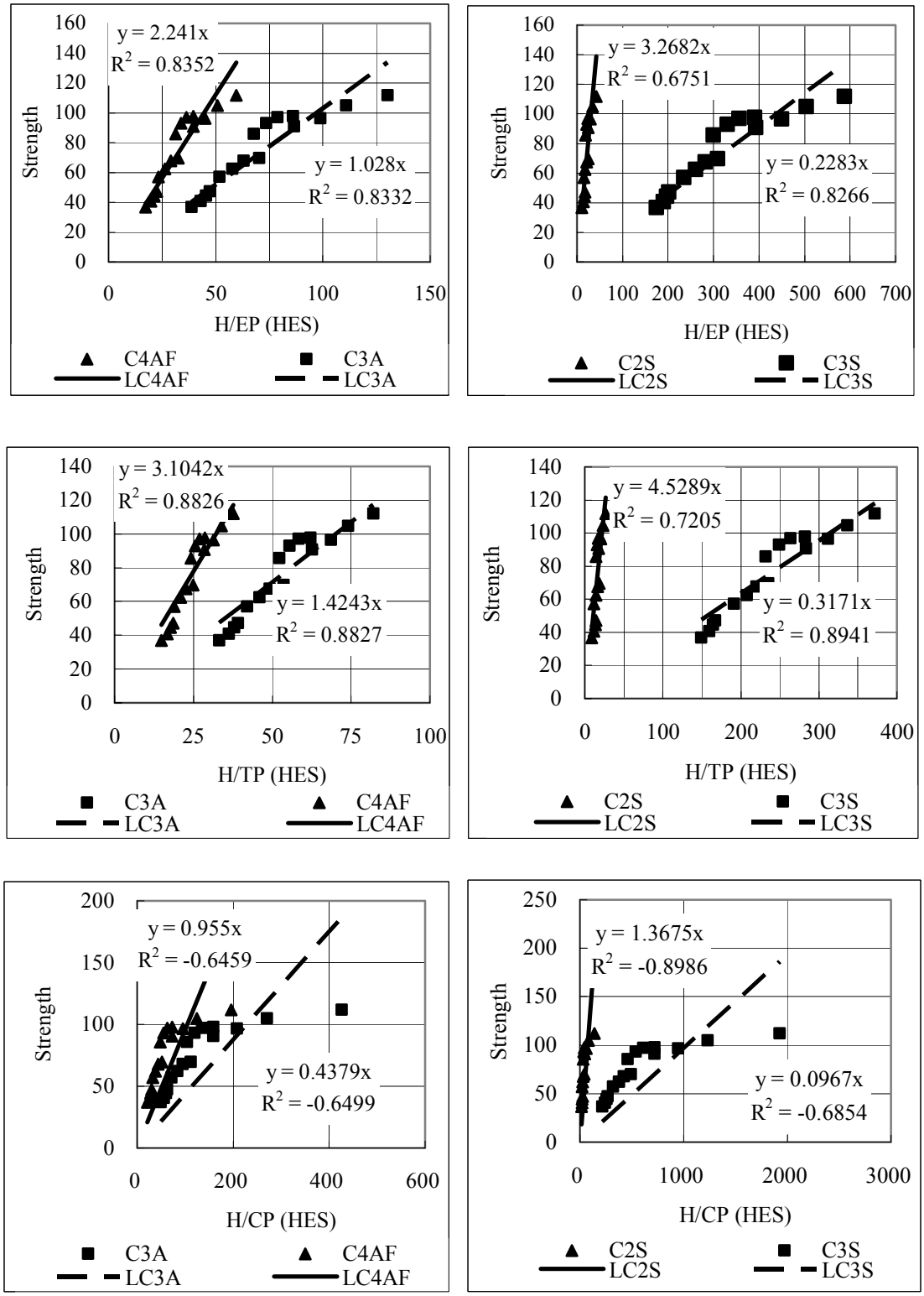

Fig VIII.2-2: Strength behavior versus heat of each component divided by pore type (High early strength Portland cement)

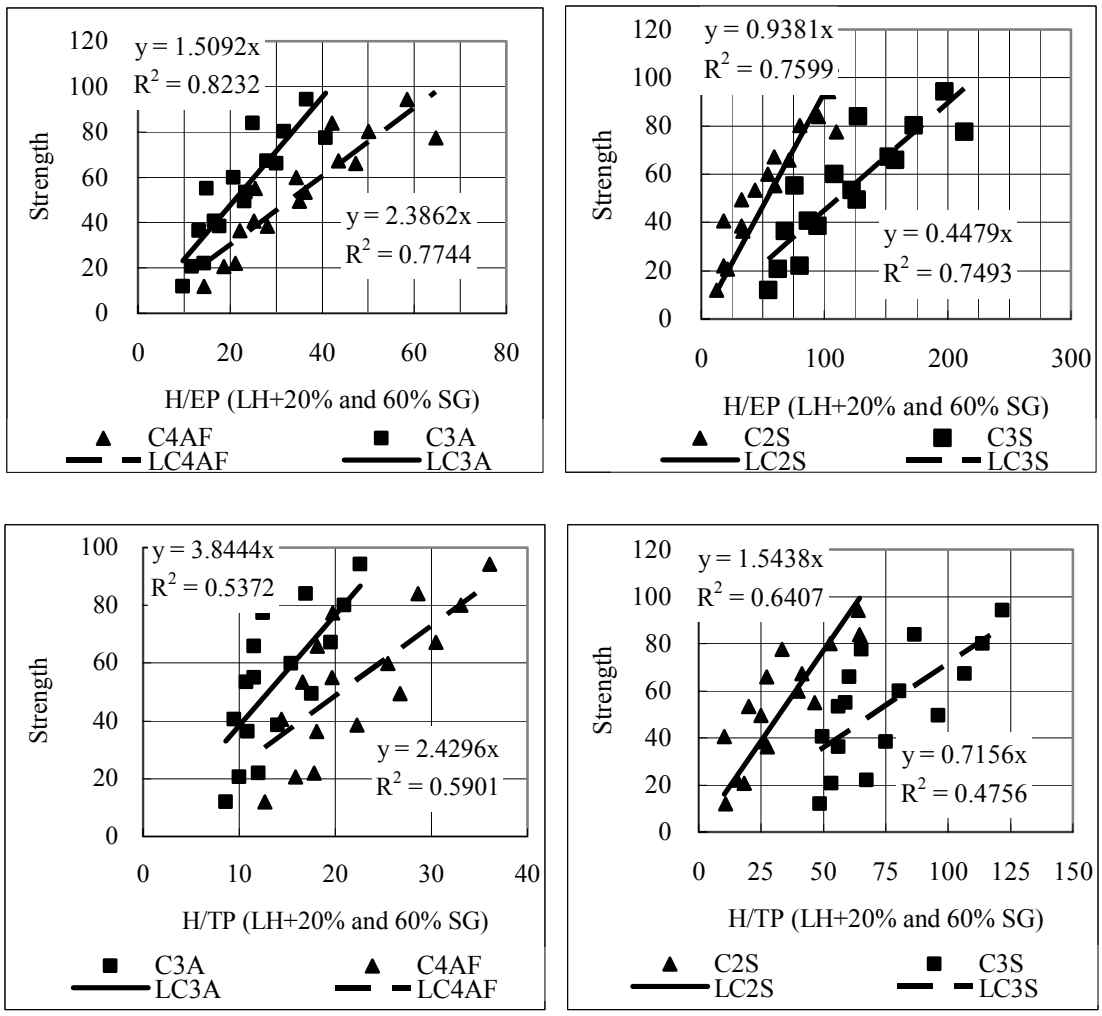

Fig VIII.2-3: Strength behavior versus heat of each component divided by pore type (Slag replacement)

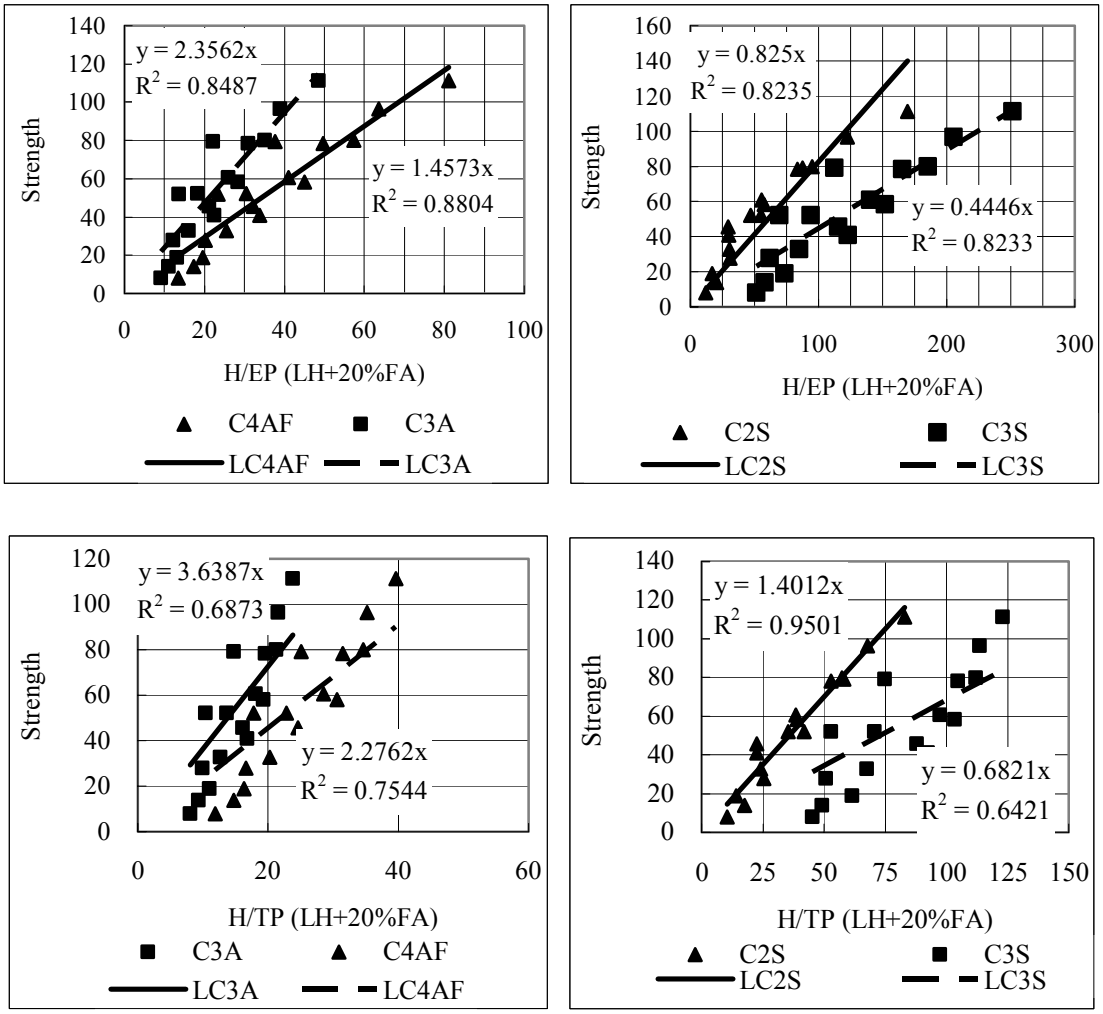

Fig VIII.2-4: Strength behavior versus heat of each component divided by pore type (Fly ash replacement)

VIII.3. Strength and porosity: Hi*(PI-EP)/PI

The symbol Hi*(Vw-EP)/Vw is represented with ComHi (Component heat of i)

Table VIII.3-1: Hi*(Vw-EP)/Vw for LH cement mortar

Age	$ComH_{C2S}$	$ComH_{C3S}$	$ComH_{C3A}$	$ComH_{C4AF}$	Tested (MPa)
7	3.15	11.32	2.00	3.04	59
14	5.81	14.23	2.57	4.06	77.33
28	8.62	16.59	3.04	4.90	100.2
91	12.05	19.13	3.59	5.88	116.35
7	3.02	10.22	1.81	2.75	57
28	6.69	13.83	2.49	3.93	81
7	1.56	6.05	1.06	1.57	27.75
14	2.91	7.58	1.41	2.24	42.5
28	4.80	8.93	1.71	2.84	61.32
91	8.59	10.84	2.12	3.60	83.13
7	1.55	5.90	1.03	1.55	33.89
14	2.87	7.38	1.36	2.16	45.33
28	4.69	8.73	1.65	2.71	56.53
91	7.51	10.30	1.99	3.34	78.14
7	0.87	3.43	0.59	0.87	13.9
14	1.62	4.26	0.80	1.27	23.4
28	2.67	4.97	0.97	1.62	38.73
91	5.23	6.19	1.22	2.08	50.31
7	0.87	3.41	0.59	0.87	13.44
28	2.66	4.96	0.96	1.61	36.28

Table VIII.3-2: Hi*(Vw-EP)/Vw for OPC and HES mortars

	Age	$ComH_{C2S}$	$ComH_{C3S}$	$ComH_{C3A}$	$ComH_{C4AF}$	Tested (MPa)
OPC	7	2.54	26.91	9.10	2.84	84.25
	14	3.10	30.87	10.33	3.27	91.74
	28	3.56	34.06	11.36	3.64	100.42
	91	4.18	38.30	12.78	4.13	108.32
	7	1.94	20.47	7.22	2.25	75.48
	14	2.24	22.73	7.88	2.47	83.82
	28	2.47	24.50	8.40	2.65	91.68
	91	2.75	26.72	9.07	2.88	96.18
	7	1.59	18.03	5.92	1.82	54.90
	14	2.25	21.42	7.15	2.29	62.48
	28	2.74	23.58	8.00	2.62	71.98
	91	3.28	25.59	8.89	2.98	77.05
	7	0.92	10.94	3.55	1.07	33.70
	14	1.39	13.14	4.45	1.42	39.85
	28	1.76	14.12	4.91	1.64	46.53
	91	1.99	14.55	5.13	1.75	51.56
HES	7	1.87	29.83	6.58	3.00	90.65
	14	2.24	33.74	7.42	3.39	96.39
	28	2.56	37.10	8.16	3.73	104.74
	91	3.02	41.77	9.24	4.24	111.87
	7	1.41	22.75	5.13	2.37	85.60
	14	1.63	25.15	5.61	2.58	92.95
	28	1.79	27.13	6.00	2.76	96.90
	91	2.01	29.68	6.53	3.01	97.67
	7	1.12	17.81	3.93	1.77	57.01
	14	1.40	20.16	4.47	2.03	62.24
	28	1.63	22.00	4.93	2.26	67.61
	91	1.93	24.29	5.53	2.56	69.67
	7	0.76	12.31	2.74	1.22	36.78
	14	1.02	13.80	3.14	1.44	40.62
	28	1.19	14.57	3.37	1.57	44.42
	91	1.33	15.05	3.53	1.67	47.20

Table VIII.3-3: Hi*(Vw-EP)/Vw for Limestone and slag mortars

Age	$ComH_{C2S}$	$ComH_{C3S}$	$ComH_{C3A}$	$ComH_{C4AF}$	Tested (MPa)
Limestone mortar					
7	2.05	6.99	1.22	1.83	51.00
28	5.82	10.29	1.94	3.18	84.00
7	0.96	3.41	0.59	0.87	20.64
14	1.76	4.23	0.79	1.26	33.15
28	2.77	4.89	0.95	1.59	46.05
91	5.10	5.98	1.18	2.01	69.24
7	0.55	1.94	0.33	0.49	12.06
14	1.00	2.41	0.45	0.71	16.24
28	1.57	2.78	0.54	0.91	26.26
91	2.95	3.41	0.67	1.15	42.78
Slag mortar					
7	2.47	9.47	1.73	2.63	49.40
14	4.52	11.64	2.14	3.33	67.27
28	6.04	13.04	2.40	3.79	80.08
91	7.61	14.51	2.69	4.29	94.17
7	1.31	6.31	1.21	1.83	40.66
14	2.76	7.68	1.47	2.28	53.41
28	3.85	8.55	1.63	2.56	65.96
91	4.84	9.43	1.80	2.86	77.48
7	1.23	5.42	0.97	1.44	22.04
14	2.47	7.09	1.33	2.11	38.47
28	4.22	8.50	1.63	2.69	59.90
91	7.48	10.04	1.96	3.32	83.94
7	0.70	3.14	0.56	0.82	11.93
14	1.41	4.11	0.77	1.23	20.64
28	2.42	4.91	0.95	1.59	36.31
91	4.61	5.83	1.15	1.95	55.10

Table VIII.3-4: Hi*(Vw-EP)/Vw for flyash mortar

Age	$ComH_{C2S}$	$ComH_{C3S}$	$ComH_{C3A}$	$ComH_{C4AF}$	Tested (MPa)
7	2.16	8.87	1.61	2.44	40.90
14	4.38	11.64	2.17	3.45	58.14
28	7.26	14.18	2.69	4.39	79.92
91	11.82	17.52	3.39	5.65	111.19
7	2.10	8.23	1.51	2.30	45.55
14	4.21	10.68	1.98	3.12	60.68
28	6.41	12.72	2.38	3.83	78.22
91	9.09	15.26	2.89	4.73	96.44
7	1.04	4.48	0.81	1.19	18.80
14	2.11	5.88	1.11	1.76	32.78
28	3.52	7.01	1.36	2.26	52.10
91	6.92	8.91	1.75	2.98	79.26
7	0.59	2.58	0.46	0.68	7.94
14	1.20	3.40	0.64	1.02	13.94
28	2.01	4.01	0.78	1.31	27.79
91	4.06	5.11	1.01	1.72	52.05

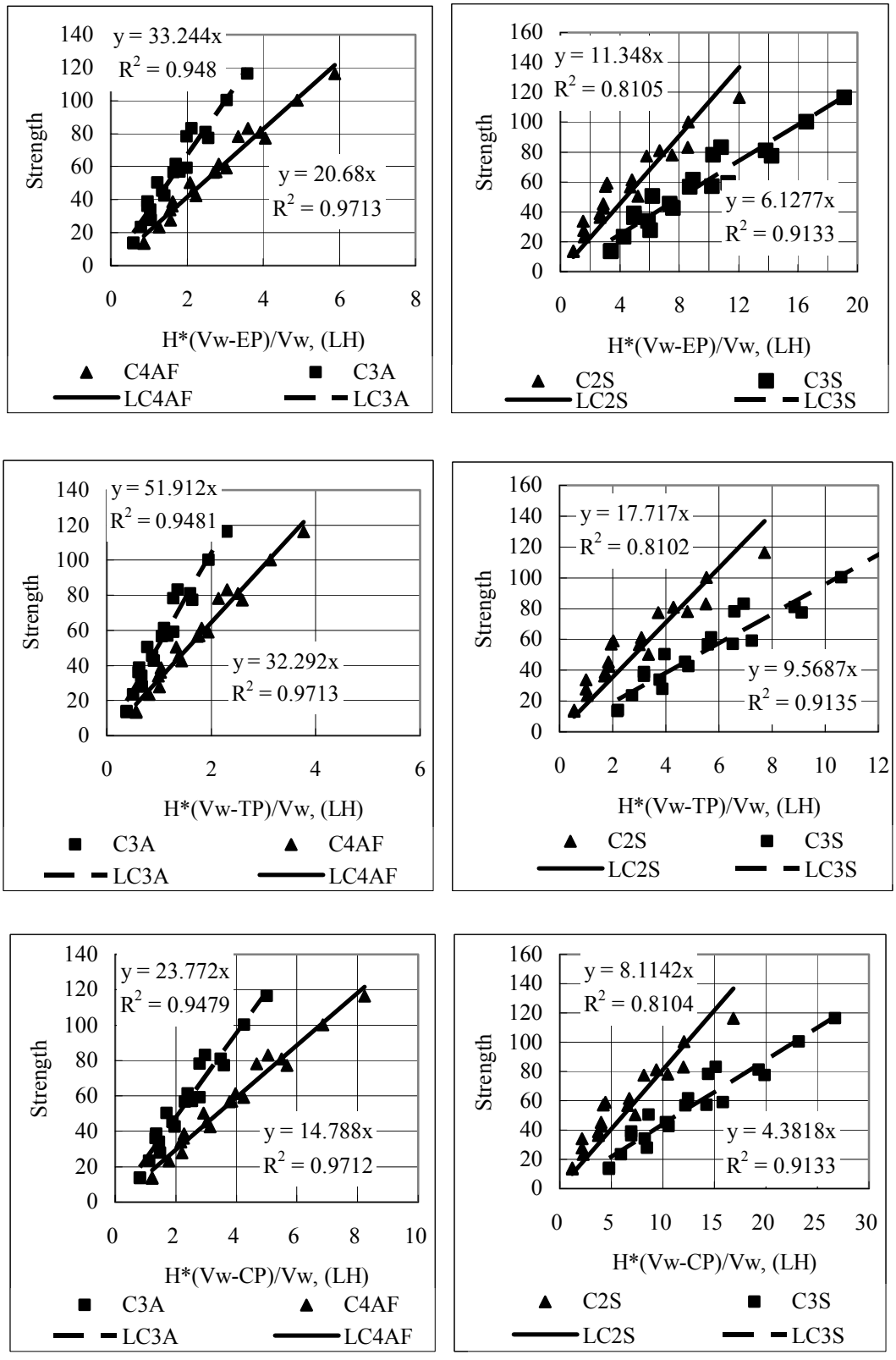

Fig VIII.3-1: Strength behavior versus $\frac{PI-P}{PI}.H_i$ (LH cements)

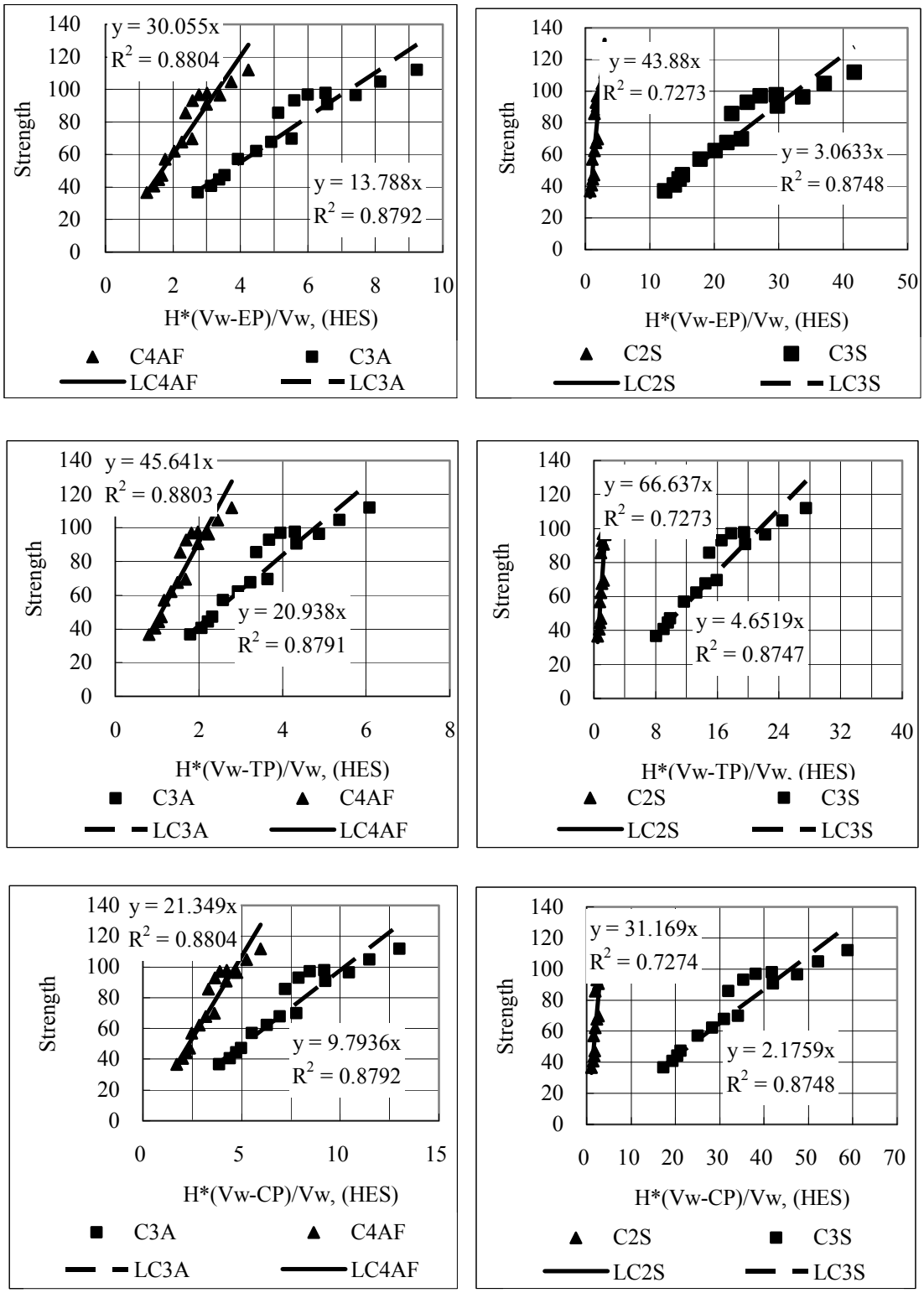

Fig VIII.3-2: Strength behavior versus $\frac{PI-P}{PI}.H_i$ (HES cements)

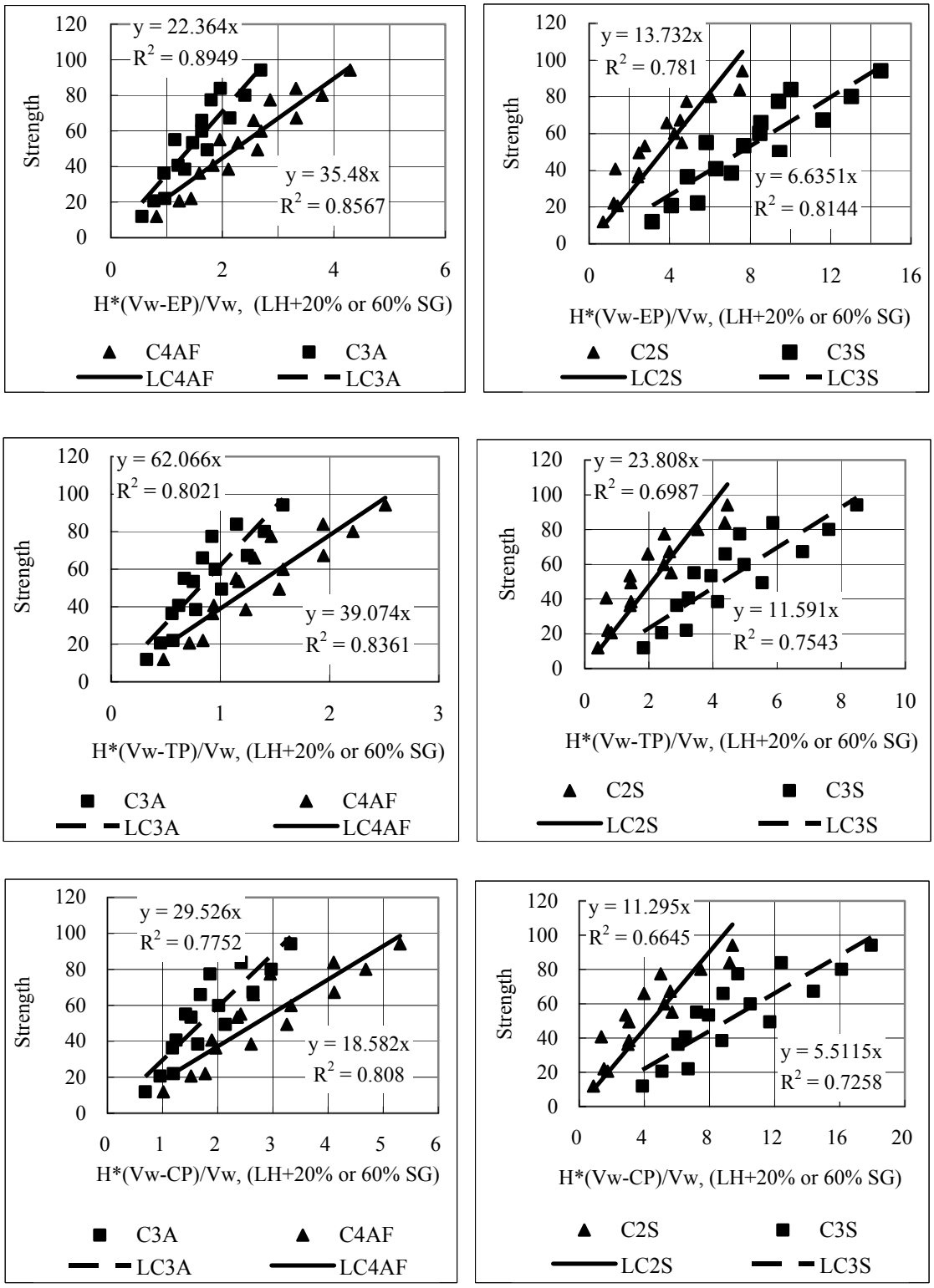

Fig VIII.3-3: Strength behavior versus $\frac{PI-P}{PI}.H_i$ (Slag replacement)

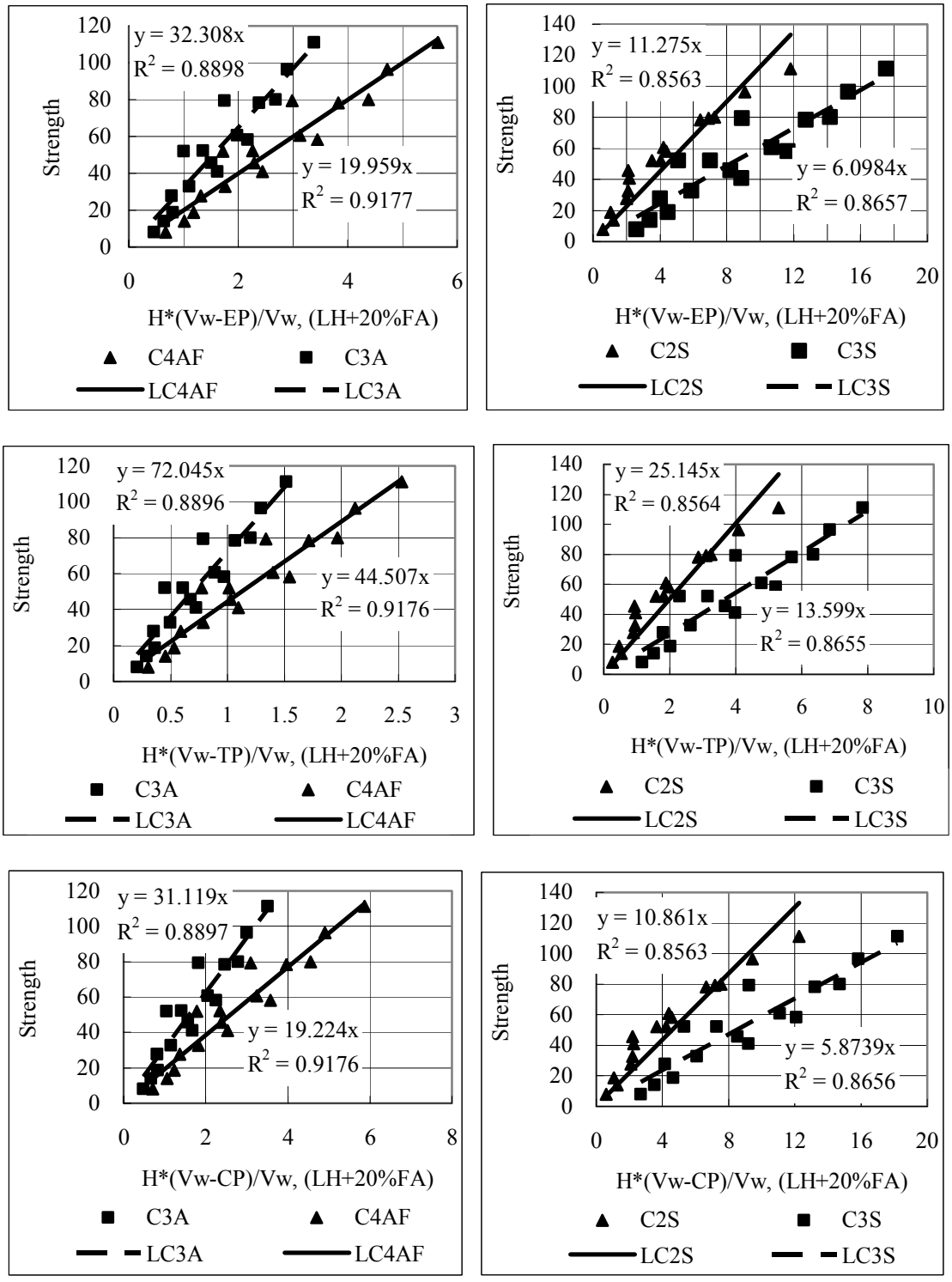

Fig VIII.3-4: Strength behavior versus $\frac{PI-P}{PI}.H_i$ (Fly ash replacement)

VIII.4. Data of Sumitomo Osaka and UBE-Mitsubishi cements

Table VIII.4-1 Compositions of cements provided by Sumitomo Osaka cement

Type	C3S	C2S	C3A	C4AF	Gypsum	Specific gravity	Fineness Modulus
LH-Used	28	53	3	10	5.0	3.24	3280
LHA	24	56	3	10	5.1	3.24	3410
LHB	25	55	3	10	5.3	3.24	3440
LHC	27	56	3	10	4.4	3.23	3380
LHD	28	54	2	10	4.6	3.24	3440
HES	63	11	9	8	6.8	3.13	4770

Table VIII.4-2 Strength of standard mortars by Sumitomo Osaka cement

Age	Used	A	B	C	D	HES
1	-	-	-	-	-	30.1
3	-	-	-	-	-	50.1
7	20.3	19.1	16.9	16.9	19.5	60.1
28	49.8	50.6	49.2	49.5	51	68.8
91	76.6	76.5	75.1	78.1	74.8	-

Table VIII.4-3 Cement composition of UBE-Mitsubishi corporation

	C3S	C2S	C3A	C4AF	Gypsum	Specific gravity	Fineness Modulus
OPC	57	17	10	8	4.6	3.16	3300
HES	66	9	9	8	6.8	3.14	4490
MH	38	42	4	10	5.2	3.21	3680
LH5	29	50	4	9	5.4	3.22	3610
LH	23	58	3	10	5.2	3.24	3470

Table VIII.4-4 Strength of standard mortars by UBE-Mitsubishi corporation

Age	OPC	HES	MH	LH5	LH
1	-	27	-	-	-
3	28.7	47.3	20	15	10.1
7	44.8	57	28.9	22.4	13.6
28	61.8	66.2	60.5	59.3	49.7
91	66.5	-	75.1	79.3	80.1

Table VIII.4-5 Mix proportions of normal concrete by UBE-MItsubishi

Cement	w/c (%)	Air %	Unit cement		Sand		Coarse aggregate	
			kg/m3	m3/m3	m3/m3	kg/m3	m3/m3	kg/m3
OPC	55	4	296	0.094	0.302	795.4	0.401	1062.4
HES		4	304	0.097	0.299	787.3	0.397	1051.6
MH		4	295	0.092	0.304	798.5	0.402	1066.6
LH5		4	293	0.091	0.304	800.7	0.404	1069.4
LH		4	291	0.090	0.305	803.1	0.405	1072.7
OPC	45	4	334.9	0.106	0.302	795.4	0.401	1062.4
HES		4	343.3	0.109	0.299	787.3	0.397	1051.6
MH		4	333.4	0.104	0.304	798.5	0.402	1066.6
LH5		4	331.3	0.103	0.304	800.7	0.404	1069.4
LH		4	329.3	0.102	0.305	803.1	0.405	1072.7
OPC	65	4	265.6	0.084	0.302	795.4	0.401	1062.4
HES		4	272.4	0.087	0.299	787.3	0.397	1051.6
MH		4	264.1	0.082	0.304	798.5	0.402	1066.6
LH5		4	262.3	0.081	0.304	800.7	0.404	1069.4
LH		4	260.6	0.080	0.305	803.1	0.405	1072.7

Table VIII.4-6 Strength of normal concrete provided by UBE-Mitsubishi

Temperature		10°C			20°C			35°C		
Cement type	w/c	45%	55%	65%	45%	55%	65%	45%	55%	65%
OPC	3	15.5	11	7.36	23.5	16.6	12.4	27.2	19.8	14.1
	7	31.3	22.5	16.8	37.5	26.5	20.1	41.6	29.7	23
	28	43	32.1	23.7	48.3	35.7	28.2	48.5	36.8	28.2
	56	49.2	38.1	29.4	50.1	37.7	29.8	49.4	37.8	28.7
	91	52.5	40.7	32	51.2	39.5	30.7	50.9	38.7	29.6
HES	1	14.4	8.22	4.07	21.2	13.7	7.68	28.7	19.9	13
	3	31.2	21.4	15.1	38.7	26.8	19.5	43.7	32.2	23.5
(High Early	7	41.8	30.3	22.9	46.2	34	26.7	47.4	35.7	26.6
strength)	14	47.5	35.3	27.2	49.9	37.2	29.3	50.6	37.9	29.1
	28	51.6	39.5	30.4	52.1	39.1	30.9	51.3	38.3	29.8
	91	54.1	42.3	32.8	54	40.7	32.7	51.8	39.1	30.1
MH	3	10.6	6.62	4.19	15.7	10.5	7.02	18.7	13.1	8.74
(Medium	7	20.2	13	7.53	24.4	16	9.76	27.2	18.4	11.8
Heat)	28	36.2	24.1	14.6	43.2	30.1	21.5	43.5	31.9	23.2
	56	50.7	38.2	28.4	52.7	39.8	30.4	52.6	41.4	31
	91	59.5	46.7	36.8	60	47.2	37.5	59.9	47.7	37.8
LH5	3	8.6	5.78	3.74	13	8.9	5.83	17.4	11.6	7.83
	7	16.7	11.4	7.02	22.6	14.3	8.92	25.2	16.6	10.8
(Low Heat)	28	32.9	26.4	21.1	42.9	35.2	29.1	46.2	37.3	31.5
	56	46.3	39.2	33.6	52.6	44.1	39	55	45.9	39.7
	91	56.7	49.5	43.6	56.8	49.5	43.2	58.3	50	42.4
LH	3	5.7	3.39	2.03	7.45	5.14	3.35	10.5	6.78	4.49
	7	9.92	6.72	4.71	12	7.92	4.67	18.9	11.8	7.4
	28	26.4	20.8	16.5	36.6	27.4	20.7	39	30.1	23.2
	56	45	36.9	31.6	51.7	43.9	37.2	55	45.7	38.3
	91	59.1	50.2	44	59.5	49.7	41.6	60.1	50.2	42.4

Table VIII.4-7 Mix proportions of high strength concrete by UBE-Mitsubishi

Cement	w/c (%)	Air %	Unit cement		Sand		Coarse aggregate	
			kg/m3	m3/m3	m3/m3	kg/m3	m3/m3	kg/m3
OPC	30	3.6	550.0	0.17	0.32	842.6	0.30	806.0
	38	3.5	421.0	0.13	0.34	891.0	0.33	883.5
	45	5.0	344.0	0.11	0.30	788.1	0.39	1023.0
LH5	30	3.6	550.0	0.17	0.32	852.8	0.30	806.0
	38	3.6	421.0	0.13	0.34	894.5	0.33	883.5
	45	5.0	344.0	0.11	0.30	794.5	0.39	1023.0
LH	30	3.7	550.0	0.17	0.32	852.8	0.30	806.0
	38	3.7	421.0	0.13	0.34	894.5	0.33	883.5
	45	5.1	344.0	0.11	0.30	794.5	0.39	1023.0

Table VIII.4-8 Strength of high strength concrete Provided by UBE-Mitsubishi

Temperature		10°C	20°C			35°C
Cement type	w/c	30%	30%	38%	45%	30%
OPC	3	41.7	49.4	35.1	23.6	58
	7	55.8	63.4	47.3	32.9	66.3
	28	70	76.3	61.9	44.4	77.6
	56	76.7	83.4	68.8	50	79.5
	91	80.2	85.1	69.7	51.7	80.2
LH5	3	31.2	34	25.7	17.6	45.6
	7	41.3	50.4	33.7	22.7	64.9
	28	63.8	70.9	63	44.9	95.6
	56	79.7	83.5	77.3	59.8	103
	91	91.8	90.1	83	66.4	106
LH	3	24.5	25	22.4	17.3	37.6
	7	34.3	34.6	25.7	20.6	55
	28	58.9	62.8	49.4	38	92
	56	77.8	78.8	70.2	57.3	98.2
	91	92.9	92.5	85.3	70.5	103

VIII.5. Pore effects

In section VI.3.B, the strength model was proposed with eq.70. One question is how much the gel pore and capillary pore share their effects in strength contribution.

$$f_c = \left(\frac{Vw - EP}{Vw}\right).(2.1\,HC2S + 1.8\,HC3S - 0.16\,HC3A + 11\,HC4AF) \quad \text{.....eq. 76}$$

$$\sum a_i H_i = (2.1\,HC2S + 1.8\,HC3S - 0.16\,HC3A + 11\,HC4AF) \quad \text{.....eq. 77}$$

Posing

$$EP = \alpha * GP + \beta * CP \quad \text{.....eq. 78}$$

The equation becomes:

$$f_c = \left(\frac{Vw - (a * GP + b * CP)}{Vw}\right).\sum a_i H_i \quad \text{.....eq. 79}$$

$$\alpha * GP + \beta * CP = Vw - Vw.\frac{f_c}{\sum a_i H_i} \quad \text{.....eq. 80}$$

Using the calculated data listed in tables VIII.5-1, VIII.5-2 and VIII.5-3, the equation eq.78 is solved for α and β, we obtain:

$$\alpha = 1.00 \; and \; \beta = 0.99 \quad \text{.....eq. 81}$$

As can be seen with eq.79, the effective coefficients of GP and CP suggest that the EP is a good parameter for pore.

Table VIII.5-1: Data for fictive porosity calculation for LH

		Heat in Mcal/m^3				Volume m^3				
LH	Age	C3A	C4AF	C2S	C3S	Water (Vw)	Interlayer	Gel	Capillary	Stregngth
w/c=0.3	7	5.044	7.672	8.398	28.456	0.308	0.040	0.044	0.153	57.0
	28	5.455	8.606	14.645	30.277	0.308	0.051	0.056	0.111	81.0
	7	5.326	8.106	8.399	30.207	0.308	0.042	0.046	0.147	59.0
	14	5.719	9.038	12.950	31.694	0.308	0.050	0.055	0.115	77.3
	28	5.976	9.625	16.930	32.560	0.308	0.057	0.063	0.089	100.2
	91	6.268	10.277	21.065	33.442	0.308	0.063	0.070	0.062	116.4
w/c=0.45	7	3.978	5.957	5.952	22.707	0.328	0.031	0.034	0.209	33.9
	14	4.350	6.921	9.219	23.683	0.328	0.037	0.041	0.185	45.3
	28	4.552	7.466	12.949	24.100	0.328	0.043	0.047	0.162	56.5
	91	4.711	7.900	17.735	24.344	0.328	0.050	0.055	0.134	78.1
	7	4.031	5.982	5.952	23.078	0.328	0.031	0.034	0.207	27.8
	14	4.459	7.099	9.219	24.016	0.328	0.037	0.041	0.183	42.5
	28	4.668	7.728	13.072	24.315	0.328	0.043	0.048	0.159	61.3
	91	4.784	8.110	19.343	24.409	0.328	0.052	0.058	0.124	83.1
w/c=0.6	7	2.983	4.397	4.372	17.191	0.321	0.023	0.025	0.232	13.4
	28	3.479	5.799	9.607	17.918	0.321	0.032	0.035	0.197	36.3
	7	2.986	4.397	4.372	17.259	0.321	0.023	0.025	0.232	13.9
	14	3.356	5.309	6.772	17.848	0.321	0.028	0.031	0.214	23.4
	28	3.498	5.849	9.607	17.929	0.321	0.032	0.036	0.196	38.7
	91	3.530	6.028	15.166	17.934	0.321	0.040	0.044	0.166	50.3

Table VIII.5-2: Data for fictive porosity calculation for OPC

		Heat in Mcal/m^3				Volume m^3				
	Age	C3A	C4AF	C2S	C3S	Water (Vw)	Interlayer	Gel	Capillary	Stregngth
w/c=0.3	7	15.562	4.840	4.185	44.092	0.304	0.047	0.057	0.106	75.48
	14	16.083	5.048	4.580	46.392	0.304	0.050	0.060	0.095	83.82
	28	16.509	5.215	4.851	48.136	0.304	0.052	0.063	0.086	91.68
	91	17.051	5.421	5.162	50.209	0.304	0.054	0.065	0.077	96.18
	7	17.153	5.352	4.789	50.722	0.304	0.054	0.065	0.077	84.25
	14	18.107	5.738	5.428	54.102	0.304	0.058	0.070	0.060	91.74
	28	18.894	6.048	5.914	56.649	0.304	0.061	0.074	0.047	100.42
	91	19.959	6.456	6.527	59.827	0.304	0.065	0.079	0.031	108.32
w/c=0.45	7	14.145	4.344	3.803	43.082	0.323	0.045	0.055	0.133	54.90
	14	15.441	4.944	4.860	46.261	0.323	0.050	0.061	0.113	62.48
	28	16.301	5.344	5.591	48.030	0.323	0.053	0.064	0.100	71.98
	91	17.180	5.766	6.351	49.483	0.323	0.056	0.068	0.088	77.05
w/c=0.6	7	10.823	3.253	2.803	33.365	0.317	0.035	0.042	0.171	33.70
	14	12.104	3.877	3.774	35.779	0.317	0.039	0.047	0.153	39.85
	28	12.676	4.227	4.534	36.476	0.317	0.041	0.050	0.144	46.53
	91	12.918	4.408	5.005	36.642	0.317	0.042	0.051	0.140	51.56

Table VIII.5-3: Data for fictive porosity calculation for HES

		Heat in Mcal/m^3				Volume m^3				
	Age	C3A	C4AF	C2S	C3S	Water (Vw)	Interlayer	Gel	Capillary	Stregngth
w/c=0.3	7	11.119	5.125	3.059	49.280	0.305	0.048	0.058	0.107	85.60
	14	11.536	5.314	3.345	51.757	0.305	0.051	0.061	0.096	92.95
	28	11.892	5.476	3.549	53.725	0.305	0.053	0.063	0.088	96.90
	91	12.362	5.690	3.796	56.152	0.305	0.055	0.066	0.078	97.67
	7	12.473	5.678	3.539	56.504	0.305	0.055	0.066	0.078	90.65
	14	13.173	6.014	3.978	59.927	0.305	0.059	0.070	0.063	96.39
	28	13.788	6.309	4.328	62.691	0.305	0.062	0.074	0.051	104.74
	91	14.662	6.729	4.792	66.311	0.305	0.066	0.078	0.034	111.87
w/c=0.45	7	9.781	4.401	2.785	44.385	0.315	0.043	0.052	0.137	57.01
	14	10.416	4.737	3.258	46.935	0.315	0.046	0.055	0.125	62.24
	28	10.930	5.011	3.605	48.799	0.315	0.049	0.058	0.115	67.61
	91	11.608	5.380	4.046	50.972	0.315	0.051	0.061	0.104	69.67
w/c=0.6	7	8.232	3.675	2.281	36.996	0.317	0.036	0.043	0.169	36.78
	14	8.801	4.036	2.872	38.684	0.317	0.039	0.046	0.158	40.62
	28	9.130	4.258	3.229	39.467	0.317	0.040	0.048	0.152	44.42
	91	9.349	4.431	3.522	39.832	0.317	0.041	0.049	0.148	47.20

REFERENCES

[1]. Maekawa K., Chaube R. and Kishi T., Modelling of Concrete Performance, ISBN 0-419-24200-7, London and New York, 1999.

[2]. Taylor H.F.W., Cement Chemistry, 2nd edition, 1997.

[3]. De Larrard F. Concrete mixture proportioning, ISBN 0 419 23500 0, London and New York, 1999.

[4]. A. M. Neville CBE and J. J. Brooks, Concrete Technology, 1990.

[5]. Dupain R., Lanchon R. and Saint-Arroman J.C. Granulats, sols, cements et betons, ISBN 2-7135-2064-9, Paris, 2000.

[6]. Lessard M. and Aitcin P.C. in Les betons a hautes performances, ISBN 2-85978-187-0, Paris, p.221-241, 1992.

[7]. Bentz D.P., Modeling the Influence of Limestone Filler on Cement Hydration Using CEMHYD3D, USA.

[8]. Suzuki, Y., Harada, S., Maekawa, K. and Tsuji, Y., Evaluation of adiabatic temperature rise of concrete measured with the new testing apparatus, Concrete Library of JSCE, 1989, No. 13, 71-83.

[9]. Suzuki, Y., Tsuji, Y., Maekawa, K. and Okamura, H., Quantification of hydration-heat generation process of cement in concrete, *Concrete Library of JSCE*, 1990, No. 16, 111-24.

[10]. Kishi. T and Maekawa. K, Multi-component model for hydration heating of blended cement with blast furnace slag and fly ash, Proceeding of JSCE, No. 550/Vol-33, 1996.

[11]. Neville, A. M., Properties of Concrete, ISBN 0-582-23070-5.

[12]. Sakai. E.,Yamada. K and Ohta. A., Molecular Structure and Dispersion-Adsorption Mechanisms of Comb-Type Superplasticizers Used in Japan, Journal of Advanced Concrete Technology Vol. 1, No.1, 16-25, April 2003.

[13]. Ferraris. F. Chiara, "Concrete Mixing Methods and Concrete Mixers: State of Art", Journal of Research of the National Institute of Standards and Technology, Vol. 106, No. 2, 391-399, March-April 2001.

[14]. Scrivener. K. L. and Gariner. E. M., "Microstructural gradients in cement paste around aggregate particles", Material Research Symposium Proc., 114, pp. 77-85 (1988).

[15]. Bentz. D. P, Replacement of "coarse" cement particles by inert fillers in low w/c ratio concretes II. Experimental validation, Cement Concrete Research, vol.35, No. 1, pp.185-188, 2005.

[16]. Bentur, A., Goldman, A. and Cohen, M.D. (1988). Mater. Res. Soc. Sym. Proc. 114, 97.

[17]. Kishi, T *et al,* Multi-component heat calculation code: developed 2005.

[18]. 小田部　裕一、複合水和発熱モデルの一般化と水和相識形成に着目した強度発現モデルの開発。

[19]. Kishi, T. and Otabe, Y., Universal Modeling for Hydration Heat Generation of Arbitrarily Blended Cementitious Materials Based on Multi-Component System, International RILEM-JCI Seminar on Concrete Durability and Service Life Planning, Concrete life'06, 14-16 March 2006, Ein-Brokek, Dead Sea, Israel.

[20]. 小田部裕一、岸利治、論文：初期空隙における水和物形成に基づいた強度発現性の評価、コンクリート工学年次論文集、Vol. 27, No 1, 2005.

[21]. 小田部　裕一、岸　利治、コンクリートの品質予測・施工管理支援に向けた水和反応・強度発現モデルの開発、生産研究　第 57 巻　第二号抜刷、2005 年 3 月。

[22]. KEN W. DAY, Concrete Mix Design, Quality Control and Specification, 2nd edition, ISBN 0-419-24330-5, 1999.

[23]. Dalgleish, B. J. and Pratt, P. L., Fractographic Studies of microstructural development in hydrated Portland cement, Journal of Material science, No 17, pp. 2199-2207, 1982.

[24]. Test records (of cement chemical compositions provided by manufacturers)

[25]. UBE-Mitsubishi cement corporation, technical reports.

ASTM Standards:

[26]. C 29-97 Standard Test Method for Bulk Density ("Unit Weight") and Voids in Aggregate.

[27]. C172-97 Standard Test Method for Sampling Freshly Mixed Concrete.

[28]. C 39-96 Standard Test Method for Compressive Strength of Cylindrical Concrete Specimens.

[29]. C109-98 Standard Test Method for Compressive Strength of Hydraulic-Cement Mortars (Using 2-in. or [50-mm] Cube Specimens)

[30]. C349-97 Standard Test Method for Compressive Strength of Hydraulic-Cement Mortars (Using Portions of Prisms Broken in Flexure)

[31]. C348-97 Standard Test Method for Flexural Strength of Hydraulic-Cement Mortars

[32]. C128-97 Standard Test Method for Specific Gravity and Absorption of Fine Aggregate.

[33]. C 136-96a Standard Test Method for Sieve Analysis of Fine and Coarse Aggregate.

[34]. C 192-95 Standard Practice for Making and Curing Concrete Test Specimens in the laboratory.

[35]. C494-98 Standard Specification for Chemical Admixtures for Concrete

[36]. C 171-97 Standard Specification for Sheet Materials for Curing Concrete.

[37]. C 618-98 Standard Specification for Coal Fly Ash and Raw or Calcined Natural Pozzolan for Use as a Mineral Admixture in Concrete.

[38]. Standard Specification for Ground Granulated Blast-Furnace Slag for Use in Concrete and Mortar